GEOCHEMISTRY AND ORIGINS OF MISSISSIPPI VALLEY TYPE MINERALIZING FLUIDS OF THE OZARK PLATEAU

A Dissertation

Presented to

The Faculty of the Graduate School

At the University of Missouri

In Partial Fulfillment

Of the Requirements for the Degree

Doctor of Philosophy

By

Zachary John Wenz

Dr. Martin Appold, Dissertation Supervisor

JULY 2011

The undersigned, appointed by the dean of the Graduate School,

have examined the Dissertation entitled

GEOCHEMISTRY AND ORIGINS OF MISSISSIPPI VALLEY TYPE MINERALIZING FLUIDS OF THE OZARK PLATEAU

Presented by Zachary John Wenz

A candidate for the degree of

Doctor of Philosophy

And hereby certify that, in their opinion, it is worthy of acceptance.

Dr. Martin Appold

Dr. Kevin Shelton

Dr. Peter Nabelek

Dr. John Bowders

ACKNOWLEDGEMENTS

First and foremost, I thank my advisor Dr. Martin Appold for his advice and encouragement during my doctoral studies. I will be forever grateful for your advice, instruction and patience throughout my graduate career at the University of Missouri. I also thank my additional geological sciences committee members Dr. Kevin Shelton, and Dr. Peter Nabelek. You both provided me with knowledge that has allowed me to critically evaluate many aspects of my research and will continue to aid me in my professional career. I also thank Dr. John Bowders for his thoughtful advice and critiques.

Former committee member Dr. Carol Wicks taught me the importance of evaluating large geochemical databases with statistical techniques and former committee member Dr. Karyn Rodgers taught me the fundamentals of designing geochemical models. Drs. Robert Bodnar and Luca Fedele and Charles Farley of the geofluids group at Virginia Polytechnic Institute and State University provided days of analytical support and valuable conversation during the early stages of this project.

TABLE OF CONTENTS

APPENDIX

LIST OF FIGURES

LIST OF TABLES

CHAPTER 1: Introduction

1.1 Purpose of the Study

Mississippi Valley-type (MVT) ore deposits represent some of the greatest enrichments of Pb, Zn, and Ba in the Earth's crust. Determining the factors responsible for creating such large base metal enrichments has been an ongoing scientific endeavor spanning over 100 years, resulting in numerous theories as to their formation. Over this time, three ore precipitation models remain credible, each of which requires a number of assumptions regarding the mineralizing fluids' chemistry. Advances in laser ablation-inductively coupled plasma-mass spectrometry (LA-ICP-MS; Longerich et al., 1996; Heinrich et al., 2003; Allan et al., 2005) and Raman microprobe analysis of individual fluid inclusions (Rosasco et al., 1975; Dubessy et al., 1989) has made possible the determination of absolute concentrations of many elements including ore metals , sulfur content, and redox state of the mineralizing fluids responsible for precipitating MVT deposits. Identifying these fluid properties can provide constraints from which the plausibility of the proposed precipitation mechanisms can be evaluated. In addition, these fluid properties may provide explanations for why MVT deposits exhibit extreme variability with respect to deposit size, stratigraphic location and ore Pb/Zn ratio.

Ozark MVT ore fluids are commonly regarded as some type of sedimentary brine (Hall and Friedmann, 1964; White, 1968; Anderson and Macqueen, 1982). However, the geochemical processes that lead to their composition are largely unknown. The salinity origin for Ozark MVT mineralizing fluids has commonly been determined based on Cl and Br systematics. Numerous studies have proposed the mineralizing fluids have Cl/Br

ratios indicative of both seawater evaporation and halite dissolution (Crocetti and Holland, 1989; Viets and Leach, 1990; Viets et al., 1996; Kendrick et al., 2002; Shelton et al., 2009). However, Ozark MVT mineralizing fluids with Cl/Br ratios indicative of highly evaporatively concentrated seawater (past the point of halite precipitation) have ionic strengths and cation concentrations inconsistent with the composition of highly evaporated seawater. These differences suggest Ozark MVT ore fluids are not as highly evaporated as suggested by their Cl/Br ratios or the seawater has been diluted significantly and/or reacted with aquifer rocks.

This dissertation focuses on using Ozark MVT mineralizing fluid compositions determined from LA-ICP-MS and Raman analysis to develop a hydrogeochemical conceptual model and reaction path and mixing models in two chapters (Chapters 2 and 3). In Chapter 2 the composition of Ozark MVT mineralizing fluids from four Ozark MVT districts are evaluated to determine a dominant ore precipitation mechanism, possible fluid migration pathways, temporal changes in fluid compositions and infer why Ozark MVT deposits are variable with respect to deposit size, stratigraphic location and ore Zn/Pb ratio. In Chapter 3 reaction path and mixing models are developed which may explain how the Ozark MVT fluids acquired their unique composition. The reaction path models consider a variety of natural evaporated seawater compositions reacting with granitic rocks. In addition, an idealized evaporated seawater was designed to allow the model to converge on the average Ozark MVT ore fluid composition. The mixing model considers a fluid composition that, upon mixing with a Cambrian highly evaporatively concentrated seawater, results in the average composition of the Ozark MVT sphalerite-hosted fluid.

1.2 References

Allan, M. M., Yardley, B. W. D., Forbes, L. J., Shmulovich, K. I., Banks, D. A., and Shepherd, T. J., 2005, Validation of LA-ICP-MS fluid inclusion analysis with synthetic fluid inclusions: American Mineralogist, v. 90, p. 1767-1775.

Anderson, G.M., and MacQueen, R.W., 1982, Ore deposit models-6. Mississippi Valley-type lead-zinc deposits: Geoscience Canada, v. 9, p. 107–117.

Crocetti, C. A., and Holland, H. D., 1989, Sulfur-lead isotope systematics and the composition of fluid inclusions in galena from the Viburnum Trend, Missouri: Economic Geology, v. 84, p. 2196-2216.

Dubessy, J., Poty, B., Ramboz, C., 1989, Advances in C–O–H–N–S fluid geochemistry based on micro-Raman spectrometric analysis of fluid inclusions: European Journal of Mineralogy, v. 1, p. 517–534.

Hall, W. E., and,F riedman, Irving, 1963, Composition of fluid inclusions Cave-in-Rock fluorite district, Illinois, and upper Mississippi Valley zinc-lead district: Economic Geolgy, v. 58, p. 886-911.

Heinrich, C.A., Pettke, T., Halter, W.E., Aigner-Torres, M., Audétat, A., Günther, D., Hattendorf, B., Bleiner, D., Guillong, M., and Horn, I., 2003, Quantitative multi-element analysis of minerals, fl uid and melt inclusions by laser-ablation inductively-coupled-plasma mass-spectrometry: Geochimica et Cosmochimica Acta, v. 67, p. 3473–3497.

Kendrick, M. A., Burgess, R., Leach, D., and Pattrick, R. A. D., 2002, Hydrothermal fluid origins in Mississippi Valley-type ore districts: Combined noble gas (He, Ar, Kr) and halogen (Cl, Br, I) analysis of fluid inclusions from the Illinois-Kentucky fluorspar district, Viburnum Trend, and Tri-State districts, mid-continent United States: Economic Geology, v. 97, p. 453-470.

Longerich, H.P., Jackson, S.E., and Günther, D., 1996, Laser ablation inductively coupled plasma mass spectrometric transient signal data acquisition and analyte concentration calculation: Journal of Analytical Atomic Spectrometry, v. 11, p. 899-904.

Rosasco, G.J., Roedder, E., Simmons, J.H., 1975, Laser-excited Raman spectroscopy for nondestructive partial analysis of individual phases in fluid inclusions in minerals: Science, v. 190, p. 557–560.

Shelton, K. L., Gregg, J. M., and Johnson, A. W., 2009, Replacement dolomites and ore sulfides as recorders of multiple fluids and fluid sources in the Southeast Missouri Mississippi Valley-type District: Halogen-$^{87}Sr/^{86}Sr$-$\delta^{18}O$-$\delta^{34}S$ systematics in the Bonneterre Dolomite: Economic Geology, v. 104, pp. 733-748.

Viets, J. G., Hostra, A. F., and Emsbo, P., 1996, Solute compositions of fluid inclusions in sphalerite from North American and European Mississippi Valley-type ore deposits: Ore fluids derived from evaporated seawater: Society of Economic Geologists Special Publication 4, p. 465-482.

Viets, J. G., and Leach, D. L., 1990, Genetic implications of regional and temporal trends in ore fluid geochemistry of Mississippi Valley-type deposits in the Ozark region: Economic Geology, v. 85, p. 842-861.

White, D. E., 1968, Environments of generation of some base-metal ore deposits: Economic Geology, v. 63, p. 301-335.

CHAPTER 2: Geochemistry of Mississippi Valley-type Mineralizing Fluids of the Ozark Plateau: A Regional Synthesis

2.1 Abstract

The compositions of fluid inclusions hosted in ore and gangue minerals from Mississippi Valley-type (MVT) Pb-Zn-Ba deposits of the Ozark Plateau region were measured to develop a regional hydro-geochemical conceptual model for ore emplacement. This model may explain the diverse compositions of fluids involved in mineral precipitation, the ore precipitation mechanism, and the temporal change in composition of fluids invading the ore districts. The conceptual model additionally provides evidence for what factors may have controlled deposit size, stratigraphic location, and Zn/Pb ratio.

High Pb concentrations up to 1,000's of ppm were identified in sphalerite-hosted fluid inclusions from all of the region's districts. If these high Pb concentrations were transported in the same fluid with sulfide, then total sulfur concentration in the fluid must have been low. Mass balance calculations demonstrate that the Arkoma Basin, a presumed source basin for the mineralizing fluids, is too small to have contained enough fluid to precipitate the observed masses of sulfur in the larger MVT districts, given the low sulfide concentrations that could coexist in the fluid with such high concentrations of Pb. High methane concentrations in sphalerite-hosted fluid inclusions from all of the region's districts, in dolomite-hosted fluid inclusions from the Tri-State and Northern Arkansas districts, and quartz-hosted fluid inclusions from the Northern Arkansas district suggest that the prevailing redox conditions during MVT mineralization were reducing,

making it unlikely that sulfate was transported in large concentrations in the fluids. During sphalerite precipitation, assuming saturation with respect to carbon dioxide, measured methane concentrations in sphalerite-hosted fluid inclusions would have required oxygen fugacity to have been at least two log units below the sulfate predominance field boundary. Fluid inclusion methane concentrations could also be used to estimate burial depths of mineralization of about 0.08 to 1.3 km.

Available evidence indicates that sulfide mineral precipitation in the Ozark Plateau MVT districts most likely occurred primarily as a result of the introduction of sulfide into a Pb- and Zn-rich ore fluid. In the two larger MVT districts, sulfide may have been supplied by local organic- and sulfur-rich carbonate facies. An apparent mixing line between high Ca/Na ratio and low Ca/Na ratio fluids hosted predominantly in main stage sulfide minerals and paragenetically late minerals, respectively, indicates the ore fluid was relatively Ca enriched. The lack of continuity in high Pb concentrations in fluid inclusions in sulfide and nonsulfide minerals from across the mineral parageneses suggests that the ore fluids either entered the districts intermittently or had variable metal contents over time.

2.2 Introduction

The Ozark Plateau of the central United States is one of the world's most important provinces of Mississippi Valley-type (MVT) mineralization (fig. 2.1). The Southeast Missouri and Tri-State districts represent two of the largest known Pb and Zn enrichments in the Earth's crust, originally containing more than 800 and 450 million tonnes of sulfide ore, respectively (Brockie and others, 1968; Ohle and Gerdemann,

1989; Hagni, 1995). Smaller accumulations of MVT sulfide mineralization occur in the Northern Arkansas and Central Missouri districts. These districts each produced several ten thousand tonnes of sulfide ore with an additional 320,000 tonnes of barite from the Central Missouri district (Leach, 1994). The Washington County barite district, frequently considered a subdistrict of the Southeast Missouri district but not included in the present study, is intermediate in size and produced at least 12 million tonnes of barite (Kaiser and others, 1987).

The Ozark MVT districts are all believed to be products of the same Pennsylvanian-Permian regional hydrothermal system (Leach and Rowan, 1986; Bethke and Marshak, 1990; Leach, 1994), yet differ significantly not only with respect to size but also stratigraphic position and mineralogy. Different MVT districts may also have formed by different precipitation mechanisms and from fluids with different chemical compositions (Plumlee and others, 1994). All of the districts are hosted predominantly by platform carbonate rocks, but the stratigraphic ages are Cambrian for Southeast Missouri, Mississippian for Tri-State, Ordovician and Mississippian for Northern Arkansas, and Ordovician for Central Missouri. All four districts contain sphalerite, galena, pyrite, marcasite, and chalcopyrite, but in highly variable proportions and amounts. In the Southeast Missouri, Tri-State, and Northern Arkansas districts, zinc and lead are the principal ore metals and have respective atomic Zn/Pb ratios of about 0.13, 16, and 50 (McKnight, 1935; Viets and Leach, 1990). Although the Central Missouri district consists predominantly of barite, its sulfide mineralogy has a Zn/Pb ratio of 0.87 (Viets and Leach, 1990).

Having likely formed from the same physical hydrothermal system, the Ozark Plateau MVT deposits mineralizing fluids share some broad similarities. For fluid inclusions hosted by sulfide minerals and dolomite, these similarities include homogenization temperatures (T_h) predominantly in the range of about 80 to 140° C and salinities predominantly in the range of 22 to 26 equivalent weight percent NaCl (eq. wt% NaCl), with Na, Ca, K, and Mg as the most abundant cations in solution and Cl as the most abundant anion in solution (Newhouse, 1933; Schmidt, 1962; Roedder, 1963, 1967, 1977; Leach and others, 1975; Leach, 1979; Hagni, 1983; Long and others, 1986; Rowan and Leach, 1989; Viets and Leach, 1990; Shelton and others, 1992; Ragan, 1994; Ragan and others, 1996; Viets and others, 1996; Coveney and others, 2000; Appold and others, 2004; Stoffell and others, 2008; Appold and Wenz, 2011). These fluid inclusion characteristics are typical of sedimentary brines, with the exception of K, which is enriched significantly in MVT fluid inclusions. Halogen compositions of the fluid inclusions are generally consistent with those of brines that formed through evaporation of seawater (Viets and others, 1996; Kendrick and others, 2002; Stoffell and others, 2008; Shelton and others, 2009). The Southeast Missouri, Tri-State, and Northern Arkansas districts contain a population of Pb-rich sphalerite-hosted fluid inclusions, which may indicate mixing between a metal-rich and a metal-poor fluid (Stoffell and others, 2008; Appold and Wenz, 2011).

Despite broadly similar fluid properties, significant heterogeneities in the Ozark MVT fluids have also been reported. Fluid inclusions from Central Missouri barite have lower T_h values and salinities than fluid inclusions hosted by sphalerite or dolomite from any of the districts (Leach, 1980). Viets and Leach (1990) reported distinctively high K

concentrations and low Ca/Mg ratios for fluid inclusions hosted by main-stage cuboctahedral galena from Southeast Missouri compared to fluid inclusions from other Ozark MVT districts. In the Southeast Missouri district, Viets and others (1992) found sphalerite coinciding paragenetically with cuboctahedral galena to be enriched in Fe, Cu, Cd, Mn, Co, and Ag relative to sphalerite from other Ozark MVT districts. Heterogeneities such as these may provide clues as to whether or not different precipitation mechanisms operated in the different Ozark MVT districts, and why the districts have different sizes, stratigraphic locations and mineralogies.

Like previous studies (Appold and others, 2004; Stoffell and others, 2008; Appold and Wenz, 2011), the present study used laser ablation-inductively coupled plasma-mass spectrometry (LA-ICP-MS) in conjunction with microthermometry to characterize the composition of fluids involved in forming MVT deposits in the Ozark Plateau. This study also presents Raman microprobe analyses of fluid inclusions from Ozark MVT districts, from which methane concentrations were determined and which constrain the redox potential and pressure of mineral deposit formation. The robust and comprehensive fluid inclusion composition dataset generated by the present study makes it possible to develop a regional hydro-geochemical conceptual model for MVT mineral deposit formation in the Ozark Plateau. This model is used to explain the variability of the fluids responsible for mineralization, the ore precipitation mechanism, temporal change in fluid composition invading the districts, and what factors may have controlled the deposits' size, stratigraphic location and Zn/Pb ratio.

2.3 Geologic Background

The Ozark Plateau of the central United States consists of a thick sedimentary succession composed predominantly of carbonate rocks (fig. 2.2). The Ozark MVT deposits, which include the Southeast Missouri, Tri-State, Northern Arkansas and Central Missouri districts, occur at different stratigraphic horizons and geographic locations within the Ozark Plateau (figs. 2.1 and 2. 2). The deposits are hypothesized to have formed from a regional hydrothermal flow system consisting of sedimentary brines discharged from the Arkoma basin and adjacent platform during the Late Pennsylvanian to Early Permian Ouachita orogeny (Leach, 1973; Leach, 1979; Leach and Rowan 1986). This orogeny would have created a strong south-north topographic gradient, which several hydrologic modeling studies have shown could have produced sufficient fluid flow, heat transport, and solute transport to account for large-scale MVT mineralization in the Ozark Plateau (Garven and others, 1993; Appold and Garven, 1999; Appold and Garven, 2000; and Appold and Nunn, 2005). According to this mechanism, long-distance fluid flow would have occurred primarily during the latter stages of the orogeny when erosion of the Ouachita fold and thrust belt would have caused isostatic rebound and uplift of the foreland.

What caused this regional hydrothermal system to form MVT deposits in each of the four districts remains uncertain. Historically, three models have been proposed for precipitating MVT deposits: a reduced sulfur model, a sulfate reduction model, and a mixing model (Jackson and Beales, 1967; Anderson, 1975, 1991, 2008; Sverjensky, 1981, 1986). In the reduced sulfur model, ore metals and reduced sulfur are transported together in solution in low concentrations, and sulfide minerals are precipitated due to

cooling, dilution, or a decrease in acidity. In the sulfate reduction model, ore metals are transported with sulfate, allowing higher concentrations of both metals and sulfur in solution. Sulfide mineral precipitation is caused when the fluid enters a sufficiently reducing environment to cause sulfate to be converted to sulfide, which dramatically lowers the solubility of the metals. In the mixing model, sulfide mineral precipitation is caused by mixing of a metal-rich, sulfide-poor fluid with a metal-poor, sulfide-rich fluid at the site of ore deposition.

Sverjensky (1981) argued for a reduced sulfur model in the Southeast Missouri district based on textural and paragenetic relationships, isotopic data and reasonable solubility constraints for simultaneous transport of low concentrations of lead and zinc with reduced sulfur. Anderson (1991) proposed thermochemical sulfate reduction of a metal- and sulfate-bearing fluid as the mechanism responsible for precipitating sulfides in the Southeast Missouri district. Anderson and Thom (2008) used two dimensional reaction path modeling to demonstrate that thermochemical sulfate reduction can provide enough sulfur to form an MVT orebody in a geologically reasonable period of time. Plumlee and others (1994) used reaction path modeling to evaluate possible ore precipitation mechanisms for each of the Ozark MVT deposits using geochemical fluid data collected from fluid inclusions. Based on modeling they concluded the Southeast Missouri and Central Missouri districts formed via mixing of a metal-rich sulfur-poor fluid with a metal-poor sulfide-rich fluid and the Tri-State and Northern Arkansas districts formed by reaction of a dolomite-saturated brine with cool limestone.

The viability of a reduced sulfur model has been questioned recently due to determinations of high Pb contents in some of the Ozark MVT ore fluids (Stoffell and

others, 2008; Appold and Wenz, 2011). The sulfate reduction model has been criticized for not explaining sufficiently the absence of low $\delta^{13}C$ values in ore-associated carbonates if organic carbon compounds were the reductant, though Anderson (1991) argues that ^{12}C-enriched carbon did not necessarily have to be incorporated into the rocks. The mixing model is supported by numerous investigations documenting the involvement of multiple fluids in mineralization (Viets and Leach 1990; Shelton and others, 1992, 2009; Goldhaber and others, 1995; Stoffell and others 2008; Appold and Wenz, 2011), though some workers have questioned its consistency with observed isotopic compositions and ore mineral assemblages (Sverjensky, 1981; Plumlee and others, 1994).

2.3.1 Southeast Missouri district

The Southeast Missouri district is composed of two principal subdistricts of sulfide mineralization, the Old Lead Belt and the Viburnum Trend. The present study considered only deposits in the Viburnum Trend, which contains the majority of the ore and where all current mining is taking place. The Viburnum Trend stretches north to south for approximately 80 km along the western flank of the St. Francois Mountains and is hosted by the Upper Cambrian Bonneterre Dolomite (fig. 2.2). The following district description of the Southeast Missouri district comes from the works of Snyder and Gerdemann (1968), Gerdemann and Myers (1972), and the review of Hagni (1995), except where otherwise referenced. Mineralization is associated closely with a dolomitized reef facies that encircles much of the St. Francois Mountains. The rocks of the St. Francois Mountains are composed predominantly of granites, rhyolites, and tuffs,

and form the basement to the Cambrian sedimentary succession in southeast Missouri (Bickford and Mose, 1975), and probably most of the Ozark Plateau. Unconformably overlying the felsic is the Lamotte Sandstone, which grades from an arkose near its contact with the basement, to a quartz arenite in its middle, to a sandy carbonate near its upper contact with the overlying Bonneterre. The Bonneterre is overlain by the Davis Formation, which consists of interbedded shales and fine-grained carbonates that act as a regional capping aquitard.

Galena is the dominant sulfide mineral in southeast Missouri, but other abundant sulfide minerals include sphalerite, chalcopyrite, marcasite, and pyrite. Mineralization occurs most commonly as porosity fillings in breccias, vugs, fractures, or bedding planes, and as replacement of the host rock (Gregg and Gerdemann, 1989). Most of the galena (~90%) was precipitated in a cuboctahedral form, with lesser amounts of cubic galena precipitated late in the paragenesis. The principal gangue mineral is dolomite, which occurs as a replacement or as four distinct cement stages that are identifiable by cathodoluminescence microscopy and that span much of the paragenesis (fig. 2.3).

2.3.2 Tri-State district

The Tri-State district consists of six major ore bodies oriented in a roughly southwest-northeast trending, 35 km long array in northeast Oklahoma, southwest Missouri, and southeast Kansas. The following represents a brief review of the geology of the Tri-State District from the works of Brockie and others (1968), McKnight and Fischer (1970), and Hagni (1976) except where otherwise referenced. Ore is hosted predominantly in cherty limestones of the Mississippian Warsaw and Keokuk

Formations, which are part of a larger hydrostratigraphic package called the Springfield Plateau Aquifer (fig. 2.2). Regionally, the Springfield Plateau Aquifer is underlain by the low-permeability Ozark Confining Unit, but in the Tri-State district the Ozark Confining Unit is absent (Imes, 1990), which may have allowed rising hydrothermal fluids to enter the Springfield Plateau Aquifer in the Tri-State district. Hydrothermal fluids may have been channeled along faults that can extend from the Precambrian basement to as high as the ground surface. Displacement along these faults has produced folds, with which most of the economic mineralization is associated.

The dominant sulfide ore mineral in the Tri-State district is sphalerite with subordinate galena and minor chalcopyrite. The paragenesis can be summarized as consisting of early gray dolomite and jasperoid alteration, overprinted successively by pink dolomite, sulfide, and calcite mineralization, with significant overlap and intermittencies (fig. 2.3). This spatial and temporal mineral zonation likely attests to the changing composition of the ore fluids over time. Mineralization in the district tends to be zoned spatially and temporally. Gray dolomite is early paragenetically, possibly predating MVT mineralization, and occurs in the center of mineralized zones, commonly as ovoid or elongate masses. These gray dolomite masses may have originated as limestone bioherms (Hagni, 1982) and served as sources of sulfur and/or organic reductant. Gray dolomite may grade into pink dolomite locally, although pink dolomite predominantly occurs as cement and more commonly occurs separate from gray dolomite. The zone of pink dolomite and sulfide mineralization grades into a zone of jasperoid alteration that can also be strongly mineralized with sulfides and calcite. Beyond the jasperoid zone is unaltered and unmineralized limestone.

2.3.3 Northern Arkansas district

The Northern Arkansas district is comprised of approximately 250 small deposits in two geographically separated clusters (McKnight, 1935; fig. 2.1). About 90% of the mineralization occurs in the western part of the district (fig. 2.1), which was the focus of the present study. Mineralization is hosted predominantly in the Ordovician Everton Formation, which consists of limestone and dolomite interbedded with sandstone and rare shale. A smaller amount of mineralization occurs in Mississippian limestones of the St. Joe and Boone Formations in the southwestern part of the district (fig. 2.2). Throughout the Northern Arkansas district, mineralization tends to occur as replacement and cavity-fill deposits along bedding planes in dolomite and silicified limestone in close proximity to faults, which can also be mineralized (McKnight, 1935). Thus, mineralizing fluids are likely to have risen through faults until they encountered high porosity and permeability horizons, into which the fluids would then have flowed laterally.

The sulfide mineralogy of the Northern Arkansas district consists predominantly of sphalerite with lesser amounts of galena, chalcopyrite, pyrite, and marcasite. Mineralization began with the precipitation of a gray dolomite phase and jasperoid, followed by sulfides, pink dolomite, coarse quartz, and calcite (McKnight, 1935).

2.3.4 Central Missouri district

The Central Missouri district consists of more than 250 small barite deposits with highly variable amounts of sulfides. Mineralization occurs in cherty granular dolomites of the Ordovician Jefferson City and Gasconade Dolomites. It began with the precipitation

of sulfide minerals, predominantly sphalerite and galena with minor marcasite and pyrite, followed by barite and calcite, with chalcopyrite precipitated throughout the paragenesis (Leach, 1980). The majority of ore is contained within circular solution collapse structures located on the crests of northwest trending folds and flexures related to the Ozark uplift (Leach, 1980).

2.4 Methodology

2.4.1 Fluid Inclusion Petrography and Microthermometry

Fluid inclusions for compositional analysis were identified in doubly polished thin sections using transmitted light microscopy. Primary and secondary fluid inclusions were distinguished following the criteria of Goldstein and Reynolds (1994). Secondary fluid inclusions were also of interest in this study because of the information that they provide about post-ore-stage fluid compositions. When possible, multiple fluid inclusions from a single fluid inclusion assemblage (FIA) were selected to ensure good data quality. However, some isolated, negative crystal-shaped, large fluid inclusions were measured as well. All inclusions observed were two-phase aqueous inclusions with the exception of a single one-phase liquid fluid inclusion hosted in barite. Fluid inclusion microthermometry was performed using a Linkam THGMS 600 heating-cooling stage at the University of Missouri. Measurement precision and accuracy for T_h measurements were ± 1° C and ± 0.1° C for last ice melting (T_m). T_h data were collected in sample chips systematically from low to high temperature to avoid stretching of the fluid inclusions. Despite this precaution, numerous inclusions were observed to have decreased liquid to vapor (L:V) ratios after heating, indicating that stretching had occurred and that the T_h

value recorded may be elevated artificially due to stretching. T_m values were measured after T_h values had been determined. Although hydrohalite was observed, ice was the last phase to melt for all of the inclusions.

2.4.2 LA-ICP-MS

After the completion of microthermometry, elemental concentrations of inclusion fluids were measured using an Agilent 7500ce quadrupole ICP-MS coupled to a GeolasPro Excimer 193 nm ArF laser ablation system housed in the Department of Geosciences Fluids Research Laboratory at Virginia Polytechnic Institute and State University. The instrument was calibrated to the NIST 610 glass standard. Samples were ablated in a 1.5 cm^3 ablation cell using a laser output energy of 150 mJ, and adjusting beam diameter to ensure ablation of the entire fluid inclusion. The ablated material was transported from the ablation cell by He gas flowing at a rate of 0.7 mL/min. The analyte was then mixed with 1.03 L/min Ar gas before introduction into the plasma. The ICP-MS was operated at a RF power value of 1500 W with a dwell time per isotope of 10 ms.

Because LA-ICP-MS analysis is destructive, data quality cannot be assessed by reproducibility tests where the same fluid inclusions are analyzed repeatedly. Instead, the relative standard deviation (RSD) is determined for fluid inclusions within a FIA, where the fluid inclusions should all represent samples of the same fluid composition. For sphalerite-hosted FIA's the average RSD values for Na, Mg, K, Ca, Sr and Ba are 4, 18, 15, 11, 12, and 24 percent, respectively. These values are less than or equal to those reported in a validation study of the LA-ICP-MS fluid inclusion analysis technique by Allan and others (2005). Despite the need to analyze multiple inclusions from a single

FIA to assess data quality, a few isolated large inclusions were measured as well. The advantages of measuring large fluid inclusions are increased signal intensity and lower limits of detection. In addition, larger inclusions on average had detectable Pb concentrations, which is likely a direct result of the better counting statistics afforded by a larger analytical volume. Reduction of LA-ICP-MS fluid and mineral matrix data was carried out using the AMS 6.1.1 software (Mutchler and others, 2008). This software calculates the absolute elemental concentrations in fluid inclusions using Na as an internal standard. An independent determination of Na concentration in the fluid inclusions was obtained from the T_m values, which was converted to eq. wt% NaCl using the equation of state of Bodnar (1993). Eq. wt% NaCl was then converted to actual weight percent NaCl using the algorithm of Heinrich and others (2003).

LA-ICP-MS elemental analysis of fluid inclusions cannot be used to determine fluid constituents that occur in comparatively high concentrations in the mineral matrix. For example the elemental concentration of Ca and Mg in dolomite-hosted fluid inclusions cannot be determined due to substantial interference of the fluid signal from the host matrix signal. As discussed by Appold and Wenz (2011), for fluid inclusions whose major elemental solute signals (e.g. Na, Ca, Mg, or K) cannot be resolved because of interferences from the host mineral matrix, then the mass balance equation for computing absolute elemental concentrations (e.g. ppm) cannot be solved, and only atomic ratios can be quantified.

For sphalerites that have detectable concentrations of Pb, the aqueous Pb component was determined by selecting the sphalerite matrix as the background during AMS data reduction. The accuracy of this approach was checked by recalculating several

fluid inclusion analyses using the Exlam software (Zacharias and Wilkinson, 2007), which utilizes an algorithm for determining the aqueous concentrations of elements that are present at low concentrations in the host mineral matrix (Wilkinson and others, 2009). These comparisons showed the AMS software to calculate similar, but slightly lower, Pb concentrations than calculated by the Exlam software.

2.4.3 Raman Spectroscopy

Raman analyses were conducted in the Vibrational Spectroscopy Laboratory in the Department of Geosciences at Virginia Polytechnic Institute and State University using a JY Horiba LabRam HR (800 mm) spectrometer with excitation provided by a 514.53 nm Laser Physics 100S-514 Ar^{+} laser. Raman spectroscopy was used to look for SO_4^{2-}, H_2S, CO_2, and CH_4 in fluid inclusions. Many fluid inclusions were either too deep or too small for the targeted species to be detected. Methane partial pressures were determined following the method of Lin and others (2007), which relies on accurate determination of the pressure dependent CH_4 wave number peak location relative to neon reference lines. Methane partial pressure was then converted to density by applying the CH_4 equation of state of Duan and others (1992). Next, the total aqueous concentration and minimum trapping pressure of CH_4 in the fluid inclusions was determined using the method of Becker and others (2010) and the H_2O-NaCl-CH_4 equation of state of Duan and Mao (2006). Burial depth at the time of mineralization was computed assuming that the CH_4 trapping pressure is equivalent to hydrostatic pressure with a water density of 1000 kg/m^3.

2.4.4 Cathodoluminescence Petrography

After completion of LA-ICP-MS and Raman analysis, dolomite samples were observed by cathodoluminescence (CL) microscopy using a Nuclide Corporation cathode luminoscope in the Department of Geology and Geophysics at the Missouri University of Science and Technology. CL microscopy was used to determine the paragentic stage of dolomite cements in the Viburnum Trend (Rickman, 1981; Voss and Hagni, 1985; Farr, 1989; Voss and others, 1989) and to determine if similar zoning patterns exist for dolomites from the other districts.

2.5 Results

A total of 528 sphalerite-hosted, 71 dolomite-hosted, 30 quartz-hosted, 12 barite-hosted, and three calcite-hosted fluid inclusions were analyzed by both microthermometry and LA-ICP-MS. Petrographic, microthermometry, and LA-ICP-MS data for sphalerite- and quartz-hosted fluid inclusions are presented in Appendix 1. Petrographic, microthermometry, and LA-ICP-MS data for barite-, calcite- and dolomite-hosted fluid inclusions are presented in Appendix 2. Fluid inclusion LA-ICP-MS analyses that included at least several seconds of mineral matrix ablation also allowed the mineral matrix composition to be calculated. Mineral matrix analyses are presented in table 2.1.

2.5.1 Fluid Inclusion Microthermometry and Petrography

T_h values for dolomite-, quartz-, and sphalerite-hosted fluid inclusions show considerable variation within each of the four Ozark MVT districts, but collectively fall mostly within a range of 85 to 140° C (fig. 2.4A). As discussed in more detail below,

fluid inclusions hosted by quartz tend to have the lowest T_h values, whereas sphalerite and dolomite have increasingly greater T_h values. Mineral parageneses for each district indicate mineral precipitation was largely sequential. Therefore, the variation in T_h among minerals may reflect temporal variation of the fluid temperature. The Ozark Plateau is not known to have been subjected to any heating events subsequent to MVT ore formation (Wisniowiecki and others, 1983; Pan and others, 1990; Symons and Sangster, 1991; Symons and others, 2005) that could have partially reset T_h values and caused their observed variability. However, stretching or leakage of some fluid inclusions could have occurred during microthermometric heating, artificially raising their T_h values. Thus, the actual mean and range of T_h values is probably lower than indicated by the measured data. A further important observation is that all fluid inclusions homogenized to a single aqueous phase, which together with the absence of any vapor-dominated fluid inclusions argues against boiling as an explanation for the observed variability in T_h values. First melting for all dolomite-, sphalerite- and quartz-hosted fluid inclusions measured range from −35 to −68 °C, indicating that the inclusions are complex brines with significant concentrations of cations other than Na. Further details about the microthermometry and petrography of fluid inclusions in each of the mineral hosts are reported below.

Sphalerite.— Microthermometry was performed on primary and secondary fluid inclusions hosted by sphalerite from all four Ozark MVT districts. T_h values for both fluid inclusion types range from 54 to 145 °C and T_m values from −2.5 to −23.4 °C, corresponding to salinities of 4.0 to 24.6 eq. wt% NaCl. These values lie within the

ranges determined from previous studies (Newhouse, 1933; Schmidt, 1962; Leach and others, 1975; Leach, 1979; Roedder, 1977, Hagni, 1983; Long and others 1986; Ragan, 1994; Ragan and others, 1996; Coveney and others, 2000; Stoffell and others, 2008). Pseudosecondary origin for fluid inclusions could not be determined with confidence, due to the absence of suitable relationships to growth bands. It is possible, therefore, that some of the inclusions classified as secondary may actually be pseudosecondary.

T_h values and salinity do not vary systematically as a function of fluid inclusion origin in any of the four districts. Instead, primary and secondary fluid inclusions have largely coincident ranges for T_h values from 54 to 145 °C and 67 to 140 °C and for salinity from 18.8 to 24.6 NaCl eq. wt%, and 16.3 to 24.5 eq. wt% NaCl (excluding two anomalous values of 4.0 eq. wt% NaCl), respectively. This suggests that fluids with similar temperature and salinity to the fluids responsible for sphalerite precipitation continued to circulate through each of the districts after sphalerite precipitation had ceased.

District mean T_h values for sphalerite-hosted fluid inclusions show a weak positive correlation with district size (fig. 2.4A). The district mean T_h value is lowest for Central Missouri and increases progressively for Northern Arkansas, Tri-State, and the Viburnum Trend. An exception to this trend is a small population of fluid inclusions from the Northern Arkansas district that has elevated T_h values, also identified by Leach (1975) and Long and others (1986). District standard deviation of salinity for sphalerite-hosted fluid inclusions shows an overall positive correlation to district size. The standard deviations of salinity are 3.8, 1.9, 0.9, and 0.8 for the Viburnum Trend, Tri-State, Northern Arkansas, and Central Missouri districts, respectively.

Calcite and Dolomite.— Microthermometric measurements were determined for fluid inclusions hosted by gangue calcite from the Granby mine in the Tri-State district. Microthermometric measurements of fluid inclusions hosted by gangue dolomite were conducted on samples from various localities in the Viburnum Trend, Tri-State, and Northern Arkansas districts. No dolomite gangue was found in the Central Missouri district. All of the dolomite- and calcite-hosted fluid inclusions measured were two-phase aqueous inclusions interpreted to be primary in origin. T_h values determined for calcite- and dolomite-hosted fluid inclusions range from 68 to 78 °C and from 77 to 193 °C, respectively, consistent with previous studies (Rowan and Leach, 1989; Shelton and others, 1992; Appold and others, 2004). As noted above, for all districts, dolomite-hosted fluid inclusions record T_h values that are greater than those of fluid inclusions hosted by any other mineral (fig. 2.4A). Some of this difference may be attributable to stretching of the fluid inclusion during heating. Stretching was observed in the majority of dolomite-hosted fluid inclusions through decreased L:V ratios upon cooling to room temperature after homogenization. T_h value ranges for fluid inclusions hosted by dolomite are similar for the Tri-State district and Viburnum Trend, whereas for Northern Arkansas district fluid inclusions, T_h values are on average about 10 °C higher (fig. 2.4A).

All calcite-hosted fluid inclusions measured in this study come from a single FIA and have a salinity of 6.7 eq. wt% NaCl. This is consistent with previous findings for the Tri-State district (Schmidt, 1962) as well as for the Viburnum Trend (Rowan and Leach, 1989; Appold and others 2004) indicating the presence of a low salinity fluid late in the district parageneses. Gangue dolomite-hosted fluid inclusions from all of the Ozark MVT

districts have salinities ranging from 8.5 to 24.6 eq. wt% NaCl, with over 90% of the inclusions exceeding 22 eq. wt% NaCl. Two low salinity (8.5 and 10.1 eq. wt% NaCl, fig. 2.1B) dolomite-hosted fluid inclusions from the Viburnum Trend occur in the same dolomite cement zone 1 as high salinity fluid inclusions. Previous studies (Rowan and Leach, 1989; Shelton and others, 1992; Appold and others, 2004) have found a similar low salinity fluid in the Viburnum Trend gangue dolomite.

Quartz.— Microthermometric measurements were made for primary and secondary fluid inclusions hosted by quartz from the Tri-State and Northern Arkansas districts. Quartz was not found in any of the Central Missouri district mines, and is rare in the Southeast Missouri district. T_h values for quartz-hosted fluid inclusions are highly variable among and within FIA's in both the Tri-State and Northern Arkansas districts, ranging overall from 63 to 140 °C and from 87 to 125 °C, respectively. Secondary fluid inclusions have some of the higher T_h values, which may have been caused by leaking or necking down during annealing of a fracture. Despite the large variation in T_h values, quartz-hosted fluid inclusions exhibit the narrowest salinity range of any mineral (from 23.4 to 24.1 eq. wt% NaCl), for both primary and secondary fluid inclusions. These results are similar to those of previous studies (Long and others, 1986; Stoffell and others, 2008), though Stoffell and others (2008) reported a population of lower salinity (~16 eq. wt% NaCl) fluid inclusions from the Picher field of the Tri-State district that was not identified in this study. Although no Viburnum Trend quartz-hosted fluid inclusions were analyzed in this study, Appold and others (2004) measured four quartz-

hosted fluid inclusions from the Viburnum Trend's Casteel mine and found T_h values to range from 90 to 108 °C with salinities of approximately 19 eq. wt% NaCl.

Barite.— Fluid inclusions hosted by barite were analyzed from the Ford, Goller, and Tiff mines of the Central Missouri district. All barite-hosted fluid inclusions analyzed were interpreted to be primary in origin. Many secondary fluid inclusions and interconnected cavities were also identified but were not measured. The L:V ratios of barite-hosted fluid inclusions are highly variable and range from pure liquid to gas-dominated, likely indicating fluid entrapment in the vadose zone (Goldstein and Reynolds, 1994). Thus, T_h values of barite-hosted fluid inclusions are unlikely to provide accurate constraints on trapping temperatures. This conclusion is supported by the observation that, with one exception, none of the barite-hosted fluid inclusions homogenized below a temperature of 140° C, which is near the maximum observed for Ozark MVT deposits in fluid inclusions hosted by other minerals. Thus, 140° C was the maximum temperature to which barite samples were heated in the present study to avoid decrepitating fluid inclusions. T_m values of barite-hosted fluid inclusions range from −0.9 to −8.1 °C, corresponding to salinities from 1.6 to 11.8 eq. wt% NaCl. This range of salinities is similar to that found by Leach (1980) and demonstrates the occurrence of large fluid compositional changes during barite precipitation. Moreover, the salinities of barite-hosted fluid inclusions are overall much lower than those of sphalerite-hosted fluid inclusions from the Central Missouri district or from sphalerite-, dolomite-, or quartz-hosted fluid inclusions from the other three Ozark MVT districts. Thus, barite precipitation in the Central Missouri district appears to have occurred from an

anomalously dilute fluid, possibly reflecting the influence of meteoric recharge in the vadose zone.

2.5.2 LA-ICP-MS Analysis of Fluid Inclusions

A major goal of this study was to determine the elemental composition of the mineral precipitating fluids in order to look for contrasts that might distinguish the districts from one another and to provide insights into how the deposits formed. This was attempted by analyzing fluid inclusions with LA-ICP-MS. The results of these analyses are shown in Appendices 1 and 2 and summarized below.

Sphalerite.— Sphalerite is common to all four Ozark MVT districts, and therefore, sphalerite-hosted fluid inclusions offer the best basis for comparing and contrasting ore fluids among the districts. Of the 528 sphalerite-hosted fluid inclusions analyzed, 75 are from the Viburnum Trend, 166 are from the Tri-State district, 180 are from the Northern Arkansas district, and 107 are from the Central Missouri district. Overall the sphalerite-hosted fluid inclusions' elemental composition was dominated by Na with lower concentrations of Ca, K, Mg, Sr, and Ba. Average concentrations for Na, Ca, K, Mg, Sr and Ba are 66,000, 18,000, 2800, 2000, 680, and 23 ppm, respectively. Three detectable Li concentrations ranged from 14 to 18 ppm, and twelve detectable Mn concentrations ranged from 7 to 46 ppm. These analyses were from some of the larger inclusions, suggesting that other fluid inclusions likely had similar low Li and Mn concentrations, but their fluid volume was too small to allow quantification.

In each of the four districts, sphalerite-hosted fluid inclusions can be subdivided into two groups based on their salinity—a "high salinity" group with eq. wt% NaCl greater than 22 that shows an inverse correlation between Na and Ca, and a low salinity group with eq. wt% NaCl less than 22 that shows little correlation between Na and Ca (fig. 2.5). In addition, the low salinity group has significantly elevated Sr/Na ratios and contains a higher proportion of secondary fluid inclusions.

In each district, only sphalerite-hosted fluid inclusions contained detectable concentrations of Pb and Cu. A total of 147 fluid inclusions from across all four districts contained detectable concentrations of Pb, ranging from 2 to 3200 ppm. These Pb concentrations were found in both primary and secondary fluid inclusions, and in both the high and low salinity groups (fig. 2.6). A total of 32 fluid inclusions contained detectable concentrations of Cu, ranging from 70 to 3900 ppm. The high Cu concentrations come from a few mines in the Tri-State and Northern Arkansas districts, which have anomalously high amounts of chalcopyrite indicating elevated aqueous Cu concentrations are a local phenomenon.

Major element concentrations for sphalerite-hosted fluid inclusions are variable among the four districts. Atomic Mg/Na ratios average between 0.026 and 0.033 and K/Na ratios between 0.023 and 0.034, though the Viburnum Trend population has a larger number of Mg- and K-rich outliers than the other districts (fig. 2.7 A and B). Atomic Ca/Na ratios average between 0.15 and 0.17 and Ca/Mg ratios between 5.6 and 6.1, within which the Viburnum Trend populations have a larger number of low value Ca/Mg ratio outliers compared to the other districts (fig. 2.8B). The Ca/Mg ratios of all of the sphalerite-hosted fluid inclusions are below the threshold value of 34 for equilibrium

replacement of calcite by dolomite (Appold and Wenz, 2011). That is, the fluids responsible for sphalerite precipitation in the Ozark MVT districts were all dolomitizing. Average atomic Sr/Na ratios vary between about 0.0023 and 0.0033 and Ba/Na ratios vary between about 4.4×10^{-5} and 5.9×10^{-5} (fig. 2.9 A and B). Fluid inclusions from the Northern Arkansas district have slightly lower Sr/Na and Ba/Na mean values than fluid inclusions from the other districts (fig. 2.9A and B).

The possible existence of geochemical similarities among the four Ozark MVT districts was investigated by carrying out Analysis of Variance (ANOVA) and Fisher Least Significant Difference (LSD) post-hoc statistical tests using the SPSS software. The ANOVA test was calculated with an α-value of 0.05 (corresponding to a confidence of 95%) such that a significance value less than 0.05 indicates that the district populations are different. The ANOVA test results (table 2.1) show the mean Mg/Na, K/Na, Sr/Na, and Ba/Na ratios from each district to be statistically distinguishable from one another, whereas the mean Ca/Na and Ca/Mg ratios are not distinguishable from one another at the 95% confidence interval. Thus, although sphalerite-precipitating fluids across the Ozark Plateau are remarkably similar with respect to their bulk salinity, T_h values and dolomitizing character given the disparate geographic and stratigraphic locations of the ore districts, the districts' fluids are chemically distinguishable from one another, reflecting original differences in the fluid composition and differences in the composition of host rocks or pore fluids with which they reacted or mixed along their flow paths.

Fisher LSD post-hoc calculations were carried out as a further test of the variability among the districts' mean atomic ratios. The results are plotted in figure 2.10 as simple binary indicators of similarity: Boxes located at the intersections of rows and

columns for different districts are shaded if the mean atomic ratios for the two compared districts are similar at a 95% confidence level and are white if they are different. Like the ANOVA tests, the Fisher LSD post-hoc tests show significant variability in the major element composition among the fluids that precipitated sphalerite in each of the four districts. The Viburnum Trend has a unique (high) K/Na ratio whereas the remaining three districts have similar (low) K/Na ratios. The Viburnum Trend is also unique with respect to its Mg/Na and Ba/Na ratio. The Tri-State district is distinguishable from the Northern Arkansas district based on its Sr/Na and Ba/Na ratios and from the Central Missouri district based on its Sr/Na ratio. The Central Missouri and Northern Arkansas districts are distinguishable from one another with respect to Mg/Na, Sr/Na and Ba/Na ratios.

As noted earlier, the Viburnum Trend has a larger population of high K/Na, Mg/Na and low Ca/Mg sphalerite-hosted fluid inclusions than any other MVT district in the Ozark Plateau (fig. 2.7 A and B; fig. 2.8B). Viets and Leach (1990) identified a population of fluid inclusions with similarly high K/Na and Mg/Na but low Ca/Mg ratios hosted by main-stage cuboctahedral galena from the Viburnum Trend, which they interpreted to represent a local ore fluid end member that they called the "Viburnum Trend brine." Viets and Leach (1990) found fluid inclusions hosted by late-stage cubic galena from the Viburnum Trend to have lower K/Na, Mg/Na, and higher Ca/Mg ratios that resemble values from fluid inclusions they analyzed from the other three Ozark MVT districts. They interpreted these fluid inclusions to represent a second ore fluid end member that was involved in MVT mineralization throughout the Ozark Plateau that they called the "regional brine."

New data presented in this study show considerably more overlap in K/Na, Mg/Na, and Ca/Mg ratios between the "Viburnum Trend brine" and the "regional brine" than is evident from the relatively small data set in the Viets and Leach (1990) study (fig. 2.11 A and B). This data overlap, coupled with the ANOVA and Fisher LSD statistical tests described above, paint a more complex picture of MVT fluid distribution in the Ozark Plateau. Namely, the Tri-State, Northern Arkansas, and Central Missouri districts are much more similar to the Viburnum Trend than the Viets and Leach (1990) data set showed, in that all four districts contain both high K/Na, Mg/Na and low Ca/Mg fluids and fluids with the converse properties. A "Viburnum Trend-type" brine could have evolved to a "regional-type" brine during ore deposition. Evidence for brine evolution can be seen in the Viburnum Trend, where sphalerite precipitated at the time of main-stage cuboctahedral galena and characterized by its high Ag content (Viets and others, 1992) contains fluid inclusions that encompass the entire range of K/Na and Ca/Mg ratios seen in cuboctahedral and cubic galena-hosted fluid inclusions (fig. 2.11 A and B).

Dolomite.— Of the 71 dolomite-hosted fluid inclusions analyzed in the present study, 32 were from the Viburnum Trend, 17 were from the Tri-State district, and 22 were from the Northern Arkansas district. All dolomite-hosted fluid inclusions contained detectable concentrations, in decreasing abundance, of Na, K and Ba. Ca, Mg, and Sr were not quantifiable in the fluid inclusions because of interferences from the host mineral matrix that overwhelmed the aqueous signal. None of the ore metals, Pb, Zn, or Cu, was detected in any of the dolomite-hosted fluid inclusions. The detection limit for Pb and Cu ranged from 1's to 10's and for Zn from 10's to 100's of ppm.

For the Viburnum Trend, Tri-State, and Northern Arkansas districts, mean atomic K/Na ratios of dolomite-hosted fluid inclusions differ slightly from sphalerite-hosted fluid inclusions, though the overall ranges of dolomite-hosted fluid inclusion K/Na values lie within the ranges of the sphalerite-hosted fluid inclusion values (fig. 2.7B). In addition, the mean K/Na ratio of the dolomite-hosted fluid for the Tri-State and Northern Arkansas districts is significantly greater than that of the Viburnum Trend dolomite cements. Because much of the dolomite was precipitated at different paragenetic stages than sphalerite, these K/Na ratio differences may reflect slight temporal variations in the compositions of the mineralizing fluids entering each district.

The most striking feature of the dolomite-hosted fluid inclusion K/Na data set is the high values of the Viburnum Trend replacement dolomites, which were collected from the basal portion of the Bonnterre Dolomite within a few centimeters of the contact with the Lamotte Sandstone, and are believed to represent a pre-ore recrystallization event (Shelton and others, 2009). These replacement dolomites exhibit elevated K/Na and Ba/Na ratios (fig. 2.7B and fig. 2.9B), both of which were likely caused by the dolomites' formation in closer proximity to K- and Ba-rich sources in the underlying arkosic Lamotte Sandstone and/or granitic basement rock.

The two low salinity dolomite-hosted fluid inclusions identified in this study from the Viburnum Trend (fig. 2.4B) exhibit the highest K/Na ratios and low Ba/Na ratios in comparison to the rest of the Viburnum Trend gangue dolomite (Appendix 1). The low salinity and difference in atomic ratios indicates this fluid is not the product of simple dilution and represents a fluid chemistry unlike that of the other dolomite-hosted fluid inclusions. Such extreme variability of fluid inclusion salinity within an individual

dolomite growth zone is unlikely as it would require the presence of two dolomite-precipitating fluids with drastically different densities. Rowan (1986) proposed the low salinity phase to be related to a pre-ore diagenetic dolomitization whereas Shelton and others (1992) hypothesized it to represent a separate, late invasive fluid. Rowan and Leach (1989) and Appold and others (2004) have determined the calcite-hosted fluid inclusions to have similar low salinities and Appold and others (2004) found some Viburnum Trend calcite to have similar elevated K/Na ratios and below detection Ba/Na ratios. The similarity between the low salinity dolomite- and calcite-hosted fluid inclusions suggests a late post-ore recrystallization of some of the dolomite during calcite precipitation.

Quartz.— Of the 30 quartz-hosted fluid inclusions that were analyzed in the present study, 18 were from the Tri-State district and 12 were from the Northern Arkansas district. No compositional differences were identified between the primary and secondary fluid inclusion populations. Quartz-hosted fluid inclusions differ significantly in composition from fluid inclusions hosted by other minerals. For the Ozark MVT deposits as a whole, quartz-hosted fluid inclusions have lower Mg/Na and Ca/Na ratios but higher Ca/Mg ratios than fluid inclusions hosted by sphalerite, and lower K/Na, Sr/Na, and Ba/Na ratios than fluid inclusions hosted by either sphalerite or dolomite (figs. 2.7-2.9). Thus, quartz in the Tri-State and Northern Arkansas districts appears to have been precipitated from fluids that were relatively more enriched in Na than the fluids that precipitated sphalerite or dolomite, and also less dolomitizing than the fluid that precipitated sphalerite.

Quartz-hosted fluid inclusions from the Viburnum Trend were not analyzed in the present study, but Appold and others (2004) analyzed fluid inclusions hosted by quartz from the Casteel mine in the Viburnum Trend. In contrast to the Tri-State and Northern Arkansas districts, quartz-hosted fluid inclusions from the Viburnum Trend were found to have significantly lower salinity (approximately 19 NaCl eq. wt%) and elevated Mg/Na, K/Na, and Sr/Na ratios. Like the Tri-State and Northern Arkansas districts, Viburnum Trend quartz-hosted fluid inclusions were found to have elevated Ca/Mg ratios. Thus, quartz in the Viburnum Trend was also precipitated from a fluid that was less dolomitizing than the fluids that precipitated sphalerite, but was significantly different in composition from the fluids that precipitated quartz in the Tri-State and Northern Arkansas districts.

Relatively low ore metal concentrations were detected in some quartz-hosted fluid inclusions from the Tri-State district. Five fluid inclusions contained Pb ranging from 1 to 3 ppm, and a single fluid inclusion contained Zn at a concentration of 33 ppm. None of the quartz-hosted fluid inclusions from the Northern Arkansas district analyzed in the present study or from the Viburnum Trend analyzed by Appold and others (2004) contained detectable ore metal concentrations. However, detection limits in the present study were on the order of 1's to 10's of ppm for Cu and Pb, 10's to 100's of ppm for Zn, and up to an order of magnitude higher in the Appold and others (2004) study.

Barite.— Twelve barite-hosted fluid inclusions were analyzed from the Brown, Tiff, and Goller mines in the Central Missouri district. These fluid inclusions, on average, have the highest K/Na and Ca/Mg and lowest Ca/Na ratios for all mineral types (figs.

2.7B and 2.8A). Magnesium, Sr, Cu, Zn, and Pb were not detected in any barite-hosted fluid inclusions. Aqueous Ba concentration was not quantifiable because of interferences from the host mineral matrix. Although Mg concentration was below detection, its detection limit could be used to calculate the Ca/Mg ratio. The barite-hosted fluid inclusion with the highest salinity was selected to calculate the minimum Ca/Mg ratio because a higher count rate of the internal standard (in this case Na) allows more accurate detection limits to be calculated. The highest salinity barite-hosted fluid inclusion had a detection limit of 36 ppm Mg, which corresponds to a minimum Ca/Mg atomic ratio of 28. This is the highest Ca/Mg ratio for any mineral from any district. The absence of gangue dolomite in the Central Missouri district in conjunction with the calculated high minimum Ca/Mg ratio is strong evidence that the barite precipitating fluid was non-dolomitizing. It is possible that the low salinity fluid inclusions have lower Ca/Mg ratios than the high salinity fluid inclusions, though the overall similarity of the measured cation ratios for the two fluid inclusion types suggests that the low salinity fluid inclusions may also have high Ca/Mg ratios.

2.5.3 LA-ICP-MS Analysis of Mineral Matrices

In the course of fluid inclusion LA-ICP-MS analysis, the adjacent host mineral matrix, particularly for the ore minerals, sphalerite, galena, and barite, was frequently also analyzed to determine the concentrations of elements that could also be quantified in the fluid inclusions. These host mineral matrix analyses commonly also identified elements that were not detectable in corresponding fluid inclusions, but that can be inferred to have existed in trace concentrations in the mineralizing fluids. These trace

element compositions may provide further insights into the origins of the Ozark MVT deposits and their relationship to one another.

Concentrations of Fe, Co, Ag, Cd, and Pb in sphalerite from the four Ozark MVT districts are plotted in figure 2.12 and average compositions are presented in table 2.3. Cadmium is the most abundant substituted element in all four districts and is on average most concentrated in sphalerites from the Central Missouri district. Iron is consistently the second most abundant element and is on average more concentrated in sphalerites from the Viburnum Trend. The Viburnum Trend sphalerite is unique based on its significantly elevated Co concentration (fig. 2.12) found in all analyses. The Viburnum Trend sphalerites are also variably enriched in Ag, Pb, and Fe compared to sphalerites from the other three districts. Sphalerites from the Viburnum Trend that are most enriched in Co, Ag, and Fe were noted by Viets and others (1992) to be enriched also in Ni and to coincide paragenetically with the main stage cuboctahedral galena mineralization. The cuboctahedral-stage sphalerite is particularly identifiable by its high Ag content, but also by its fluid inclusions with elevated K/Na ratios like those in cuboctahedral galena (fig. 2.7B and fig. 2.11 A and B). Thus, Ag-rich sphalerite in the Viburnum Trend appears to have precipitated largely from the same fluid from which cuboctahedral galena precipitated.

2.5.4 Raman Spectroscopy

Prior to laser ablation, fluid inclusions were analyzed by Raman spectroscopy to provide additional compositional information of the fluid inclusions. Of particular importance was quantifying the concentration of sulfur in the fluid, an element that

cannot be easily detected by LA-ICP-MS due to its high first ionization potential and mass interference with oxygen gas. Raman spectrometry can also provide more detailed information on the redox state of the fluid due to its ability to discriminate among various sulfur and carbon species.

Sulfate was not detected in any analyzed fluid inclusions in dolomite, quartz, sphalerite, or barite from any of the four Ozark MVT districts. The instrumental detection limit for SO_4^{2-} was about 5×10^{-3} molal, which is similar to the values reported in previous studies (Rosasco and Roedder, 1979; Dubessy and others, 1983), and was determined in the present study from a series of standards consisting of synthetic halite-hosted fluid inclusions with variable concentrations of SO_4^{2-}. This detection limit is relatively high, so it is possible that concentrations of SO_4^{2-} were high enough in the ore fluids to have played a significant role in mineralization. For barite-hosted fluid inclusions, the aqueous SO_4^{2-} peak and one of the barite peaks overlap so that even a very sulfate-rich fluid would not be recognizable in these fluid inclusions.

Hydrogen sulfide was also not detected in any fluid inclusions hosted by barite, dolomite, sphalerite, or quartz from any of the four Ozark MVT districts. Carbon dioxide was not detected in any fluid inclusions hosted by barite, quartz, or sphalerite from any of the Ozark MVT districts. Without synthetic fluid inclusion standards for H_2S or CO_2, their instrumental detection limits could not be quantified. However, the concentrations of H_2S in the fluid inclusions are inferred to be low, as H_2S has a high Raman scattering cross section (Σ=6.8, Burke, 2001). In contrast, CO_2 is only detectable in fluid inclusions at relatively high concentrations, as its Raman scattering cross-section is small at 0.80 and 1.23 for the ν_1 and $2\nu_2$ peaks, respectively (Burke, 2001).

Methane has a large Raman scattering cross-section ($\Sigma = 8.63$, Burke, 2001) and was detected consistently in dolomite-, quartz- and sphalerite-hosted fluid inclusions. Moreover, the amount of methane in many fluid inclusions was quantifiable. These tended to be large fluid inclusions located close to the sample surface, as Raman scattering intensity decreases with increasing depth from the sample surface and decreasing fluid volume. In total, CH_4 content was quantified in seven dolomite-, three quartz-, and 31 sphalerite-hosted fluid inclusions (table 2.3).

Figure 2.13 shows fluid inclusion CH_4 concentrations by host mineral for each district. Methane concentrations in sphalerite-hosted fluid inclusions vary widely, and for the Viburnum Trend, Tri-State, and Northern Arkansas districts largely overlap, covering a range from 89 to 661 ppm. Concentrations in sphalerite-hosted fluid inclusions from the Central Missouri district are on average much lower, ranging from 43 to 279 ppm with a single outlier at 416 ppm. The Viburnum Trend and Tri-State district sphalerite-hosted fluid inclusions have the highest median CH_4 concentrations among all the districts at 331 and 390 ppm, respectively, though the Northern Arkansas district range extends higher. Nonetheless, these observations suggest that methane was generally more concentrated in the Viburnum Trend and Tri-State district fluids.

Methane concentrations can be used to estimate fluid inclusion trapping pressures using the algorithm of Becker and others (2010) which incorporates the equation of state of Duan and Mao (2006). Applying this method, which assumes that measured methane concentrations are saturated values, estimated trapping pressures range from 8 to 126 bars for sphalerite-hosted fluid inclusions. Because there was no evidence of a separate phase of methane in the fluid inclusions that would indicate supersaturation, it is possible that

methane is actually undersaturated in the fluid inclusions, meaning that trapping pressures could be higher than calculated. Assuming a hydrostatic pressure gradient and an average fluid density of 1000 kg/m^3, the measured minimum trapping pressures correspond to minimum burial depths of approximately 80 to 1300 meters (table 2.3). The wide range in pressure and depth presented here is due to the variable concentration of methane in the fluid where the highest concentrations correspond to the greatest depths and pressures. Because of the assumption of methane saturation in the approach of Becker and others (2010), the higher minimum trapping pressures and depths calculated are probably closer to the actual trapping pressures and depths, as the higher methane concentrations to which they correspond are probably closer to saturation.

Average measured CH_4 concentrations of 308 and 154 ppm for the dolomite- and quartz-hosted fluid inclusions, respectively, are lower than the average CH_4 concentration of 352 ppm in sphalerite from the Tri-State and Northern Arkansas districts. However, the predominance of CH_4 over CO_2 in these gangue minerals indicates overall reducing conditions throughout the parageneses.

Fluid inclusions that were not analyzed quantitatively for methane were analyzed qualitatively to determine the presence of aqueous and gas species present at room temperature. These qualitative analyses found CO_2 to be absent from all sphalerite-, quartz- and barite-hosted fluid inclusions. However, three dolomite-hosted fluid inclusions analyzed had detectable concentrations of CH_4 and CO_2. These dolomite-hosted fluid inclusions are from the Viburnum Trend zone 4 dolomite (WF2_D2a_1_1_6), Tri-State gray dolomite (TSPC7-1_D4_1_3) and Northern Arkansas pink dolomite (NALD1-1_D1_1_3), none of which precipitated concurrently with main

stage sulfide mineralization (fig. 2.3). The presence of CO_2 with CH_4 demonstrates that during some periods of nonsulfide mineralization, fluids were modestly more oxidizing. This suggests that fluid responsible for sulfide mineralization was relatively more reducing. A previous study by Hofstra and others (1989) identified a population of gas-rich and CO_2-dominated (up to 10 mole percent) inclusions from each of the Ozark MVT districts. These findings were based on mass spectrometry analysis of thermally decrepitated dolomite-hosted fluid inclusions. Fluid inclusions measured in the present study did not exhibit any phenomena such as a separate liquid CO_2 phase at room temperature, melting at the CO_2 eutectic or development of clathrates during cooling runs that would indicate such high concentrations of CO_2. In addition, previous microthermometric studies of Ozark MVT dolomites (Rowan and Leach, 1989; Shelton and others, 1992; Appold and others, 2004; Stoffell and others, 2008) do not report finding gas-rich CO_2 dominated fluid inclusions.

2.6 Discussion

2.6.1 Genetic Importance of High Lead Concentrations

The wide range of Pb concentrations in fluid inclusions hosted by sphalerite, including a population of very Pb-rich fluid inclusions in each district with concentrations of 100's to 1000's of ppm, may represent the invasion of Pb-rich and possibly overall metal-rich brine into each of the districts during sulfide precipitation that mixed with and displaced a Pb-poor brine (see also Stoffell and others, 2008; and Appold and Wenz, 2011). Some of the variability in Pb concentration may reflect uncertainty in fluid inclusion origin (post-ore secondary inclusions are likely to be Pb-poor), variability in the

degree to which the fluid has precipitated Pb, as well as variable proportions of mixing between Pb-rich and Pb-poor fluids.

As noted by Stoffell and others (2008) and Appold and Wenz (2011), high Pb concentrations would require low sulfide concentrations in the mineralizing fluids due to galena solubility constraints. Mass-balance calculations performed in these studies for the Tri-State and Southeast Missouri districts showed that sulfide concentrations would have been too low to allow a fluid simultaneously carrying Pb and Zn to have deposited the observed masses of ore in a geologically reasonable period of time (<100 million years) at hydrologically reasonable flow rates (<10 m/yr). In contrast, if Pb and Zn were transported with sulfur in the form of sulfate that was reduced at the site of ore deposition, then based on the Ba concentration in fluid inclusions and barite solubility, the observed masses of ores could have been deposited in millions of years or less even for low groundwater flow rates on the order of one cm/yr. Stoffell and others (2008) showed that for the Tri-State district, if sufficient sulfur were available to bond with all of the available Pb and Zn in solution (about 100 and 4000 ppm, respectively), either as sulfate (ultimately reduced at the deposit site) in the metal-rich fluid or as sulfide in a second, metal-poor fluid, then only a relatively small volume of about 2 km^3 of metal-rich fluid would be needed to precipitate all of the observed mass of ore. The Southeast Missouri district, whose size is of similar magnitude to the Tri-State district but that has fluid inclusions as much as an order of magnitude more Pb-rich, and the Northern Arkansas and Central Missouri district, which are much smaller than the Tri-State district and have fluid inclusions that are more Pb-rich than those from the Tri-State district,

should all require fluid volumes for ore formation that are smaller than the 2 km^3 needed for the Tri-State district.

A similar fluid volume analysis can be conducted to evaluate the feasibility of ore deposition from a fluid transporting simultaneously Pb and sulfide. For all four districts, the high Pb concentrations in fluid inclusions indicate that coexisting sulfide concentrations would had to have been low and thus would have acted as the controlling factor with respect to the fluid volume required to precipitate ore. For the Viburnum Trend, if Pb concentrations in the ore fluid equaled the highest Pb concentration found in fluid inclusions (1500 ppm), then calculations carried out using the Geochemist's Workbench SpecE8 software show that a maximum of 1.8×10^{-6} mol/kg sulfide could have been carried simultaneously in solution, assuming a temperature of 120° C and a pH of 3.5, which is near the lower limit of typical sedimentary brines (Hanor, 1994).

Based on this sulfide concentration, 5.9×10^4 km^3 of fluid would have been required to precipitate all of the 1.1×10^{11} moles of sulfur comprising the Viburnum Trend ore (Ohle and Gerdemann, 1989). Assuming a porosity of 10 percent, then a rock volume of 5.9×10^5 km^3 would have been required to entrain all of this fluid. The Lamotte Sandstone is believed to have been the principal conduit for metal-bearing fluid into the Southeast Missouri district (Gerdemann and Myers, 1972; Goldhaber and others, 1995). Assuming an average thickness of 30 meters for the Lamotte, then fluid would had to have been derived from an area of the Lamotte encompassing 2×10^7 km^2. This area is nearly three orders of magnitude larger than the actual 8.8×10^4 km^2 area of the Arkoma Basin (Perry, 1995) demonstrating that the entire basin could not have contained enough sulfur in the Lamotte at this high of a metal concentration if the sulfur was in the form of

sulfide and coexisted with Pb in solution. However, for every order of magnitude decrease in Pb concentration or for every 0.5 unit decrease in pH, the volume of aquifer rock required decreases by one order of magnitude. Therefore, by decreasing the Pb concentration by three orders of magnitude to ~1.5 ppm while maintaining the pH at 3.5 or lower, the aquifer source volume requirement can be reduced to the volume of Lamotte Sandstone present in the Arkoma basin.

Although what geologic formations served as the ore fluid conduit aquifer for the other three Ozark MVT districts is not as clear as for Southeast Missouri, if they had comparable thicknesses to the Lamotte Sandstone then they also could not have contained enough sulfide to precipitate all of the observed MVT mineralization. It can further be questioned whether all of the pore fluid in a particular source aquifer like the Lamotte Sandstone, from throughout the Arkoma Basin, could be funneled toward one particular district. More likely, only a fraction of the available fluid in the source aquifer in the basin would ever flow through any particular district, making simultaneous transport of sulfide and metals an even less feasible component of any sulfide mineral precipitation mechanism.

Alternatively, for the Viburnum Trend, if sulfide was present in the solid matrix of the Bonneterre Dolomite, the principal host rock for the ore, then for the 35 km^3 volume of Bonneterre Dolomite present within the Viburnum Trend, a sulfide concentration of only 100 ppm would have been required to precipitate all of the ore. This value is well below the 1,700 to 8,800 ppm total sulfur concentrations found by Leventhal (1990) in whole rock analyses of unmineralized Bonneterre Dolomite, which also contained total organic C concentrations of 1,700 to 26,000 ppm that could have

served as a reductant for sulfur. Further, insoluble residues from ore samples were found by Leventhal (1990) to contain even greater amounts of sulfur ranging from 77,000 to 215,000 ppm, which could have served as a rich source of organic sulfide for ore precipitation. These mass balance arguments do not address the sulfur isotope composition of the ores, which may require multiple sulfur sources (Sverjensky, 1979, 1981; Deloule and others, 1986; Burstein and others, 1993; Shelton and others, 1995).

2.6.2 Genetic Significance of High Methane Concentrations

Redox state fundamentally affects fluids' ability to transport and precipitate metals and sulfur, however, redox state in MVT fluids has historically not been known with much certainty. The redox state of crustal fluids is frequently buffered by their host rocks (Yardley, 2005). In the case of the Viburnum Trend, whose mineralizing fluids are likely to have had prolonged contact with arkose in the lower Lamotte Sandstone and felsic igneous rocks in the underlying basement, the redox state of the mineralizing fluids likely was governed by equilibrium with granite. The redox state of most felsic igneous rocks is relatively reducing, lying two to three log f_{O_2} units above the quartz-fayalite-magnetite (QFM) buffer (Haggerty, 1976). At 120° C the log f_{O_2} value of the QFM buffer is −57, which lies in the sulfide and methane species predominance fields (fig. 2.14). At 120° C, more oxidizing granites would have log f_{O_2} values near −54, which are still within the sulfide and methane species predominance fields and are consistent with the high methane concentrations found in fluid inclusions in this study.

Host rocks in the Tri-State, Northern Arkansas, and Central Missouri districts do not provide such clear records of redox state as do host rocks of the Viburnum Trend,

although for all four districts, CO_2/CH_4 ratios of fluid inclusions can provide some constraints. Although CO_2 concentration was not measured in any fluid inclusions in this study, its experimental solubility can be used in conjunction with the measured methane concentrations to determine maximum redox state. According to Duan and Sun (2003), CO_2 has a solubility of 3.733×10^{-1} mol/kg in a 4 molal NaCl solution at 120° C and 100 bars. For the range of CH_4 concentrations found in sphalerite-hosted fluid inclusions from the Viburnum Trend, Tri-State, Northern Arkansas, and Central Missouri districts, maximum CO_2/CH_4 mole ratios can be calculated, which range from 10 to 51, 12 to 67, 9 to 35, and 14 to 140, respectively. Using the Geochemist's Workbench SpecE8 software, these ranges of CO_2/CH_4 mole ratios correspond to maximum log f_{O_2} values of approximately -53 to -52 for all of the districts. Inspection of figure 2.14 clearly shows that the measured CH_4 concentrations are too high to allow a redox state to have been reached where SO_4^{2-} was the dominant sulfur species.

Whether these high methane concentrations were transported with metal-rich fluids along their flow paths to the ore districts or were introduced into the metal-rich fluids through mixing in the ore districts is not absolutely clear. However, the fact that many of the sphalerite-hosted fluid inclusions that have high Pb concentrations also have high methane concentrations suggests that Pb and methane were transported together at relatively high concentrations, and that the Pb-rich fluids for each district were reducing enough such that sulfur would have been transported predominantly as sulfide rather than as sulfate. Thus, the most likely precipitation mechanism for each district is mixing between two relatively reducing fluids, one Pb- and possibly over all metal-rich and sulfur-poor, and the other, metal-poor and sulfur-rich. Alternatively, sulfide could have

been added to the metal-rich fluids by their reaction with sulfide-rich host rocks, such as organic-rich reef facies in the Viburnum Trend or bioherms in the Tri-State district.

2.6.3 Genetic Significance of Ca/Mg Ratios

The low average Ca/Mg ratio (~6) of sphalerite-hosted fluid inclusions from all of the Ozark Plateau MVT districts places important constraints on possible ore fluid flow paths. As noted previously, thermodynamic calculations by Appold and Wenz (2011) demonstrated that a fluid with a Ca/Mg ratio below 34 should cause calcite to be replaced by dolomite. Therefore, the ore fluid could not have flowed through a limestone aquifer without the fluid's Ca/Mg ratio becoming significantly elevated. In addition, the low Ca/Mg ratio of the ore fluid indicates that it is likely responsible for precipitation of some of the dolomite in each of the districts.

In the Southeast Missouri district, the dolomitizing nature of the ore fluid is corroborated by field evidence of a dolomitizing fluid having flowed through the Lamotte Sandstone. Gregg (1985) reported that approximately the lower six meters of the Bonneterre Dolomite have been dolomitized over an area of more than 1.7×10^4 km^2 outside of the ore district, whereas the upper Bonneterre, which apparently did not have contact with the ore fluid flowing through the Lamotte, has remained limestone.

The Tri-State district is contained within a thick succession of Mississippian limestones in the Springfield Plateau aquifer that has not been dolomitized significantly in the vicinity of the Tri-State district (Brockie and others, 1968). Thus, it seems unlikely that the ore fluids that precipitated sphalerite in the Tri-State district could have traveled through the Springfield Plateau aquifer or they would have left a wake of dolomite

alteration along their travel path in the limestone succession. This limiting flow path scenario can be demonstrated quantitatively by computing the reaction potential with respect to calcite of a fluid with the average composition of the high salinity group of Ozark MVT sphalerite-hosted fluid inclusions. Calculations were carried out using the Geochemist's Workbench React software in which the model fluid was assumed to have a CH_4 concentration of 200 ppm, a log f_{O_2} value of −53, and a pH of 3.5. The results of the reaction path (table 5) show that only about 5 cm^3 of calcite are required to exhaust the dolomitizing potential of one kilogram of ore fluid from each of the districts. By extension, only 5.0×10^{-2} km^3 of limestone would have been required to exhaust the dolomitizing potential of the fluid occupying the entire pore volume of the Lamotte Sandstone in the Arkoma Basin, assuming a porosity of 10% and an initial Ca/Mg ratio of six.

Thus, fluid responsible for sphalerite mineralization in the Tri-State district could not have flowed very far through the limestone Boone Formation that hosts the ore or through any other limestone aquifers. As noted previously, fluids responsible for MVT mineralization in the Tri-State district have long been thought to have risen from lower stratigraphic levels, based on the presence of mineralization in deep-seated faults and a local window in the Ozark confining unit, which underlies the Springfield Plateau aquifer (Brockie and others, 1968; Appold and Nunn, 2005). Thus, long distance flow of the ore fluid more likely occurred through a deeper non-limestone aquifer such as the St. Peter Sandstone, the clastic Roubidoux Formation, which is the most important groundwater resource in the Tri-State district today, or the Lamotte Sandstone, and ascended into the Boone Formation via permeable conduits in the Tri-State district.

As in the Tri-State district, some of the Northern Arkansas mineralization is hosted by Springfield Plateau aquifer limestones and has strong spatial association with faults and fractures along which mineralizing fluids could have risen from deeper non-limestone aquifers. The remainder of the Northern Arkansas mineralization, as well as the Central Missouri mineralization, is hosted by deeper Ordovician formations that have been dolomitized extensively and that could have provided conduits for flow that would have preserved the dolomitizing character of the mineralizing fluids.

2.6.4 Correlations to Deposit Size

The four Ozark Plateau MVT districts differ greatly in the size of their sulfide mineral endowments, raising the question of what might have caused these differences. A possibility to consider is that the fluids that precipitated the Viburnum Trend and Tri-State deposits were much more metal-rich than fluids that precipitated the Northern Arkansas and Central Missouri deposits. However, lead concentrations in fluid inclusions from the Viburnum Trend and Tri-State districts are not significantly or consistently elevated above lead concentrations in fluid inclusions from the other districts, suggesting that aqueous metal concentration did not affect ore deposit size.

In contrast, variability in salinity of fluid inclusions hosted by sphalerite and dolomite correlates strongly with district size, where fluid inclusions from the Viburnum Trend and Tri-State district have the highest variability and fluid inclusions from the Northern Arkansas and Central Missouri districts have the least (fig. 2.4B). This variability of fluid inclusion salinity could be explained by mixing of fluids with different salinities. Fluids that differed with respect to salinity may also have differed with respect

to other aspects of composition, such as metal and sulfur content. Because mixing of metal-rich and sulfide-rich fluids is an efficient sulfide mineral precipitation mechanism, then perhaps the Viburnum Trend and Tri-State deposits grew large because mixing of this type occurred to a much larger degree than in the Northern Arkansas and Central Missouri districts.

Figure 2.8B shows that the fluids that produced MVT mineralization in each of the four Ozark districts were all consistently dolomitizing. Yet, field observation indicates the amount of dolomite gangue present in the districts varies greatly, with the largest amounts of dolomite gangue present in the larger Viburnum Trend and Tri-State district, considerably less dolomite gangue in the Northern Arkansas district, and little or no dolomite gangue in the Central Missouri district. Thus, abundance of dolomite gangue correlates with district size. Moreover, abundance of dolomite gangue may be a proxy for magnitude of mineralizing fluid flux, meaning that the larger districts were formed by higher fluxes of mineralizing fluid.

District size may also correlate to the amount of locally available sulfur. The ores of the Viburnum Trend are predominantly associated with organic-rich reef facies of the Bonneterre Dolomite (Gerdemann and Myers, 1972), and Hagni (1976 and 1982) has suggested that the gray dolomitic cores of the Tri-State district ore bodies are replaced bioherms that may also have been organic-rich. Organic compounds are commonly rich in reduced sulfur. Typical carbonate rocks have 1200 ppm sulfur, whereas coals can have up to 110,000 ppm sulfur (Faure, 1998; Speight, 2005). Therefore, organic material in the carbonates could have promoted the precipitation of metal sulfide minerals from a metal-bearing ore fluid. Sulfide could also have been contributed through pore fluids that

derived their sulfur from elsewhere in the local stratigraphic section. In contrast, mineralization in the Northern Arkansas and Central Missouri districts is not clearly related to any organic-rich facies, but rather is associated strongly with fracturing and brecciation in a variety of facies (McKnight, 1935; Long and others, 1986). Without a local reduced sulfur source, sulfide mineral deposits in Northern Arkansas and Central Missouri could not have grown to a very large size.

2.6.5 Genetic Implications of Geochemical Trends

Data presented in this study indicate that the dominant ore precipitation mechanism for Ozark MVT deposits is likely to have been mixing between two relatively reducing fluids, one Pb- and possibly overall metal-rich and sulfur-poor, the other metal-poor and sulfide-rich, based on the consistently high methane concentrations and highly variable Pb concentrations of sphalerite-hosted fluid inclusions. As a result, sphalerite-hosted fluid inclusions represent a mixture of variable proportions of at least two fluids. The same can probably be said for fluid inclusions hosted by galena, which would explain the overlap of K/Na and Ca/Mg ratios for early cuboctahedral and late cubic galena from the Southeast Missouri district noted earlier.

For each district, the most Pb-rich sphalerite-hosted fluid inclusions should most closely approximate the composition of the metal-rich ore fluid end member that entered the district. In theory, further characteristics of these end member ore fluids should be inferable through correlations with aqueous Pb concentration. However, Pb concentration was not found to correlate strongly with other element concentrations, perhaps because more than two fluids were involved in sulfide mineral precipitation, which would cause

the compositions to plot as two-dimensional mixing arrays rather than one dimensional mixing lines (Appold and Wenz, 2011). Alternatively, element correlations with Pb could have been obscured due to high matrix Pb concentrations in some sphalerites, preventing quantification of the aqueous Pb signal. The paragenetically early sphalerite from the Southeast Missouri district is an example of such, where the matrix Pb contribution from the sphalerite is so great that it overwhelms the fluid inclusion's aqueous Pb signal.

Other element concentrations do correlate strongly with one another. Figure 2.15A shows an inverse correlation between Ca/Na ratio and Na concentration for sphalerite-hosted fluid inclusions from all four Ozark MVT districts and for quartz-hosted fluid inclusions from the Tri-State and Northern Arkansas districts. This inverse correlation may represent mixing between high Ca/Na and low Ca/Na fluids. The quartz-hosted fluid inclusion data in figure 15A are from paragenetically late quartz, indicating that a low Ca/Na fluid was present in the Tri-State and Northern Arkansas districts after the main period of sphalerite precipitation. If the quartz-hosted fluid inclusions captured a greater proportion of a non-ore (that is, Pb- and Zn-poor) fluid, then the high Ca/Na end member in figure 2.15A is most likely the metal-rich ore fluid.

The Cl/Br data of Stoffell and others (2008) plotted in figure 2.15B show that not only do quartz-hosted fluid inclusions from the Tri-State and Northern Arkansas districts have low Ca/Na ratios, they also have high Cl/Br ratios (300 to 2100) compared to sphalerite-hosted fluid inclusions (80 to 100). Thus, in the Tri-State and Northern Arkansas districts, mixing occurred between a high Ca/Na, low Cl/Br, Pb-rich fluid and a fluid with the converse properties. Similar mixing appears to have occurred in the Southeast Missouri district. Data from this study, Shelton and others (2009), and Crocetti

and Holland (1989) plotted in figures 2.16A and B show that fluid inclusions in main stage cuboctahedral and Ag-rich sphalerite have high Ca/Na and low Cl/Br ratios, whereas fluid inclusions in late stage cubic galena have much lower Ca/Na and higher Cl/Br ratios.

In the Central Missouri district, barite mineralization postdates sulfide mineralization and was precipitated from a cooler, lower salinity fluid than the fluids that precipitated sulfides elsewhere in the Ozark Plateau. Based on fluid inclusion data from barite, Leach (1980) hypothesized that the Central Missouri district barite deposits formed by dilution of a late stage ore fluid by mixing with a cooler, dilute groundwater. Fluid inclusion microthermometry data from the present study support a dilution hypothesis, but show that the groundwater must have had elevated K/Na and Ca/Mg ratios, as these ratios are much higher in barite-hosted fluid inclusions than in sphalerite-hosted fluid inclusions.

2.6.6 Hydro-geochemical Conceptual Model

The results of the present study reveal several important characteristics of MVT deposit formation in the Ozark Plateau. Perhaps the most important is the identification of a Pb-rich population of sphalerite-hosted fluid inclusions in each of the four districts (see also Stoffell and others, 2008; Wilkinson and others, 2009; and Appold and Wenz, 2011). These fluid inclusions probably represent the influx of a Pb-rich fluid into each of the districts where mixing occurred with one or more relatively Pb-poor fluids. Though Zn concentration could not be determined in any of the sphalerite-hosted fluid inclusions because of interference from the host mineral matrix, the fact that sphalerite is the host

mineral suggests that the Pb-rich fluid was also Zn-rich and thus could be characterized as overall metal-rich. Mass balance and solubility constraints make it unlikely that much sulfide was transported in solution with the high Pb concentrations observed. In addition, relatively high methane concentrations in sphalerite-, dolomite- and quartz-hosted fluid inclusions indicate that redox conditions during MVT mineralization were generally reducing, with the exception of barite mineralization in the Central Missouri district. Thus, sulfide mineralization in the four districts is less likely to have precipitated as a result of reduction of sulfate in a metal-rich fluid or as a result of cooling, dilution, or alkalinization of a metal- and sulfide-rich fluid, but rather due to mixing of a metal-rich fluid with a sulfide-rich fluid, or perhaps reaction of a metal-rich fluid with sulfide-rich host rocks. Barite in the Central Missouri district was probably precipitated due to mixing of a hotter, more reducing brine with a cooler, more oxidizing groundwater.

Though Pb concentration does not correlate strongly with other element concentrations in the fluid inclusions, the Pb-rich fluid in each of the four districts can be inferred to have had high Ca/Na and low Cl/Br ratios. Some of the variability in fluid inclusion Pb concentration could also be a function of the metal content of the ore fluid entering the districts being variable over time. At times when metal concentration in the ore fluid was high, sulfide mineral precipitation would have been favored, whereas when metal concentration was low, gangue mineral precipitation would have been favored. Furthermore, because sulfide precipitation is an acid-generating process (Anderson and Garven, 1987), times of high metal concentration leading to sulfide mineral precipitation would have inhibited dolomite precipitation, whereas times of low metal concentration without sulfide mineral precipitation would have promoted dolomite precipitation. That

the fluid that precipitated sphalerite and dolomite in any district was the same other than with respect to its metal content is supported by the similar K/Na and Ba/Na ratios of the sphalerite- and dolomite-hosted fluid inclusions, and that the sphalerite-hosted fluid inclusions have dolomitizing Ca/Mg ratios. Thus, the dolomite- and sphalerite-hosted fluid inclusions likely represent a single ore fluid that varied temporally with respect to its Pb and Zn content which controlled whether dolomite or sulfides would precipitate.

Alternatively, Appold and Wenz (2011) hypothesized that the lack of strong correlation in Pb concentration with other element concentrations for the Viburnum Trend was the result of mixing between more than two fluids. They argued that Pb-rich fluid entered the Viburnum Trend intermittently, based on the observation that fluid inclusions hosted by different stages of dolomite cement that largely alternate paragenetically with sulfide minerals are Pb-poor. Similar interpretations may also hold for the Tri-State and Northern Arkansas districts, where fluid inclusions hosted by gangue minerals, which only partially overlap sulfide deposition paragenetically, are poor in metals. Paragenetically late calcite was precipitated from a much more dilute fluid than the earlier precipitated minerals, and may either represent a very high level of dilution of the MVT fluids or a fluid that was uninvolved in the earlier mineralization.

One of the distinctions among the Ozark Plateau MVT deposits is the large differences in their Zn/Pb ratios. The stratigraphically lowest Southeast Missouri district ores have Zn/Pb ratios of 0.13 whereas the stratigraphically higher Central Missouri, Northern Arkansas and Tri-State districts have Zn/Pb ratios of 0.87, 16, and 50, respectively. Considering that the solubility of Pb in the presence of sulfide is approximately one order of magnitude less than that of Zn, then except for fluids with

high Zn/Pb ratios, galena should precipitate before sphalerite as sulfide is introduced into an ore fluid, causing relative enrichment of Zn in the ore fluid over time. Calculations using the Geochemist's Workbench React software show that for a fluid with a 4 molal NaCl concentration, a pH of 5, and a log f_{O_2} value of -54, galena would precipitate as sulfide was introduced into the fluid as long as the Zn/Pb ratio was less than 43. Therefore, even for fluids relatively enriched in Zn compared to Pb, galena would precipitate first as sulfide is introduced into the ore fluid, but with continued galena precipitation, the Zn/Pb ratio of the fluid would eventually increase enough to allow sphalerite precipitation to dominate. In the case of the Southeast Missouri district, where the host for mineralization (the Bonneterre Dolomite) is adjacent to the presumed aquifer for the metal-bearing ore fluid (the Lamotte Sandstone), the short distance between the ore fluid aquifer and mineralization host may not have allowed enough sulfide to be introduced into the ore fluid to raise the Zn/Pb ratio to a level where sphalerite precipitation would start to dominate over galena precipitation. In contrast, in the Tri-State, Northern Arkansas, and Central Missouri districts, the greater distance that ore fluids would need to have risen from the nearest non-limestone aquifers into the hosts for mineralization may have allowed enough sulfide to be introduced en route to allow sphalerite precipitation to dominate over galena by the time the ore fluids reached the main hosts for mineralization. Evidence for an extended ore fluid travel path is documented by the occurrence of sub-economic to economic sulfide mineralization in Ordovician rocks up to 300 meters below the majority of the ores hosted in the Mississippian limestones in the Tri-State district (Siebenthal, 1916; Brockie and others, 1968). Although the Zn/Pb ratio of these ores is unknown, the presence of mineralization

at depth indicates ore fluids may have ascended from non-limestone aquifers in the Tri-State district. It is also possible that the different Pb/Zn ratios of the four Ozark MVT districts could be a result of variation in the compositions of the rocks from which the ore fluids extracted their Pb and Zn.

2.7 Conclusions

The results of the present study have provided several new insights into the origin of MVT deposit formation in the Ozark Plateau.

1. A Pb-rich population of sphalerite-hosted fluid inclusions in each of the four Ozark MVT districts documents the invasion of a Pb- and possibly overall metal-rich fluid into each district during the period of sulfide precipitation.

2. High methane concentrations in dolomite-, sphalerite- and quartz-hosted fluid inclusions indicate that the overall oxidation state during MVT mineralization was relatively reducing, enough for sulfide to have been the dominant sulfur species.

3. Evidence for the existence of a Pb-rich fluid in each district and prevailing reducing conditions indicates the dominant precipitation mechanism to have been mixing between a metal-rich, sulfide-poor fluid and a metal-poor, sulfide-rich fluid.

4. The ore fluid also appears to have had high Ca/Na ratios, demonstrating major cation ratios can be used to identify the ore fluid in the Ozark Plateau MVT districts.

5. In order for measured fluid inclusion methane concentrations to have been fully dissolved in aqueous solution, MVT mineralization must have occurred at a minimum depth between 0.08 and 1.3 km, with the higher end of this range being more likely.

6. With the exception of calcite, MVT mineralization in each district was produced from dolomitizing fluids. Geochemical modeling demonstrates that these fluids could not have travelled a long distance through limestone without losing their ability to make dolomite, because of rapid equilibration with calcite.

7. The geochemical similarity between dolomite- and sphalerite-hosted fluid inclusions suggests that dolomite and sulfides in each of the districts may have precipitated from the same fluid whose Pb and Zn concentration varied over time.

8. The largest Ozark MVT districts contain the highest proportions of low-salinity fluid inclusions, the greatest volumes of gangue dolomite, and are hosted in organic-rich carbonate facies. High aqueous Pb concentration does not appear to have been a controlling factor in ore deposit size, as all four districts have a population of Pb-rich sphalerite-hosted fluid inclusions with concentrations on the order of 100’s to 1000’s of ppm.

2.8 Acknowledgments

Funding for this research was provided by U.S. Geological Survey Mineral Resources External Research Program grant 06HQGR0178, and by U.S. Department of Agriculture- National Institute of Food and Agriculture Cooperative Agreement No. 0217299, contribution No. 2011-008, Cooperative Research Programs, Lincoln University. We thank George Moellering, chief mine geologist of Doe Run Company, for providing us with some of the samples from the Viburnum Trend, and Luca Fedele and Charles Farley of the Fluids Research Laboratory of Virginia Polytechnic Institute and State University for their valuable assistance in operating the LA-ICP-MS and Raman spectrometer. We also thank Dr. Robert Bodnar of the Virginia Polytechnic Institute and State University for valuable conversations that helped develop some of the results of this study.

2.9 References

Allan, M. M., Yardley, B. W. D., Forbes, L. J., Shmulovich, K. I., Banks, D. A., and Shepherd, T. J., 2005, Validation of LA-ICP-MS fluid inclusion analysis with synthetic fluid inclusions: American Mineralogist, v. 90, p. 1767-1775.

Anderson, G. M., 1975, Precipitation of Mississippi Valley-type ores: Economic Geology, v. 70, p. 937-942.

Anderson, G. M., 1991, Organic maturation and ore precipitation in southeast Missouri: Economic Geology, v. 86, p. 909-926.

Anderson, G. M., 2008, The mixing hypothesis and the origin of Mississippi Valley-type deposits: Economic Geology, v. 103, p. 1683-1690.

Anderson, G. M., and Garven, G., 1987, Sulfate-sulfide-carbonate associations in Mississippi Valley-type lead-zinc deposits: Economic Geology, v. 82, p. 482-488.

Anderson, G. M., and Thom, J., 2008, The role of thermochemical sulfate reduction in the origin of Mississippi Valley-type deposits. II. Carbonate-sulfide relationships: Geofluids, v. 8, p. 27-34.

Appold, M. S. and Garven, G., 1999, The hydrology of ore formation in the Southeast Missouri district: Numerical models of topography-driven fluid flow during the Ouachita orogeny: Economic Geology, v. 94, p. 913-936.

Appold, M. S. and Garven, G., 2000, Reactive flow models of ore formation in the southeast Missouri district: Economic Geology, v. 95, p. 1605-1626.

Appold, M. S., Numelin, T. J., Shepherd, T. J., and Chenery, S. R., 2004, Limits on the metal content of fluid inclusions in gangue minerals from the Viburnum Trend, southeast Missouri, determined by laser ablation ICPMS: Economic Geology, v. 99, p. 185-198.

Appold, M. S. and Nunn, J. A., 2005, Hydrology of the western Arkoma basin and Ozark platform during the Ouachita orogeny: implications for Mississippi Valley-type ore formation in the Tri-State Zn-Pb district: Geofluids, v. 5, p. 308-325.

Appold, M. S., and Wenz, Z. J., 2011, Composition of ore fluid inclusions from the Viburnum Trend, Southeast Missouri District, United States: Implications for transport and precipitation mechanisms: Economic Geology, v. 106, p. 55-78.

Becker, S. P., Eichhubl, P., Laubach, S. E., Reed, R. M., Lander, R. H., and Bodnar, R. J., 2010, A 48 m.y. history of fracture opening, temperature, and fluid pressure: Cretaceous Travis Peak Formation, East Texas basin: Geological Society of America Bulletin, v. 122, p. 1081-1093.

Bethke, C. M., and Marshak, S., 1990, Brine migrations across North America: the plate tectonics of groundwater: Annual Review of Earth and Planetary Sciences, v. 18, p. 228- 315.

Bickford, M . D., and Mose, D. G., 1975, Geochronology of Precambrian rocks in the St. Francois mountains, southeast Missouri: Geological Society of America Special Paper 165, 48 p.

Bodnar, R. J., 1993, Revised equation and table for determining the freezing point depression of H_2O−NaCl solutions: Geochimica et Cosmochimica Acta, v. 57, p. 683-684.

Brockie, D. C., Hare, E. H., Jr, and Dingess, P. R., 1968, The geology and ore deposits of the Tri-State district of Missouri, Kansas and Oklahoma, *in* Ridge, J. D., editor, Ore deposits of the United States, 1933–1967: The Graton- Sales Volume: New York, American Institute of Mining, Metallurgical and Petroleum Engineers, p. 400-430.

Burke, E. A. J., 2001, Raman microspectroscopy of fluid inclusions: Lithos, v. 55, p. 139-158.

Burstein, I. B., Shelton, K. L., Gregg, J. M., and Hagni, R. D., 1993, Complex, multiple ore fluids in the world class southeast Missouri Pb-Zn-Cu deposits: Sulfur isotope evidence *in*, Shelton, K. L., and Hagni, R. D., editors., Geology and geochemistry of Mississippi Valley-type ore deposits: Proceedings volume: Rolla, University of Missouri-Rolla Press, p. 1-16.

Coveney, R. M., Jr., Ragan, V. M., Brannon, J. C., 2000, Temporal benchmarks for modeling Phanerozoic flow of basinal brines and hydrocarbons in the southern mid-continent based on radiometrically dated calcite: Geology, v. 28, p. 795-798.

Crocetti, C. A., and Holland, H. D., 1989, Sulfur-lead isotope systematics and the composition of fluid inclusions in galena from the Viburnum Trend, Missouri: Economic Geology, v. 84, p. 2196-2216.

Deloule, E., Allegre, C., and Doe, B., 1986, Lead and sulfur isotope microstratigraphy in galena crystals in Mississippi Valley-type deposits: Economic Geology, v. 81, p. 1307-1321.

Duan, Z., and Mao, S., 2006, A thermodynamic model for calculating methane solubility, density and gas phase composition of methane-bearing aqueous fluids from 273 to 523 K and from 1 to 2000 bar: Geochimica et Cosmochimica Acta, v. 70, p. 3369-3386.

Duan, Z., Möller, N., and Weare, J. H., 1992, An equation of state for the CH_4-CO_2-H_2O system: I. Pure systems from 50 to 1000°C and from 0 to 8000 bar: Geochimica et Cosmochimica Acta, v. 56, p. 2605-2617.

Duan, Z., and Sun, R., 2003, An improved model calculation CO_2 solubility in pure water and aqueous NaCl solutions from 273 to 533 K and from 0 to 2000 bar. Chemical Geology, v. 193, p. 257-271.

Dubessy, J., Geisler, D., Kosztolanyi, C., Vernet, M., 1983, The determination of sulphate in fluid inclusions using the MOLE Raman microprobe. Application to a Keuper halite and geochemical consequences: Geochimica et Cosmochimica Acta, v. 47, p. 1-10.

Farr, M. R., 1989, Compositional zoning characteristics of late dolomite cement in the Cambrian Bonneterre Formation, Missouri: Implications for parent fluid migration pathways: Carbonates and Evaporites, v. 4, p. 177-194.

Faure, G., 1998, Principles and applications of geochemistry 2nd edition: New Jersey, Prentice Hall, 600 p.

Garven, G., Ge, S., Person, M. A., Sverjensky, D. A., 1993, Genesis of stratabound ore deposits in the mid-continent basins of North America. I. The role of regional groundwater flow: American Journal of Science, v. 293, p. 497-568.

Gerdemann, P. E., and Myers, H. E., 1972, Relationships of carbonate facies patterns to ore distribution and to ore genesis in the southeast Missouri lead district: Economic Geology, v. 67, p. 426-433.

Goldhaber, M. B., Church, S. E., Doe, B. R., Aleinikoff, J. N., Brannon, J. C., Podosek, F. A., Mosier, E. L., Taylor, C. D., and Gent, C. A, 1995, Lead and sulfur isotope investigation of Paleozoic sedimentary rocks from the southern midcontinent of the United States: Implications for paleohydrology and ore genesis of the southeast Missouri lead belts: Economic Geology, v. 90, p. 1875-1910.

Goldstein, R. H., and Reynolds, T. J., 1994, Systematics of fluid inclusions in diagenetic minerals: Society of Economic Geologists and Paleontologists Short Course 31, 199 p.

Gregg, J. M., 1985, Regional epigenetic dolomitization in the Bonneterre Dolomite (Cambrian), southeastern Missouri: Geology, v. 13, p. 503-506.

Gregg, J. M., and Gerdemann, P. E., 1989, Sedimentary facies, diagenesis, and ore distribution in the Bonneterre Formation (Cambrian), southeast Missouri, *in* Gregg, J.M., Palmer, J.R., and Kurtz, V.A., editors., Field guide to the Upper Cambrian of southeastern Missouri: Stratigraphy, sedimentology, and economic geology: Rolla, University of Missouri-Rolla, p. 43–55.

Haggerty, S. E., 1976, Opaque mineral oxides in terrestrial igneous rocks: Reviews in Mineralogy, v. 3, p. Hg101-Hg300.

Hagni, R. D., 1976, Tri-State ore deposits: the character of their host rocks and their genesis, *in* Wolf, K. H., editor, Handbook of strata-bound and stratiform ore deposits. II. Regional studies and specific deposits: Amsterdam, Elsevier, p. 457-494.

Hagni, R. D., 1982, The influence of original host rock character upon alteration and mineralization in the Tri-State District of Missouri, Kansas, and Oklahoma, U.S.A., *in* Amstutz, G. C., El-Goresy, A., Frenzel, G., Kluth, C., Moh, G., Wauschkuhn, A., and Zimmermann, R. A., editors, Ore genesis: The State of the Art: Berlin, Springer-Verlag, p. 97-107.

Hagni, R. D., 1983, Ore microscopy, paragenetic sequence, trace element content, and fluid inclusion studies of the coper-lead-zinc deposits of the southeast Missouri district, *in* Kisvarsanyi, G., Grant, S. K., Pratt, W. F., and Koenig, J. W., editors, International Conference on Mississippi Valley-type Lead-Zinc Deposits: Rolla, Missouri, University of Missouri-Rolla Press, Proceedings, p. 243-256.

Hagni, R. D., 1995, The southeast Missouri lead district: Society of Economic Geologists Guidebook Series, v. 22, p. 44-78.

Hanor, J. S., 1994, Origin of saline fluids in sedimentary basins, in Parnell, J., editor, Geofluids: Origin, migration and evolution of fluids in sedimentary basins: Geological Society Special Publication 78, p. 151-174.

Heinrich, C. A., Pettke, T., Halter, W. E., Aigner-Torres, M., Audetat, A., Günther, D., Hattendorf, B., Bleiner, D., Guillong, M., and Horn, I., 2003, Quantitative multi element analysis of minerals, fluid and melt inclusions by laser-ablation inductively-coupled plasma mass-spectrometry: Geochimica et Cosmochimica Acta, v. 67, p. 3473-3496.

Hofstra, A. H., Leach, D. L., Landis, G. P., Viets, J. G., Rowan, E. L., and Plumlee, G. S., 1989, Fluid inclusion gas geochemistry as a monitor of ore depositional processes in Mississippi Valley-type deposits of the Ozark region, U.S. Geological Survey Circular 1043, p. 11-12.

Imes, J. L., 1990, Major geohydrologic units and adjacent to the Ozark Plateaus province, Missouri, Arkansas, Kansas, and Oklahoma: U.S. Geological Survey Hydrologic Investigations Atlas HA-711-A, scale 1:750,000.

Imes, J. L., and Smith, B. J., 1990, Areal extent, stratigraphic relation, and geohydrologic properties of regional geohydrologic units in southern Missouri: U.S. Geological Survey Hydrologic Investigations Atlas HA-711-I.

Jackson, S. A., and Beales, F. W., 1967, An aspect of sedimentary basin evolution: the concentration of Mississippi Valley-type ores during the late stages of diagenesis: Bulletin of Canadian Petroleum Geology, v. 15, p. 383-433.

Johnson, J. W., Oelkers, E. H., and Helgeson, H. C., 1992, SUPCRT92: A software package for calculating the standard molal thermodynamic properties of minerals, gases, aqueous species, and reactions from 1 to 5000 bar and 0° to 1000°C: Computers and Geosciences, v. 18, p. 899-947.

Kaiser, C. J., Kelly, W. C., Wagner, R. J., and Shanks III, W. C., 1987, Geologic and geochemical controls of mineralization in the southeast Missouri barite district: Economic Geology, v. 82, p. 719-734.

Kendrick, M. A., Burgess, R., Leach, D., and Pattrick, R. A. D., 2002, Hydrothermal fluid origins in Mississippi Valley-type ore districts: Combined noble gas (He, Ar, Kr) and halogen (Cl, Br, I) analysis of fluid inclusions from the Illinois-Kentucky fluorspar district, Viburnum Trend, and Tri-State districts, mid-continent United States: Economic Geology, v. 97, p. 453-470.

Leach, D. L., 1973, Possible relationship of Pb-Zn mineralization in the Ozarks to Ouachita Orogeny: Geological Society of America Abstracts with Programs, v. 5, no. 3, p. 269.

Leach, D. L., 1979, Temperature and salinity of the fluids responsible for minor occurrences of sphalerite in the Ozark region of Missouri: Economic Geology, v. 74, p. 931-937.

Leach, D. L., 1980, Nature of mineralizing fluids in the barite deposits of central and southeast Missouri: Economic Geology, v. 75, p. 1168-1180.

Leach, D. L., 1994, Genesis of the Ozark Mississippi Valley-type metallogenic province, Missouri, Arkansas, Kansas and Oklahoma, USA, *in* Fontboté, L., and Boni, M., editors,Sediment-hosted Zn-Pb ores: Berlin, Springer-Verlag, p. 104-138.

Leach, D. L., Nelson, R. C., and Williams, D., 1975, Fluid inclusion studies in the northern Arkansas zinc district: Economic Geology, v. 70, p. 1084-1091.

Leach, D. L. and Rowan, E. L., 1986, Genetic link between Ouachita fold belt tectonism and theMississippi Valley-type lead-zinc deposits of the Ozarks: Geology, v. 14, p. 931-935.

Leventhal, J. S., 1990, Organic matter and thermochemical sulfate reduction in the Viburnum trend, southeast Missouri: Economic Geology, v. 85, p. 622-632.

Lin, F., Bodnar, R. J., and Becker, S. P., 2007, Experimental determination of the Raman CH_4 symmetric stretching (v1) band position from 1–650 bar and 0.3–22°C: Application to fluid inclusion studies: Geochimica et Cosmochimica Acta, v. 71, p. 3746-3756.

Long, K. R., Kelly, W. C., Ohle, E. L., and Lohmann K. C., 1986, Ground preparation and zinc mineralization in bedded and breccia ores of the Monte Cristo mine, northern Arkansas: Economic Geology, v. 81, p. 809-830.

McKnight, E. T., 1935, Zinc and lead deposits of northern Arkansas: U.S. Geological Survey Bulletin 853, 311 p.

McKnight, E. T., and Fischer, R. P., 1970, Geology and ore deposits of the Picher Field, Oklahoma and Kansas: U.S. Geological Survey Professional Paper 588, 165 p.

Mutchler, S. R., Fedele, L., and Bodnar, R. J., 2008, Appendix A5: Analysis management system (AMS) for reduction of laser ablation ICP-MS data: Mineralogical Association of Canada Short Course 40, p. 318-327.

Newhouse, W. H., 1933, Temperature of formation of the Mississippi Valley lead-zinc deposits: Economic Geology, v. 28, p. 744-750.

Ohle, E. L., and Gerdemann, P. E., 1989, Recent exploration history in southeast Missouri: Society of Economic Geologists Guidebook Series, v. 5, p. 1-11.

Pan, H., Symons, D. T. A., and Sangster, D. F., 1990, Paleomagnetism of the Mississippi Valley type ores and host rocks in the northern Arkansas and Tri-State districts: Canadian Journal of Earth Sciences, v. 27, p. 923-931.

Perry, W. J., Jr., 1995, Arkoma Basin Province (062), *in* Gautier, D. L., Dolton, G.L., Takahashi, K.I., and Varnes, K.L., editors., 1995 National assessment of United States oil and gas resources--Results, methodology, and supporting data: U.S. Geological Survey Digital Data Series DDS-30, Release 2, one CD-ROM.

Plumlee, G. S., Leach, D. L., Hofstra, A. H., Landis, G. P., Rowan, E. L., and Viets, J. G., 1994, Chemical reaction path modeling of ore deposition in Mississippi Valley type deposits of the Ozark region, U.S. midcontinent: Economic Geology, v. 89, p. 1361-1383.

Ragan, V. M., 1994, Mineralogy and fluid inclusion geochemistry of Tri-State–type mineralization in eastern Kansas: Economic Geology, v. 89, p. 1411-1418.

Ragan, V. M., Coveney, R. M., Jr., and Brannon, J. C., 1996, Migration paths for fluids and the northern limits of the Tri-State district from fluid inclusions and radiogenic isotopes, *in* Sangster, D.F., editor, Carbonate-hosted lead-zinc deposits: Society of Economic Geologists Special Publication 4, p. 419-431.

Rickman, D. L., 1981, A thermochemical study of the Milliken mine, New Lead Belt, Missouri: Ph.D. thesis, University of Missouri-Rolla, Rolla, 310 p.

Roedder, E., 1963, Studies of fluid inclusions II: Freezing data and their interpretations: Economic Geology, v. 58, 167-211.

Roedder, E., 1967, Fluid inclusions as samples of ore fluids, *in* Barnes, H. L., editor, Geochemistry of Hydrothermal Ore Deposits: New York, Holt, Rinehart, and Winston, p. 515-574.

Roedder, E., 1977, Fluid inclusion studies of ore deposits in the Viburnum Trend, southeast Missouri: Economic Geology, v. 72, p. 474-479.

Rosasco, G. J., and Roedder, E., 1979, Application of a new Raman microprobe spectrometer to nondestructive analysis of sulfate and other ions in individual phases in fluid inclusions in minerals: Geochimica et Cosmochimica Acta, v. 43, p. 1907-1915.

Rowan, E. L., 1986, Cathodoluminescent zonation in hydrothermal dolomite cements: Relationship to Mississippi Valley-type Pb-Zn mineralization in southern Missouri and northern Arkansas, *in* Hagni, R. D., editor, Process mineralogy IV: Warrendale, Pennsylvania, Metallurgical Society, p. 69-87.

Rowan, E. L., and Leach, D. L., 1989, Constraints from fluid inclusions on sulfide precipitation mechanisms and ore fluid migration in the Viburnum Trend lead district, Missouri: Economic Geology, v. 84, p. 1948-1965.

Schmidt, R. A., 1962, Temperatures of mineral formation in the Miami-Picher district as indicated by liquid inclusions: Economic Geology, v. 57, p. 1-20.

Shelton, K. L., Bauer, R. M., and Gregg, J. M., 1992, Fluid inclusion studies of regionally extensive epigenetic dolomites, Bonneterre Dolomite (Cambrian), southeast Missouri: Evidence of multiple fluids during dolomitization and lead-zinc mineralization: Geological Society of America Bulletin, v. 104, p. 675-683.

Shelton, K. L., Burstein, I. B., Hagni, R. D., Vierrether, C. B., Grant, S. K., Hennigh, Q. T., Bradley, M. F., and Brandom, R. T., 1995, Sulfur isotope evidence for penetration of MVT fluids into igneous basement rocks, southeast Missouri, U.S.A.: Mineralium Deposita, v. 30, p. 339-350.

Shelton, K. L., Gregg, J. M., and Johnson, A. W., 2009, Replacement dolomites and ore sulfides as recorders of multiple fluids and fluid sources in the Southeast Missouri Mississippi Valley-type District: Halogen-$^{87}Sr/^{86}Sr$-$\delta^{18}O$-$\delta^{34}S$ systematics in the Bonneterre Dolomite: Economic Geology, v. 104, pp. 733-748.

Siebenthal, C. E., 1916, Origin of the zinc and lead deposits of the Joplin region, Missouri, Kansas, Oklahoma: U.S. Geological Survey Bulletin 606, 283 p.

Snyder, F. G., and Gerdemann, P. E., 1968, Geology of the southeast Missouri lead district, *in* Ridge, J. D., editor, Ore deposits of the United States, 1933−1967 (Graton-Sales volume): New York, American Institute of Mining, Metallurgical, and Petroleum Engineers, p. 327-358.

Speight, J. G., 2005, Handbook of coal analysis: New Jersey, John Wiley & Sons, Inc., 222 p.

Stoffell, B., Appold, M. S., Wilkinson, J. J., McClean, N. A., and Jeffries, T. E., 2008, Geochemistry and evolution of Mississippi Valley-type mineralizing brines from the Tri- State and northern Arkansas districts determined by LA-ICP-MS microanalysis of fluid inclusions: Economic Geology, v. 103, p. 1411-1435.

Sverjensky, D. A., Rye, D. M., and Doe, B. R., 1979, The lead and sulfur isotopic compositions of galena from a Mississippi Valley-type deposit in the New Lead Belt, southeast Missouri: Economic Geology, v. 74, p. 149-153.

Sverjensky, D. A., 1981, The origin of a Mississippi Valley-type deposit in the Viburnum Trend, southeast Missouri: Economic Geology, v. 76, p. 1848-1872.

Sverjensky, D. A., 1986, Genesis of Mississippi Valley-type lead-zinc deposits: Annual Review in Earth and Planetary Sciences, v. 14, p. 177−199.

Symons, D. T. A., and Sangster, D. F., 1991, Paleomagnetic age of the central Missouri barite deposits and its genetic significance: Economic Geology, v. 86, p. 1-12.

Symons, D. T. A., Pannalal, S. J., Coveney, R. M., Jr., and Sangster, D. F., 2005, Paleomagnetism of late Paleozoic strata and mineralization in the Tri-State lead zinc ore district: Economic Geology, v. 100, p. 295-309.

Viets, J. G., Hopkins, R. T., and Miller, B. M., 1992, Variations in minor and trace metals in sphalerite from Mississippi Valley-type deposits of the Ozark region: Genetic implications: Economic Geology, v. 87, p. 1897-1905.

Viets, J. G., Hostra, A. F., and Emsbo, P., 1996, Solute compositions of fluid inclusions in sphalerite from North American and European Mississippi Valley-type ore deposits: Ore fluids derived from evaporated seawater: Society of Economic Geologists Special Publication 4, p. 465-482.

Viets, J. G., and Leach, D. L., 1990, Genetic implications of regional and temporal trends in ore fluid geochemistry of Mississippi Valley-type deposits in the Ozark region: Economic Geology, v. 85, p. 842-861.

Voss, R. L., and Hagni, R. D., 1985, The application of cathodoluminescence microscopy to the study of sparry dolomite from the Viburnum Trend, southeast Missouri, *in* Hausen, D. M., and Kopp, O. C., editors, Mineralogy–applications to the Minerals Industry: New York, American Institute of Mining, Metallurgical, and Petroleum Engineers, Inc., p. 51-68.

Voss, R. L., Hagni, R. D., and Gregg, J. M., 1989, Sequential deposition of zoned dolomite and its relationship to sulfide mineral paragenetic sequence in the Viburnum Trend, southeast Missouri: Carbonates and Evaporites, v. 4, p. 195-209.

Wilkinson, J. J., Stoffell, B., Wilkinson, C. C., Jeffries, T. E., Appold, M. S., 2009, Anomalously metal-rich fluids from hydrothermal ore deposits: Science, v. 323, p. 764-767.

Wisniowiecki, M. J., Van der Voo, R., McCabe, C., and Kelly, W. C., 1983, A Pennsylvanian paleomagnetic pole from the mineralized Late Cambrian Bonneterre Formation, southeast Missouri: Journal of Geophysical Research, v. 88, p. 6540-6548.

Yardley, B. W. D., 2005, 100th anniversary special paper: Metal concentrations in crustal fluids and their relationship to ore formation: Economic Geology, v. 100, p. 613-632.

Zacharias, J., and Wilkinson, J., 2007, ExLAM 2000: Excel VBA application for processing of transient signals from laser ablation (LA-ICP-MS) of fluid inclusions and solid phases [abs.]: ECROFI-XIX Biennial Conference on European Current Research on Fluid Inclusions, Bern, Switzerland, Abstracts.

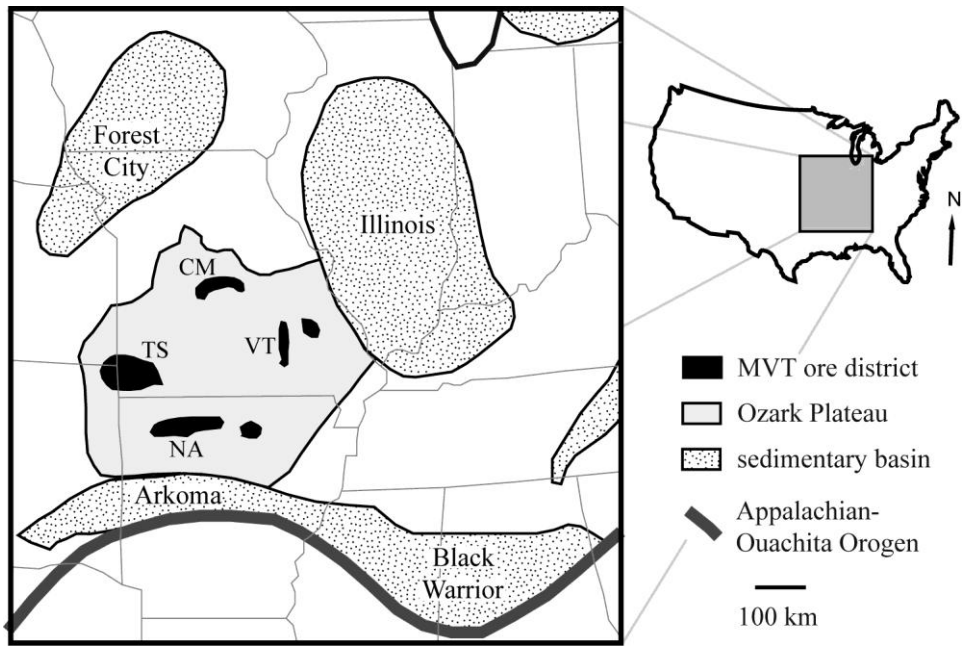

Fig. 2.1 Regional map of the Ozark Plateau and sedimentary basins showing the location of the Ozark MVT deposits (modified after Appold and Garven, 1999). Abbreviations: CM- Central Missouri district, NA- Northern Arkansas district, TS- Tri-State district, VT- Viburnum Trend.

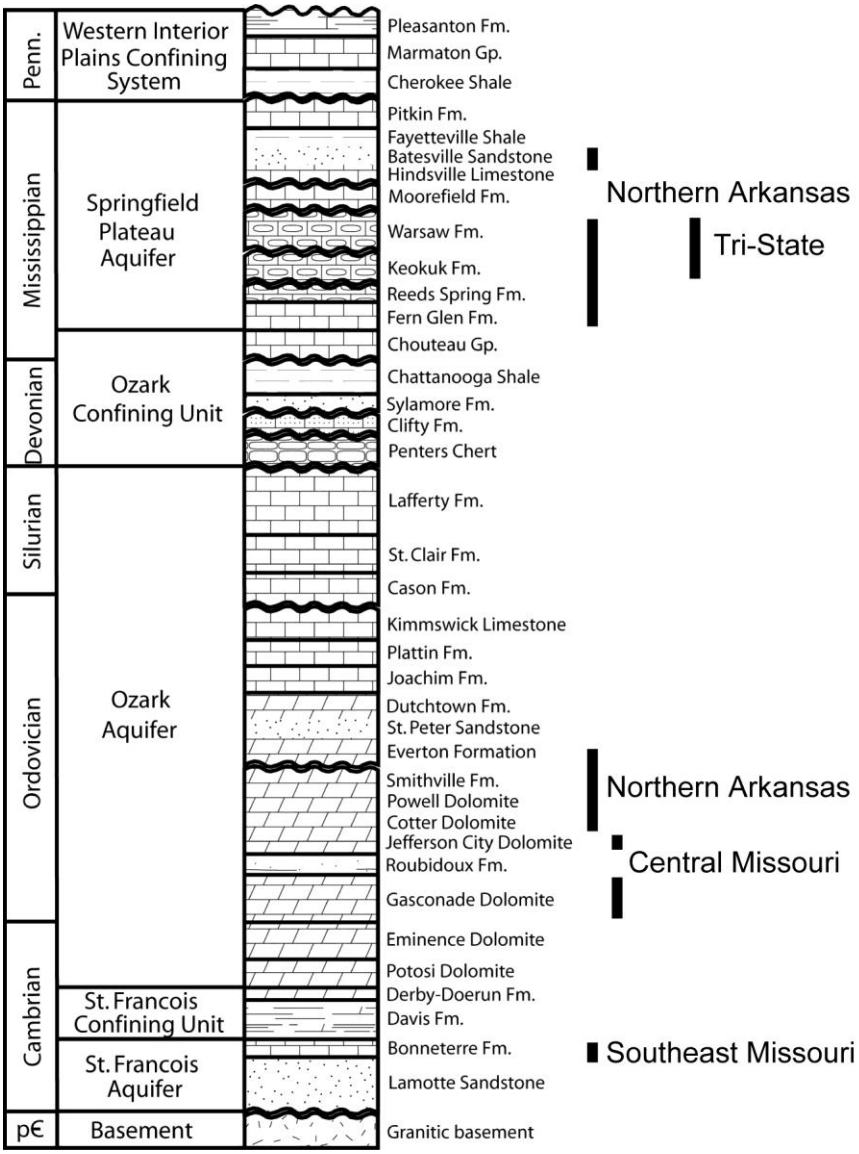

Fig. 2.2 Generalized stratigraphic section for the Ozark Plateau. Stratigraphic locations of the ore deposits are indicated by black bars (from Appold and Garven, 1999; data assembled from Brockie and others, 1968; Leach and others, 1975; Thacker and Anderson, 1977; Imes, 1990 and Imes and Smith, 1990).

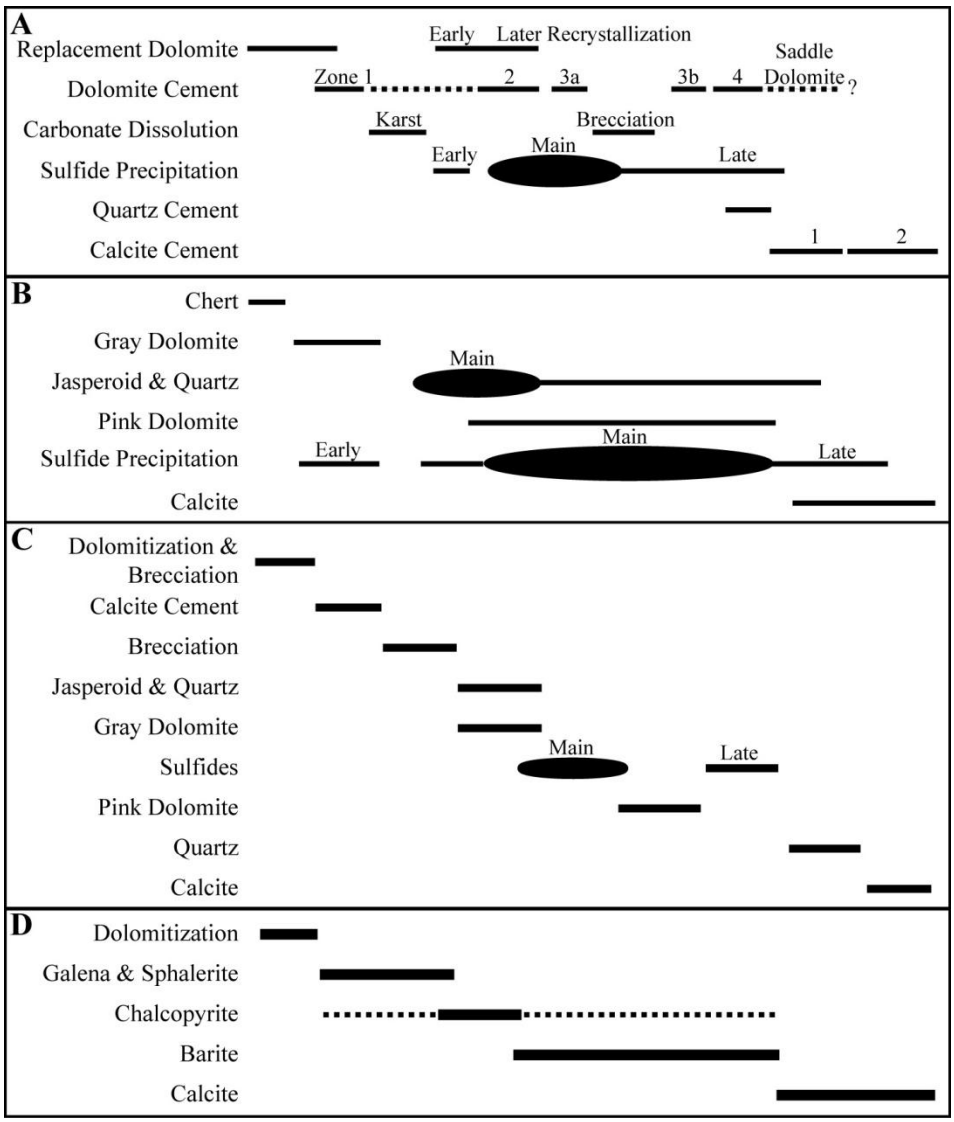

Fig. 2.3 Part A- Simplified paragenesis of the Southeast Missouri district (after Voss and others, 1989). Part B- Synthesized paragenesis of the Tri-State district (incorporating data from Hagni and Grawe, 1964; Brockie and others, 1968 and McKnight and Fischer, 1970). Part C- Synthesized paragenesis of the Northern Arkansas district (incorporating data from McKnight, 1935 and Long and others, 1986). Part D- Synthesized paragenesis for the Central Missouri district (incorporating data from Leach, 1980).

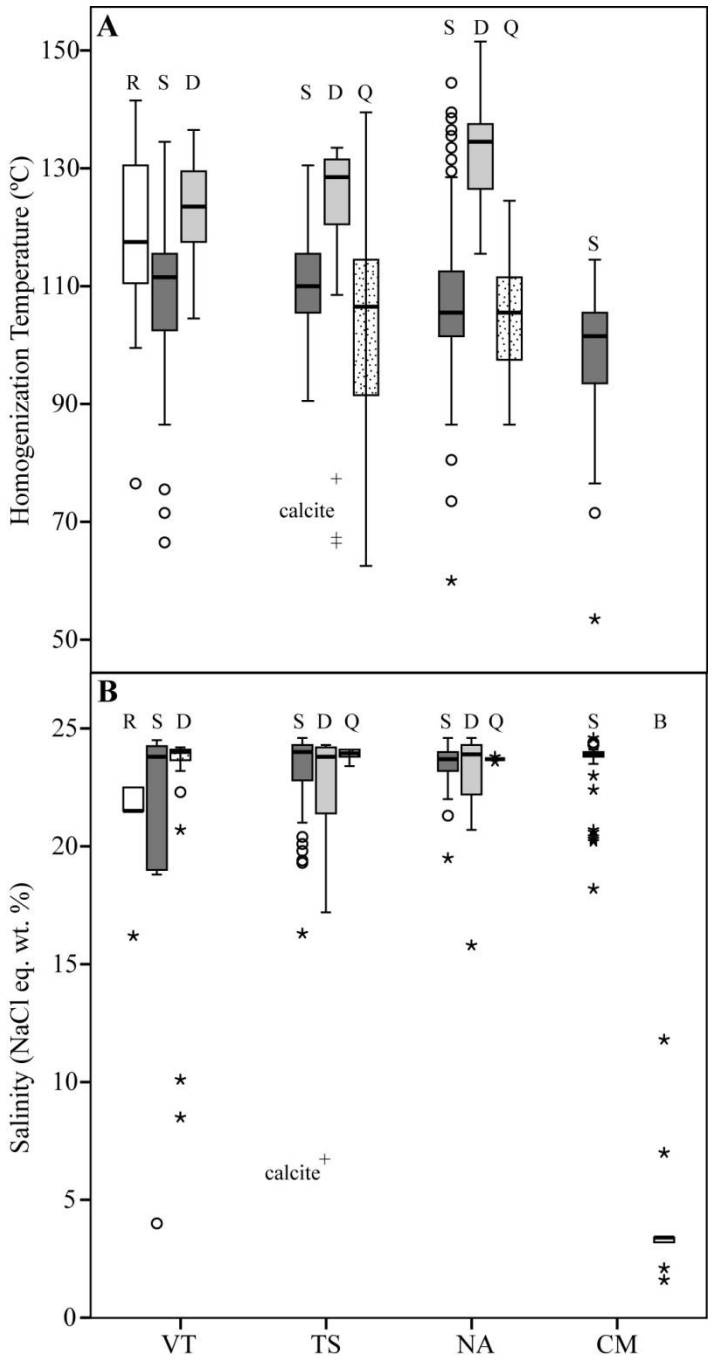

Fig. 2.4 Part A- Box and whisker plot of fluid inclusion T_h values for each district by mineral. Part B- Box and whisker plot of salinity for each district by mineral. Each box encompasses the inter-quartile range (the 25th to 75th percentile). The horizontal line in each box represents the median. Whiskers represent the highest and lowest values within a factor of 1.5 outside the inter-quartile range. Open circles and stars beyond the whiskers represent outliers that exceed the inter-quartile range by a factor of 1.5 to 3and greater than 3, respectively. Axis abbreviations same as in fig. 1. Mineral type abbreviations as follows: B- barite, D- dolomite, Q- quartz, R- replacement dolomite, S- sphalerite, +- calcite.

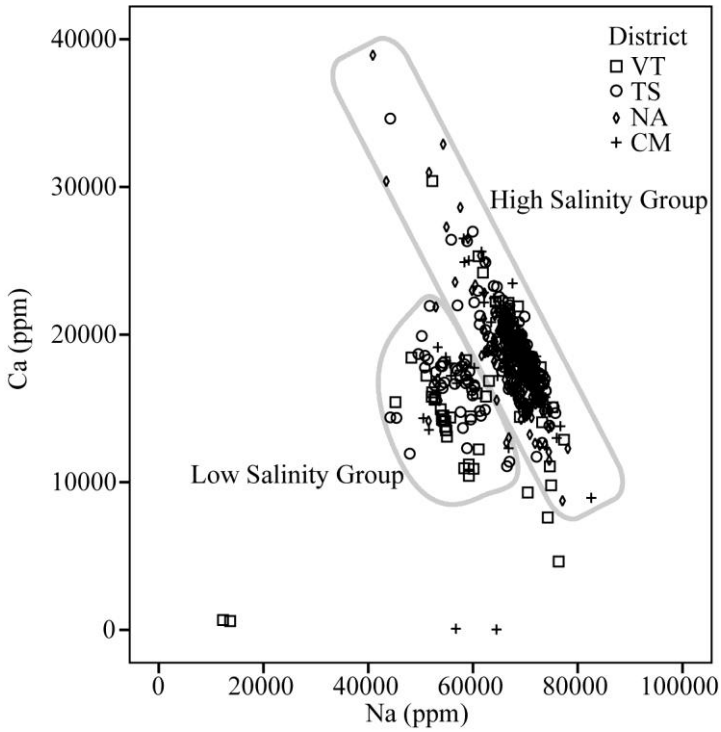

Fig. 2.5 Scatter plot of all sphalerite-hosted fluid inclusion data illustrating the existence of two salinity groups. The high salinity group has a salinity greater than 22 NaCl eq. wt% and a negative correlation between Ca and Na. The low salinity mode has a salinity less than 22 NaCl eq. wt% and exhibits little correlation between Ca and Na.

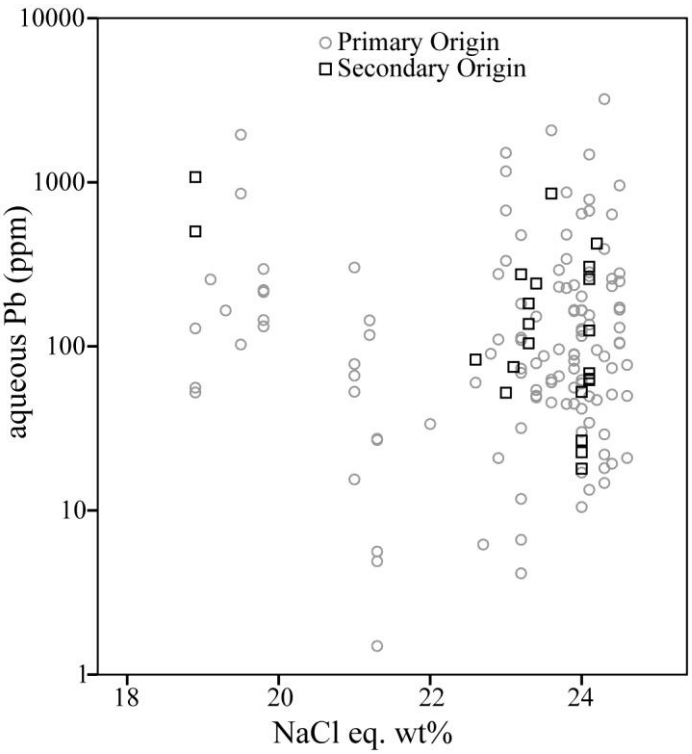

Fig. 2.6 Scatter plot of detectable aqueous Pb concentrations of sphalerite-hosted fluid inclusions. High Pb concentrations exist in both high and low salinity fluid inclusions, as well as in primary and secondary fluid inclusions.

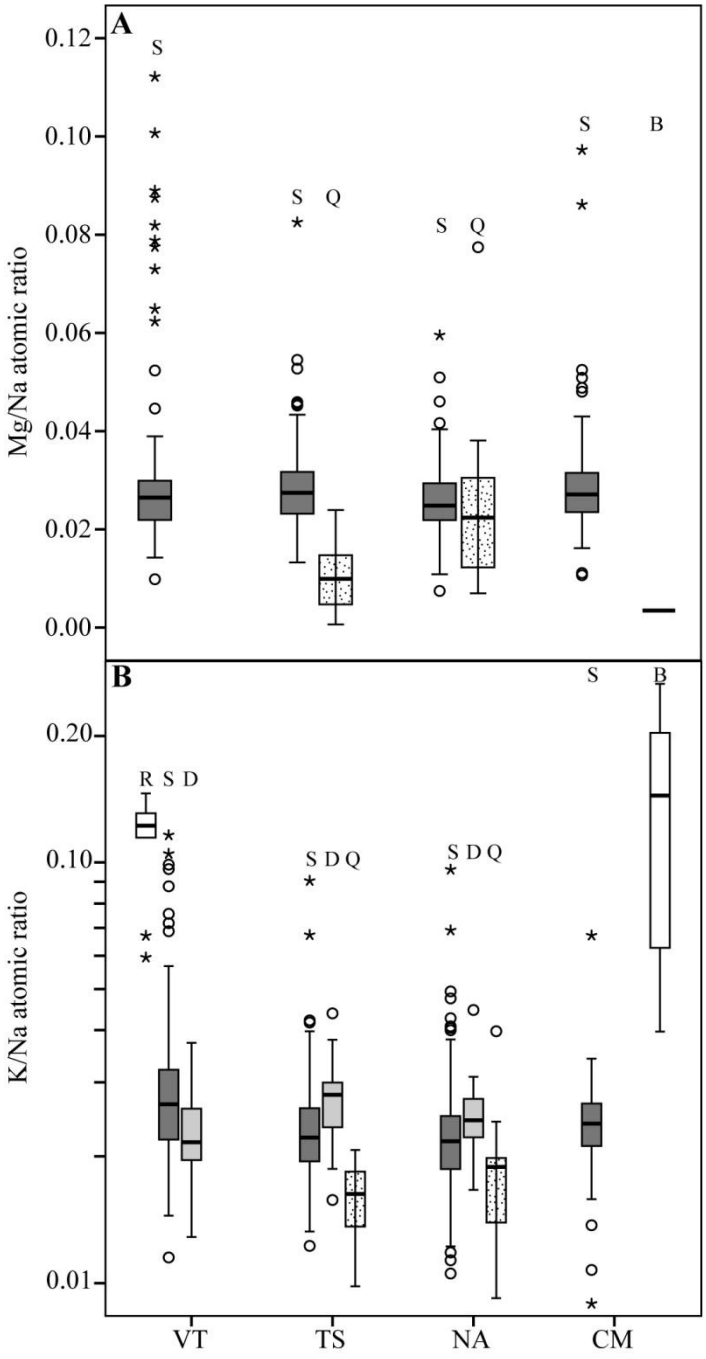

Fig. 2.7 Part A- Mg/Na atomic ratios of fluid inclusions for each district by mineral. Part B- Log K/Na atomic ratios of fluid inclusions for each district by mineral. Abbreviations same as in figs. 1 and 4.

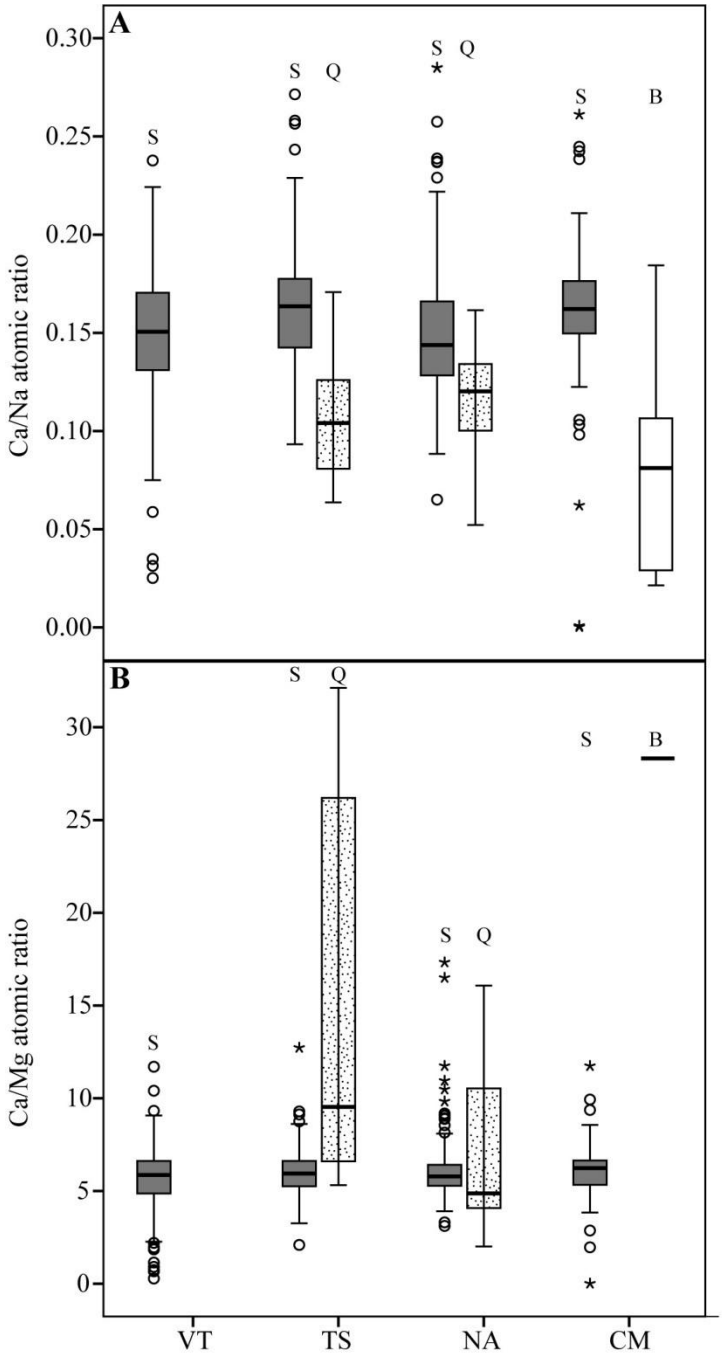

Fig. 2.8 Part A- Ca/Na atomic ratios of fluid inclusions for each district by mineral. Part B- Ca/Mg atomic ratios of fluid inclusions for each district by mineral. Abbreviations same as in figs. 1 and 4.

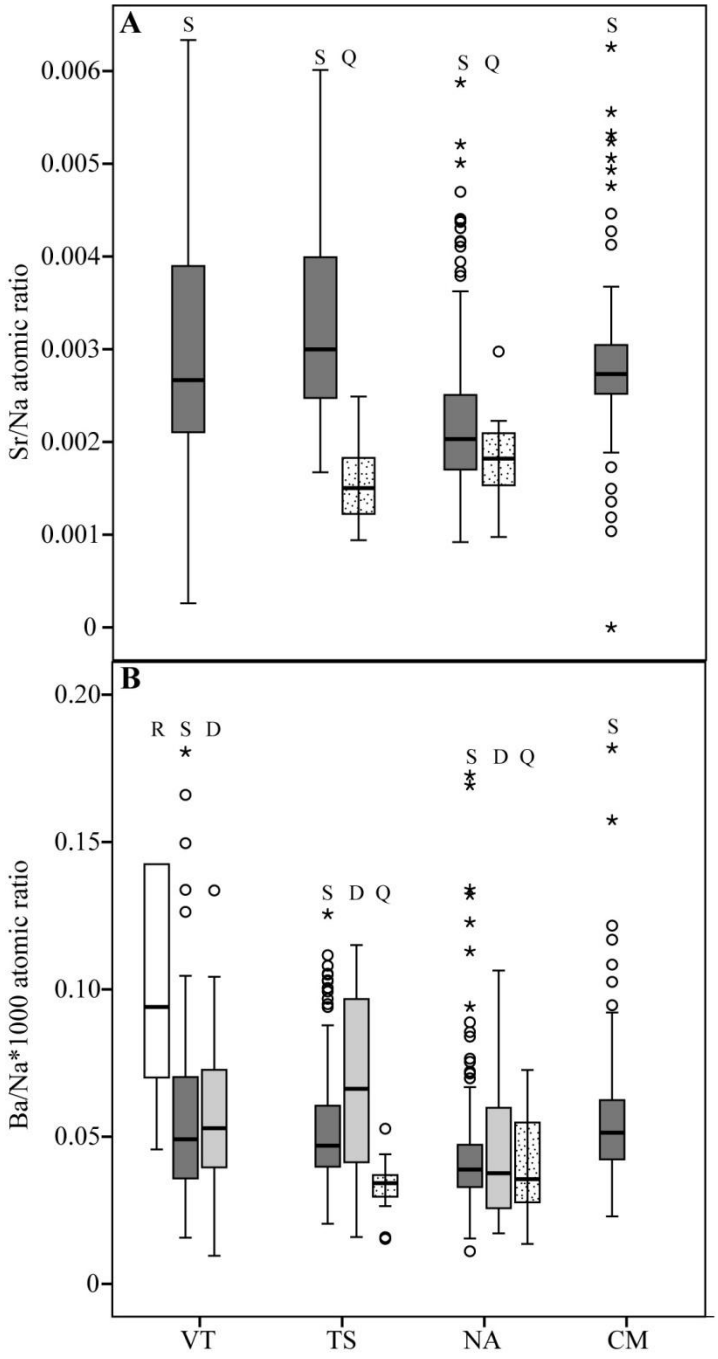

Fig. 2.9 Part A- Sr/Na atomic ratios of fluid inclusions for each district by mineral. Part B- Ba/Na atomic ratios of fluid inclusions for each district by mineral. Abbreviations same as in figs. 1 and 4.

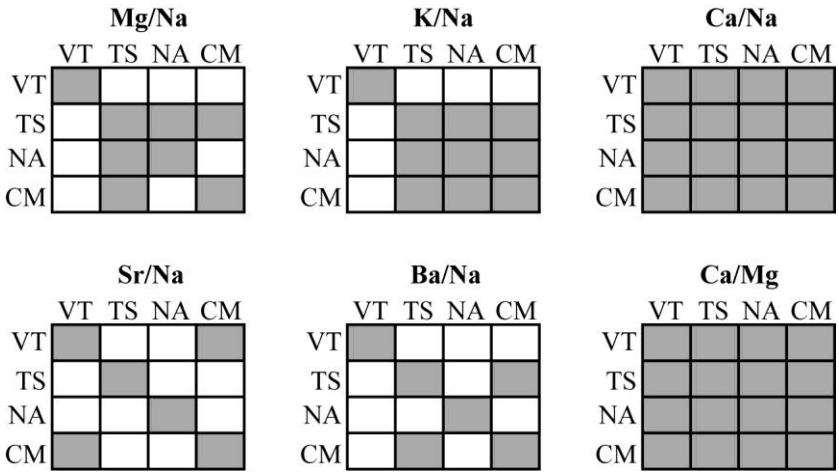

Fig. 2.10 Post Hoc results for a Fishers Least Significant Difference statistical test on atomic cation ratios for the high salinity group of sphalerite-hosted fluid inclusions among the districts. Shaded boxes indicate that the populations of cation ratio values of two districts are similar at the 95% confidence interval. Abbreviations same as in fig. 1.

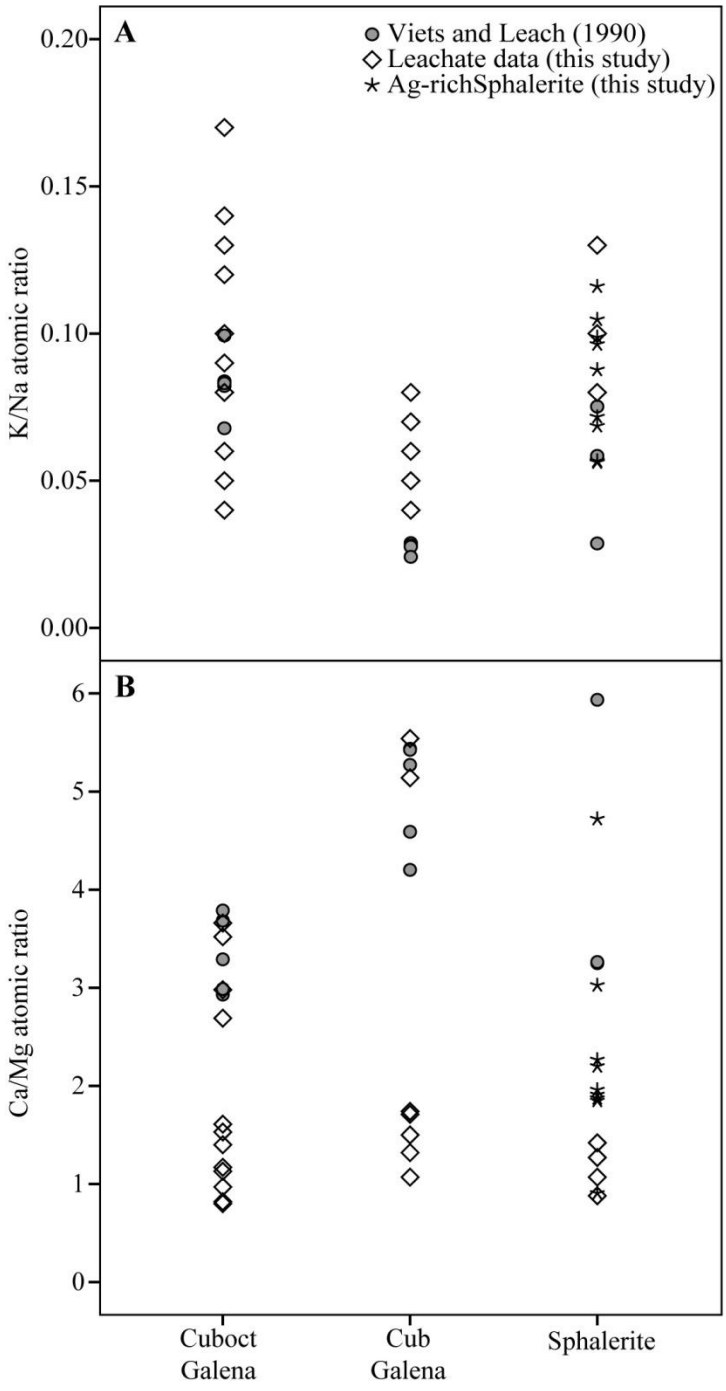

Fig. 2.11 Atomic ratio plots for leachate and LA-ICP-MS analysis of fluid inclusions hosted in cuboctahedral and cubic galena and main stage sphalerite from Viets and Leach (1990) and the present study. In part A, a substantial overlap exists for the K/Na atomic ratio among ore mineral fluids. Cubic galena has the lowest range, cuboctahedral has the highest, and sphalerite spans most of the ranges of both galena types. In part B, the cubic galena fluids have the highest Ca/Mg atomic ratios for the galena types, while the sphalerite fluids encompass the ranges of both cuboctahedral and cubic galena.

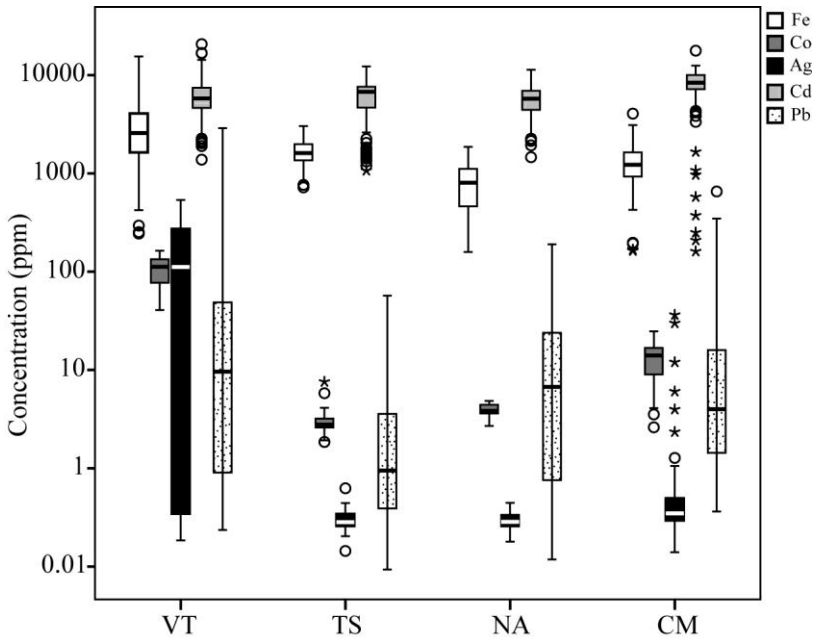

Fig. 2.12 Boxplot of trace element concentrations in sphalerite by district. Abbreviations same as in fig. 1.

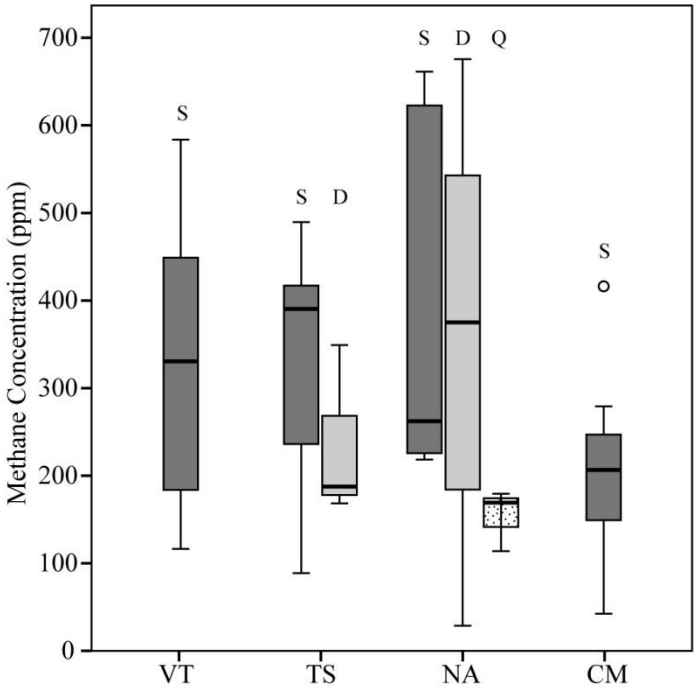

Fig. 2.13 Boxplot of CH_4 concentrations in fluid inclusions from each mineral by district. Abbreviations same as in fig. 1.

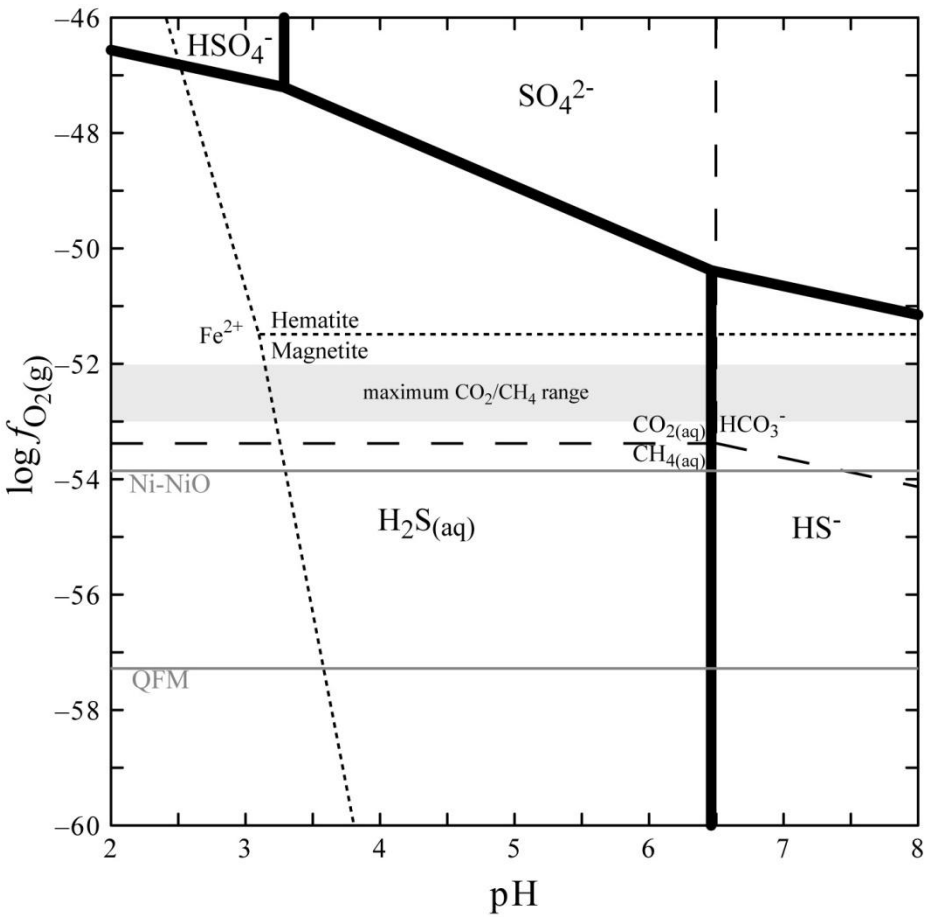

Fig. 2.14 Log f_{O_2} vs. pH plot illustrating the predominance fields of aqueous carbon and sulfur species and the stability fields of hematite and magnetite, calculated at 120° C and 100 bars pressure. Broad gray horizontal bar depicts the maximum possible oxidation state using calculated CH_4 concentrations and CO_2 saturation determined from Duan and Sun (2003). Figure constructed using Geochemists Workbench. Ni-NiO and QFM oxidation buffers calculated under the same temperature and pressure conditions using the SUPCRT92 program (Johnson and others, 1992).

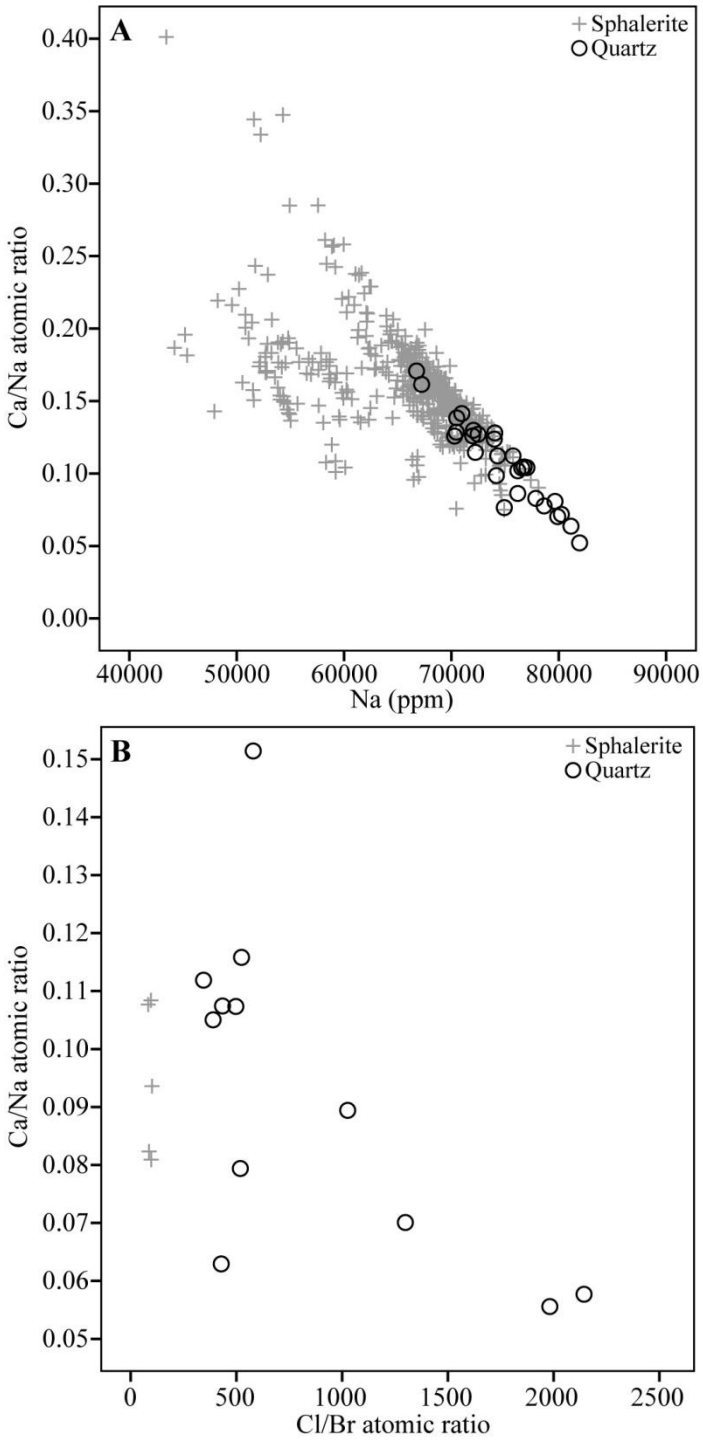

Fig. 2.15 Part A- Ca/Na ratio and Na concentration plot for illustrating an apparent mixing line between two end member fluids represented as high and low Ca/Na ratio fluids. The quartz-hosted fluid inclusions predominantly capture the low Ca/Na end member fluid. Part B- Ca/Na and Cl/Br plot of Tri-State and Northern Arkansas sphalerite- and quartz-hosted fluid inclusions illustrating that the quartz-hosted inclusions have lower Ca/Na ratios and higher Cl/Br ratios (data from Stoffell and others, 2008).

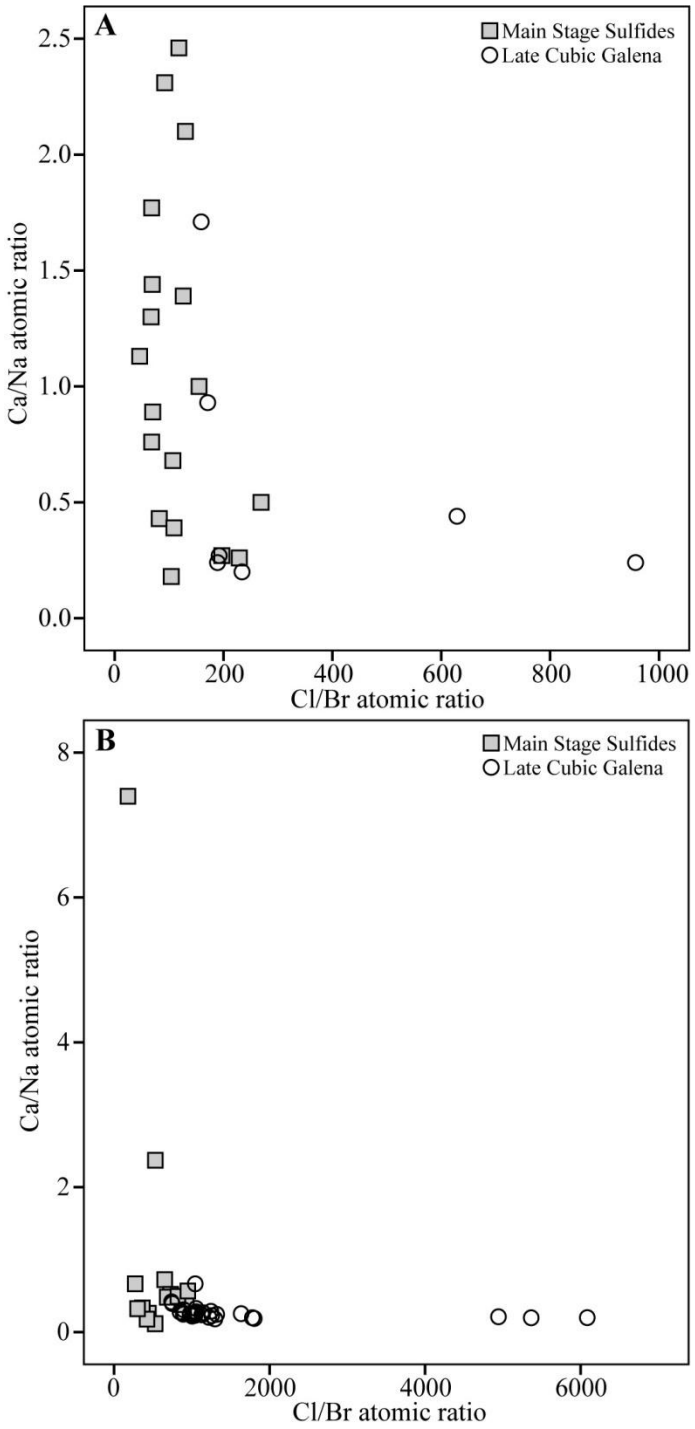

Fig. 2.16 Part A- Ca/Na and Cl/Br ratio plots of main and late stage sulfide minerals illustrating late stage sulfide mineralization has lower Ca/Na ratios (this study) and higher Cl/Br ratios (data from Shelton and others, 2009). Part B- same as in Part A with expanded axis ranges (data from Crocetti and Holland, 1989).

Table 2.1 ANOVA test results for high salinity group sphalerite-hosted fluid inclusions.

Atomic Ratio		SS	df	MS	F	F_{crit}	Sig
Mg/Na	between groups	2.00E-03	3	1.00E-03	5.86	2.63	0.001
	within groups	4.40E-02	400	1.10E-04	na	na	na
K/Na	between groups	6.00E-03	3	2.00E-03	17.78	2.63	7.91E-11
	within groups	4.50E-02	385	1.16E-04	na	na	na
Ca/Na	between groups	6.00E-03	3	2.00E-03	1.14	2.63	0.333
	within groups	7.02E-01	414	2.00E-03	na	na	na
Sr/Na	between groups	3.76E-05	3	1.25E-05	25.22	2.63	5.23E-15
	within groups	2.06E-04	415	4.97E-07	na	na	na
Ba/Na	between groups	2.05E-08	3	6.83E-09	8.50	2.63	1.74E-05
	within groups	3.23E-07	402	8.04E-10	na	na	na
Ca/Mg	between groups	5.01E+00	3	1.67E+00	0.60	2.63	0.617
	within groups	1.12E+03	399	2.80E+00	na	na	na

Based on a α=0.05 (95% confidence interval). Variation of atomic ratio among districts is significant for a Sig < 0.05. Abbreviations: SS= sum of squares, df= degrees of freedom, MS= mean square (variance), F= Fischer's F statistic, F= Fischer's F-critical statistic, Sig= significance (or p-value)

Table 2.2 Trace element concentrations in sphalerite and barite.

Location		Fe (ppm)	Co (ppm)	Zn (ppm)	Ag (ppm)	Cd (ppm)	Pb (ppm)
District		Sphalerite Matrix					
Viburnum Trend	average=	3.0E+03	1.1E+02	6.6E+05	1.6E+02	6.4E+03	9.1E+01
	std dev=	2.2E+03	3.5E+01	4.2E+03	1.8E+02	3.5E+03	3.5E+02
	n=	89	42	89	38	89	89
Northern Arkansas	average=	8.5E+02	3.9E+00	6.6E+05	2.9E-01	5.9E+03	2.3E+01
	std dev=	4.2E+02	5.7E-01	2.0E+03	7.1E-02	2.1E+03	3.8E+01
	n=	207	14	207	15	207	206
Tri-State	average=	1.7E+03	3.3E+00	6.6E+05	3.1E-01	6.2E+03	6.8E+00
	std dev=	4.9E+02	1.5E+00	2.2E+03	1.1E-01	2.4E+03	1.3E+01
	n=	167	15	167	15	167	161
Central Missouri	average=	1.4E+03	1.3E+01	6.6E+05	1.4E+00	8.1E+03	2.4E+01
	std dev=	6.6E+02	5.3E+00	2.7E+03	5.0E+00	3.0E+03	7.2E+01
	n=	121	113	121	91	121	120
		Fe (ppm)	Zn (ppm)	Sr (ppm)	Ba (ppm)	Pb (ppm)	
Mine		Barite Matrix					
Brown	average=	6.3E-01	8.3E+01	9.3E+03	5.8E+05	1.5E+00	
	std dev=	na	1.9E+00	2.3E+03	2.3E+03	na	
	n=	1	3	3	3	1	
Ford	average=	-	6.0E+01	3.0E+03	5.8E+05	-	
	std dev=	na	5.0E+01	2.6E+03	2.4E+02	na	
	n=	na	2	2	2	0	
Goller	average=	-	8.5E+01	5.8E+03	5.8E+05	-	
	std dev=	na	2.9E+00	2.9E+03	2.9E+03	na	
	n=	na	6	6	6	0	
Lee	average=	-	9.8E+01	5.7E+03	5.8E+05	-	
	std dev=	na	1.8E+01	6.8E+02	4.4E+03	na	
	n=	na	3	3	3	na	
Tiff	average=	1.3E+00	1.8E+02	3.5E+03	5.8E+05	3.3E+00	
	std dev=	5.0E-02	3.3E+02	3.0E+03	2.9E+03	5.9E+00	
	n=	2	10	10	10	6	

Abbreviations as follows: - = below detection limit, na = not applicable.

Table 2.3 Fluid inclusion methane concentrations and mineralization depth calculations.

Sample ID	mineral	P_{CH4} (bars)	position	ρ_{CH4} (g/cm^3)	CH_4 (ppm)	P_T (bars)	depth (m)
Viburnum Trend							
MAG13_1_1_6	sphalerite	4.8	2917.52	3.16E-03	181	27	275
MAG13_1a_1_1_6	sphalerite	4.5	2917.53	2.97E-03	184	31	319
MAG13_1b_1_1_6	sphalerite	8.5	2917.46	5.63E-03	339	60	609
MAG13_2_1_6	sphalerite	5.6	2917.51	3.73E-03	207	31	318
MAG13_2a_1_1_6	sphalerite	12.9	2917.38	8.64E-03	474	76	778
MAG13_2a_2_1_6	sphalerite	12.1	2917.4	8.08E-03	449	71	728
MAG13_5_1_6	sphalerite	9.0	2917.45	6.01E-03	331	51	521
WF2_1a_1_1_6	sphalerite	15.1	2917.34	1.01E-02	584	114	1166
WF2_3_1_1_6	sphalerite	3.6	2917.55	2.39E-03	116	22	223
Tri-State							
TSPC2-1_1b_1_1_6	sphalerite	2.5	2917.57	1.62E-03	89	16	164
TSPC2-1_1c_1_1_6	sphalerite	7.1	2917.49	4.68E-03	236	45	456
TSTR1-2_1a_1_1_6	sphalerite	14.6	2917.35	9.76E-03	490	90	921
TSTR1-2_1a_2__6	sphalerite	11.5	2917.41	7.71E-03	390	69	706
TSTR1-7_1c_1_1_6	sphalerite	12.9	2917.38	8.64E-03	417	85	865
TSTR1-3_D1_1_6	dolomite	4.2	2917.53	2.77E-03	168	29	296
TSTR1-3_D2_2_6	dolomite	8.8	2917.45	5.82E-03	349	62	632
TSTR1-3_D3_3_6	dolomite	4.8	2917.53	3.16E-03	188	33	333
Northern Arkansas							
NALB1-1_1_1_6	sphalerite	5.4	2917.52	3.54E-03	218	37	375
NALD1-4_2_1_1_6	sphalerite	18.0	2917.29	1.22E-02	623	119	1217
NALD1-4_2_3_1_6	sphalerite	18.6	2917.28	1.25E-02	661	126	1288
NALD1-4_2_4_1_6	sphalerite	6.5	2917.49	4.30E-03	231	38	391
NAPA1-13_1a_1_1_6	sphalerite	9.6	2917.44	6.39E-03	293	56	572
NAPA1-13_1b_1_1_6	sphalerite	7.6	2917.48	5.06E-03	226	43	435
NAEX1-7_1_2_1_7	dolomite	7.9	2917.47	5.25E-03	340	51	517
NAEX1-7_1_3_1_7	dolomite	10.7	2917.42	7.14E-03	410	66	673
NALD1-1_2_3_1_7	dolomite	15.9	2917.32	1.07E-02	676	113	1156
NALD1-1_3_5_1_7	dolomite	0.4	2917.6	4.70E-04	29	6	63
NAPA1-13_2a_1_1_6	quartz	4.8	2917.53	3.16E-03	169	30	308
NAPA1-13_2c_1_1_6	quartz	3.1	2917.56	2.01E-03	114	20	204
NAPA1-13_2c_2__6	quartz	5.9	2917.51	3.92E-03	179	34	347
Central Missouri							
CMBN_1_1_1_6	sphalerite	4.8	2917.53	3.16E-03	151	28	288
CMBN_1_2__6	sphalerite	8.2	2917.47	5.44E-03	258	50	508
CMBN_2_1_1_6	sphalerite	7.1	2917.49	4.68E-03	218	42	426
CMBN_2_2_1_6	sphalerite	6.8	2917.49	4.49E-03	207	40	405
CMFT_2_1_1_6	sphalerite	8.8	2917.45	5.82E-03	279	54	549
CMFT_2_2_1_6	sphalerite	1.3	2917.59	8.51E-04	43	8	84
CMFT_2_3_1_6	sphalerite	4.5	2917.53	2.97E-03	147	27	276
CMFT_2_4_1_6	sphalerite	7.1	2917.49	4.68E-03	236	44	448
CMTF_1_1_1_6	sphalerite	5.1	2917.52	3.35E-03	167	31	315
CMTF_1_2_1_6	sphalerite	4.2	2917.53	2.77E-03	135	25	255
CMTF_1_3_1_6	sphalerite	13.2	2917.38	8.83E-03	416	86	874

Table 2.4 Ore fluid and calcite reaction path model results.

Variable	District			
	VT	TS	NA	CM
Na (ppm)	68249	68460	68299	67386
Mg (ppm)	2291	1985	1826	2009
K (ppm)	4017	2605	2633	2761
Ca (ppm)	17815	18932	17819	18729
Sr (ppm)	656	729	544	696
Ba (ppm)	27	22	17	24
Ca/Mg	4.7	5.8	5.9	5.7
calcite (g)	15.91	13.3	12.19	13.52
CH_4aq (ppm)	200	200	200	200
calcite (cm^3)	5.87	4.91	4.50	4.99
Ca* (ppm)	16880	17360	16350	17270
Mg* (ppm)	317	326.1	306.8	324.3
Ca/Mg*	32.3	32.3	32.3	32.3

All calculations made with an initial pH of 3.5 and log f_{O_2} of -53. Abbreviations: same as in fig. 3.2 and *-reacted fluid composition.

CHAPTER 3: Fluid Evolution Models of Ozark Plateau Mississippi Valley-type Ore Fluids

3.1 Abstract

The Cl/Br ratios of Ozark Mississippi Valley-type fluids have historically been used as an indicator of salinity origin. Low Cl/Br ratios of Ozark MVT ore fluids have been interpreted to indicate a highly evaporatively concentrated seawater origin. However, the absolute concentrations of Na, Mg, K, and Ca in Ozark MVT ore fluids are significantly different from the composition of highly evaporatively concentrated seawater. Reaction path and binary mixing models were developed to investigate possible evolutionary histories that could produce a fluid with a composition similar to the Ozark MVT ore fluid. The reaction path models considered reaction between evaporatively concentrated seawater and granite. These models demonstrate that neither ancient nor modern seawater evaporatively concentrated to any degree was the sole contributor to the salinity of Ozark MVT ore fluids. This finding suggests the Cl/Br ratios of Ozark MVT ore fluids have been modified. Binary mixing models considered mixing between Cambrian highly evaporatively concentrated seawater and a lower salinity halite dissolution brine. In this mixing scenario the cation composition of the Ozark MVT ore fluid is reached at about 80 percent mixing with the halite dissolution brine. However, to produce a fluid mixture with an Ozark MVT ore fluid Cl/Br ratio, the halite dissolution brine must have either dissolved Br-rich halite or equilibrated with Br-rich halite evaporates allowing Cl to exchange for Br.

3.2 Introduction

Several decades of research on fluid inclusions in Mississippi Valley-type (MVT) deposits of the Ozark Plateau established that the deposits were most likely formed from sedimentary brines whose composition was dominated by Na, Cl, and Ca with lesser concentrations of K and Mg (Newhouse, 1933; Schmidt, 1962; Roedder, 1963, 1967, 1977; Leach et al., 1975; Leach, 1979; Hagni, 1983; Long et al., 1986; Rowan and Leach, 1989; Viets and Leach, 1990; Shelton et al., 1992; Ragan, 1994; Ragan et al., 1996; Viets et al., 1996; Coveney et al., 2000; Appold et al., 2004; Stoffell et al., 2008; Appold and Wenz, 2011). The most recent of these studies (Stoffell et al., 2008; Appold and Wenz, 2011; Chapter 2 this volume) have generated detailed characterizations of the concentrations not only of major constituents but also of minor and trace constituents like Sr, Ba, Pb, and CH_4. These recent studies have shown that sulfide mineralization most likely formed as a result of mixing under reducing conditions between a Pb- and probably overall metal-rich, sulfur-poor ore fluid with a sulfide-rich, metal-poor fluid. However, how these fluids acquired their overall composition remains unclear.

Some insights into the origin of the salinity of MVT fluids have been gained from studies of the halogen concentrations in fluid inclusions (Crocetti and Holland, 1989; Viets and Leach, 1990; Viets et al., 1996; Kendrick et al., 2002; Stoffell et al., 2008; Shelton et al., 2009). These studies suggest that Ozark MVT fluids acquired their salinity predominantly through evaporation of seawater, with a lesser component acquired through halite dissolution. Nonetheless, the major cation chemistry of Ozark MVT fluids is different from that of modern or ancient evaporated seawater (table 3.1). In particular, Ozark MVT ore fluids' Na concentrations are significantly greater and Mg concentrations

are less than one-tenth of those of ancient evaporated seawater. Previous researchers have offered some explanations for these differences in fluid composition. Stoffell et al. (2008) compared sphalerite- and quartz-hosted fluid inclusion compositions from the Tri-State and Northern Arkansas MVT districts to the evaporated modern seawater trend of McCaffery et al. (1987). They found the fluid inclusions to be enriched in Ca and depleted in Mg relative to the evaporated seawater trend. They attributed this pattern to be the result of the mineralizing fluids having replaced calcite in their host rocks with dolomite. In addition, the Tri-State district fluid inclusions had K concentrations that lay along the evaporated seawater trend whereas the Northern Arkansas district fluid inclusions had K concentrations that were variably elevated above the seawater evaporation trend. They attributed these elevated K concentrations to be the result of variable interaction of the mineralizing fluids with K-rich source rocks. In the Southeast Missouri district, numerous investigators (Deloule et al., 1986; Gregg and Shelton, 1989; Goldhaber et al., 1994; Shelton et al., 1995) have used S, Pb, and Sr isotopes to demonstrate that MVT fluids interacted with granitic basement rocks prior to precipitating sulfides. Although these studies did not specifically address the major cation composition of the fluids, they do demonstrate that the fluids were modified through water-rock reactions.

The purpose of this study was to develop reaction path and fluid mixing models that can explain how Ozark Plateau MVT ore fluids acquired their observed compositions. The models investigated two specific genetic scenarios: (1) reaction between evaporated seawater and granite, and (2) mixing of evaporated seawater with a hypothetical halite-dissolution brine. The models demonstrate that very specific water-

rock reactions, fluid compositions, and mixing ratios are necessary to develop the low Cl/Br ratios and high Na concentrations characteristic of Ozark Plateau MVT fluids. The models also demonstrate that Cl/Br ratios of Ozark MVT fluids may not be accurate indicators of salinity origin.

3.3 Geology and Hydrology of Ozark Plateau MVT deposits

The Ozark Plateau of the central United States consists of a thick succession of Paleozoic carbonate rocks interbedded with thinner and less frequent shales and sandstones (figure 3.1). The Ozark MVT deposits, which include the Southeast Missouri, Tri-State, Northern Arkansas and Central Missouri districts, occur at different stratigraphic horizons within the Ozark Plateau (figures 3.1 and 3.2). The Ozark MVT deposits formed in the Late Paleozoic during flexural rebound of the Ouachita mountain belt as erosion began to outpace uplift (Leach, 1973; Leach, 1979; Leach and Rowan 1986). This flexural rebound resulted in uplift of the Arkoma basin, forcing basinal fluids to travel northward via gravity-driven flow (Garven and others, 1993; Appold and Garven, 1999; and Appold and Nunn, 2005). Thus, based on the timing of the orogeny, which is also thought to be the age of mineralization (Leach and Rowan, 1986; Leach, 1994), the Ozark MVT ore fluids cannot be younger than Permian in age.

Further constraints on the age of the mineralizing fluids can be deduced by considering their likely flow paths. Numerous investigations have demonstrated that the ore fluids rose into the ore host rocks at the deposit sites from stratigraphically lower aquifers based on hydrogeologic models, dolomitization paths of ore fluids and the presence of significant mineralization below some of the major ore bodies (Siebenthal,

1916; Brockie et al., 1968; Gregg, 1985; Appold and Garven, 1999; Appold and Nunn, 2005). Numerical models of topography-driven flow have demonstrated that Permian meteoric recharge in the highest elevations of the Arkoma foreland basin would have displaced older resident brines initially downward and ultimately northward and upward onto the platform where MVT deposition occurred (Appold and Garven, 1999; Appold and Nunn, 2005). Because the Ozark MVT fluids are consistently highly saline, they could not have mixed with much of this Permian, presumably dilute, meteoric recharge, providing further evidence that the Ozark MVT ore fluids could not have been younger than Permian. Moreover, because the ore fluids in each Ozark MVT district were dolomitizing (Appold and Wenz, 2011; Chapter 2 this volume) and because each district is overlain by thick sections of limestone (figure 3.1), each district's ore fluids could not have originated in or traversed far through rocks stratigraphically younger than its ore host rocks, or the ore fluids would have equilibrated with limestone and lost their dolomitizing character. Thus, each district's ore fluids most likely originated in rocks no younger than the district's ore host rocks, unless the ore fluids were able to descend through the limestone successions via faults or other pathways that inhibited reaction with calcite.

3.4 MVT Ore Fluid Composition

Numerous fluid inclusion studies have shown the Ozark MVT fluids to have shared some important characteristics. Besides having had similar temperatures and bulk salinities, the ore fluids had broadly similar major element compositions with average concentrations of Na = 68,000 ppm, Ca = 18,000 ppm, K = 2,800 ppm, and Mg = 2,000

ppm (Chapter 2 this volume). The ore fluids in each of the Ozark MVT districts were at least transiently Pb- and possibly overall metal-rich, with Pb concentrations on the order of 100's to1000's of ppm (Stoffell et al., 2008; Appold and Wenz, 2011; Chapter 2 this volume). High CH_4/CO_2 ratios, based on direct measurements of CH_4 in sphalerite- and dolomite-hosted fluid inclusions and assuming CO_2 saturation, indicate that redox conditions during mineralization were predominantly reducing, such that any S in the fluids would have existed predominantly in the form of sulfide (Chapter 2 this volume). To date, sulfur concentration has not been reliably measured in any previous fluid inclusion studies. However, because the solubility of sulfide is low in the presence of such high Pb concentrations, the ore fluids must have been sulfur-poor overall, though other Pb-poor fluids with which the ore fluids may have mixed could have had high sulfide concentrations (Chapter 2 this volume). Dolomite-, quartz-, and sphalerite-hosted fluid inclusion Cl/Br ratios determined from bulk leachate and individual LA-ICP-MS analyses range from 63 to 6100, with the sphalerite-hosted fluids tending toward the lower end of this range between about 50 and 270 (table 3.1; Crocetti and Holland, 1989; Viets and Leach, 1990; Viets and others, 1992; Stoffell et al., 2008; Shelton et al., 2009). On the whole, this range of Cl/Br ratios has been interpreted to indicate that MVT mineralizing fluids in the Ozark Plateau were derived predominantly from evaporatively concentrated seawater and to a lesser extent from halite dissolution.

3.5 Approach

The purpose of the present study was to investigate how the Ozark MVT ore fluids could have attained their observed compositions. This investigation was carried out

in part through reaction path modeling using the Geochemist's Workbench^{TM} software in conjunction with the Lawrence Livermore National Laboratory thermodynamic database, version 8, release 6. Two types of reaction path models were conducted, titration and flow-through. In the titration models, a prescribed volume of reactant was added stepwise to one kilogram of fluid, where at each step a new fluid and rock equilibrium state was calculated before more reactant was added. This model simulates the geochemical evolution of a fluid that is static or moving slowly through its host rock. In the flow-through models, a prescribed volume of reactant was also added stepwise to a prescribed volume of fluid, but minerals that precipitated from the previous step were removed from the system prior to calculating the new equilibrium state of the system. This model simulates a fluid flowing more rapidly through its host rock. Reaction path model results are presented in terms of a reaction progress variable, ξ, which represents the fraction of the total prescribed reactant volume added to the system. A total of 100 ξ steps were calculated for the titration and flow-through models for a total reactant volume of 3000 cm^3.

The reaction path models evaluated a scenario in which an evaporatively concentrated seawater is reacted progressively with granite. In this scenario, the initial fluid was assumed to be evaporatively concentrated Cambrian seawater, with a composition derived from analyses of halite-hosted fluid inclusions from Cambrian evaporites from Eastern Siberia analyzed by Horita et al. (2002). These fluid inclusions have average Cl/Br ratios of ~170, which for modern seawater would correspond to evaporation past the point of halite precipitation (see compilation by Fontes and Matray, 1993). Though the Cl/Br ratios of these fluid inclusions are similar to those of MVT ore

fluids, the ionic strengths of about eight of the fluid inclusions are about a factor of two greater than those of MVT ore fluids. Thus, the model ore fluid composition was obtained by diluting the average halite-hosted fluid inclusion compositions of Horita et al. (2002) by a factor of two. This step could represent dilution by fresh meteoric water, which is consistent with hydrogen and oxygen isotope evidence that suggests that most sedimentary brines contain a significant component of meteoric water (Faure and Mensing, 2005). It is worth noting that this ionic strength or salinity reduction could possibly also have been achieved through mineral precipitation, though this scenario could not be tested because an ionic strength of eight lies beyond the limit of the extended Debye-Hückel activity model of Helgeson et al. (1981) utilized by the Geochemist's Workbench^{TM} software. In addition, the Pitzer equation-based thermodynamic database used by the software lacks data for the necessary mineral phases to model likely water-rock reactions at high ionic strength and temperature.

The reaction path models required additional parameters that are not included in the Horita et al. (2002) data set. These parameters include pH, f_{O_2}, and the concentrations of Al, Fe and S. The initial pH and log f_{O_2} values were set at 8 and −53 assuming a similar pH to modern seawater and a redox state likely for Ozark MVT ore fluids (Chapter 2 this volume). The starting concentrations for Al and Fe were set at 0.002 ppm and for SO_4^{2-} at 9 ppm, concentrations for which no Al, Fe or S bearing minerals are saturated. The model temperature was held constant at 120 °C, which represents the average homogenization temperature of sphalerite-hosted fluid inclusions from Ozark MVT deposits. A summary of the initial fluid compositions is given in table 3.2.

The sedimentary succession of the entire Ozark Plateau is underlain predominantly by felsic igneous rocks (Bickford et al., 1981). Numerous studies have suggested that the Ozark MVT ore fluids derived their Pb from these felsic basement rocks based on Pb isotope compositions (McKnight and Fischer, 1970; Doe and Delevaux, 1972; Crocetti et al., 1988; Goldhaber et al., 1994). Therefore a reactant assemblage was used in the model that is consistent with the average modal mineral abundances in granitic rocks from the St. Francois Mountains in Missouri, (table 3.3; Bickford et al.,1981; Nabelek and Russ-Nabelek ,1990), which are an outcropping of the Precambrian basement thought to underlie the Ozark Plateau.

In addition to the reaction path modeling calculations, a suite of non-thermodynamic binary fluid mixing calculations was carried out between a fluid with the composition of the halite-hosted fluid inclusions of Horita et al. (2002) and a hypothetical halite dissolution (HHD) brine. The major cation concentrations of the HHD brine were varied systematically until their mixing with the evaporatively concentrated seawater produced a fluid composition that resembles the Ozark MVT ore fluid. An initial Cl/Br atomic ratio of 650 was selected for the HHD brine. This is the Cl/Br ratio of modern seawater and represents the absolute minimum value possible for halite precipitated from seawater and was selected as a starting point for the binary mixing models.

3.6 Results

3.6.1 Titration Model

Figure 3.3A and B show the results of a titration model in which 3000 cm^3 of granite was allowed to react progressively with one kilogram of Cambrian evaporatively

concentrated seawater (table 3.2). The model fluid rapidly becomes saturated with respect to quartz, microcline, annite, pyrite, and muscovite early in the reaction path resulting in the net accumulation of these minerals over the remainder of the reaction path (figure 3.3B). The reactant minerals, albite, anorthite, phlogopite, hematite, and magnetite were either not saturated or become saturated late in the reaction path. New minerals that were not part of the original granite reactant mineral assemblage that become saturated during the reaction path include the smectite minerals, saponite and nontronite, and the zeolite, mesolite. A list of the mineral compositions is provided in table 3.4.

Figure 3.3A shows the changes in concentration of the four major elements, Na, Ca, K, and Mg, during the reaction path, relative to the average concentrations of these elements in Ozark MVT ore fluids. In this simulation, average MVT ore fluid concentrations of Na, Ca, K, and Mg were never simultaneously reached. The Na concentration of the model fluid begins more than an order of magnitude below that of the average Na concentration of the Ozark MVT ore fluids. However, as a result of continual albite dissolution, the concentration of Na in the model fluid increases steadily during the simulation, reaching the ore fluid concentration of 66,000 ppm at a ξ value of 0.66, and continuing to increase thereafter. The model fluid's Ca concentration begins and remains near the Ozark MVT ore fluid's Ca concentration up to a ξ value of about 0.4, but plunges steeply thereafter due to precipitation of mesolite. The concentrations of Mg and K in the model fluid both start out significantly higher than the average concentrations in Ozark MVT ore fluids. The Mg concentration of the model fluid decreases throughout the simulation as a result of the continual precipitation of Mg minerals like nontronite and saponite and the fact that no Mg minerals are present in the

reactant mineral assemblage. Thus, the Mg concentration in the model fluid reaches the average Mg concentration of the Ozark MVT ore fluids by a ξ value of about 0.25, but decreases by more than another order of magnitude thereafter. The concentration of K in the model fluid increases briefly through a ξ value of about 0.1 due to the dissolution of K-feldspar. Though K-feldspar continues to accumulate throughout the simulation, K concentration decreases after ξ = 0.1. The reason for K loss can be explained by conversion of muscovite into microcline, illustrated by the decrease in slope of muscovite accumulation and a more rapid rate of microcline accumulation beginning at a ξ value of about 0.1, and by reaction 1.

$$KAl_3Si_3O_{10}(OH)_2 + 6SiO_2(aq) + 2K^+ \rightarrow 3KAlSi_3O_8 + 2H^+ \qquad (1)$$

In reaction 1 muscovite and K are converted into microcline, resulting in a pH decrease. However, the pH of the system at this point is increasing, likely the result of consumption of H^+ by precipitation of abundant smectite minerals. After a ξ of about 0.25, the pH and K concentration of the fluid stabilize at about 5 and 7200, respectively. Saturation of albite in the system further increases the pH, lowering the K concentration in the reactant fluid to the average K concentration of the the Ozark MVT ore fluids at a ξ value of about 0.85. Overabundance of K in the reactant fluid until late in the reaction path was a consistent feature of the models, regardless of the initial K concentration.

The model results were found to be relatively insensitive to changes in the initial values of pH, log f_{O_2}, and total sulfur content of the model fluid. During sensitivity analysis, the initial pH was varied from 2 to 10, log f_{O_2} was varied from −40 to −60, and

total sulfur concentration was varied from 0.001 to 100 ppm. In all of the simulations, the pH was buffered to a value of about 5 to 6, depending upon changes in the silicate mineral assemblage over the course of the reaction path. The log f_{O_2} was buffered to a value of about −52 due to reactions with ferrous Fe-silicates and pyrite. The total sulfur concentration was buffered to a value of about 30 ppb due to saturation with respect to pyrite.

The sensitivity analysis was extended to evaluate the effects of other variations in fluid composition on the reaction path results. Specific scenarios evaluated included the use of a reactant fluid with the composition of (1) Middle Devonian and (2) Late Silurian evaporatively concentrated seawater that was diluted by a factor of two (table 3.2), and (3) a volume reactant exchange of 300 cm^3 of albite for the same volume of K-feldspar in the granitic reactant mineral assemblage. The Devonian and Silurian evaporatively concentrated seawater compositions were selected because they represent plausible ages for the Ozark MVT ore fluid and have significantly different compositions from Cambrian evaporatively concentrated seawater. The models in which the modified Middle Devonian and Late Silurian evaporatively concentrated seawaters reacted with the original granite mineral assemblage predict overall similar mineral precipitation sequences compared to the base case model shown in figure 3.3. As for the base case model, at no point in the Middle Devonian and Late Silurian evaporatively concentrated seawater models did the concentrations of Na, Ca, K, and Mg in the reactant fluid simultaneously match the average concentrations of these elements in the Ozark MVT ore fluids (figures 3.4 and 3.5). In the Late Silurian model, the Na concentration of the reactant fluid reached the average concentration of Ozark MVT ore fluids at a slightly

lower ξ value compared to the base case model, but the Ca and Mg concentrations in the reactant fluid were also depleted below the average concentrations of the Ozark MVT fluids at lower ξ values compared to the base case model (figure 3.4). In the Middle Devonian model, the Na concentration of the reactant fluid never reaches the average concentration of the Ozark MVT ore fluid and the Ca and Mg concentrations in the reactant fluid were depleted at much lower ξ values compared to the base case model (figure 3.5).

Increasing the proportion of albite in the reactant mineral assemblage while retaining the initial modified evaporatively concentrated Cambrian seawater composition for the reactant fluid from the base case model resulted in a faster increase in the reactant fluid's Na. The increased proportion of albite reactant also resulted in a faster decrease in the reactant fluid's Ca and Mg concentration such that the Na, Ca, and Mg concentrations in the reactant fluid never simultaneously matched the averages of the concentrations of these elements in Ozark MVT ore fluids.

In order to determine if a reactant fluid composition exists that could evolve to the composition of Ozark MVT ore fluid through reaction with granite, a series of reaction path models was carried out in which the concentrations of the major elements were varied systematically. The results show that an optimal fluid with initial elemental concentrations of Na= 18,000 ppm, Mg= 23,000 ppm, K= 6,000 ppm and Ca= 22,000 ppm would match closely the average concentrations of Na, Mg and Ca in Ozark MVT ore fluids after reacting with 1,560 cm^3 of granite at a ξ value of about 0.5 (figure 3.6 and table 3.2). As for the previous simulations, the concentration of K in the model reactant fluid remained above the average concentration of K in Ozark MVT fluids until much

later in the reaction path, no matter what initial K concentration was tried. However, the model K concentration predicted at $\xi = 0.5$ does lie within the range of K concentrations in fluid inclusions hosted by main-stage, Ag-rich sphalerite-hosted fluid inclusions from the Viburnum Trend, which are much higher than the average K concentration of Ozark MVT fluids (Fig. 2.7). Thus, this reaction path model represents a reasonable possible scenario by which the mineralizing fluid mixture in the Viburnum Trend formed. For the other three Ozark MVT districts, an additional mechanism to decrease the K concentration further would have been required. One possibility is mixing of the ore fluid with a saline, K-poor fluid. Such mixing would have been more likely in the other three districts because their higher stratigraphic positions would have created a longer flow path and therefore greater opportunities for mixing for an ore fluid ascending from the granitic basement (figure 3.1).

To identify any possible geologic analogues to the optimal fluid composition requires developing an evaporation reaction path in which Ca can be concentrated in seawater. The relative depletion of Ca in evaporatively concentrated modern seawater is due to the abundance of sulfate, which causes anhydrite to precipitate. Seawater from 350 to 500 Ma (Devonian to Late Cambrian) had SO_4^{2-} concentrations three times lower and Ca concentrations three times higher than modern seawater but comparable concentrations of Mg and K (Horita et al., 2002), allowing high Ca concentrations to be maintained during evaporative concentration. The Ca and SO_4^{2-} concentrations of Devonian to Late Cambrian seawater represent the most extreme deviation from modern seawater compositions, which allow the highest possible Ca concentrations in evaporatively concentrated seawater. The average seawater composition from this period

of time was evaporatively concentrated using the Geochemist's Workbench Harvie-Möller-Weare thermodynamic database. When the optimal fluid is progressively concentrated without reaction by a factor of two, its resultant Na and K concentrations resemble those of Devonian to Late Cambrian seawater that has been evaporatively concentrated by a factor of about 45 (table 3.1). The concentration of K in Early Paleozoic seawater that has been evaporatively concentrated by a factor of 45 is about 12,000 ppm, which led to the choice of 6,000 ppm in the model reactant fluid for the simulation shown in Figure 3.6, though as noted above, the models were relatively insensitive to the choice of initial K concentration because of the abundance of K-feldspar in the reactant mineral assemblage. Once the optimal fluid has been concentrated by a factor of two, its Ca and Mg concentrations are a factor of ~1.6 greater than those of Devonian to Late Cambrian seawater that has been evaporatively concentrated by a factor of 45. If Devonian to Late Cambrian seawater were evaporated further to a factor of about 90, it would have a Ca concentration of about 44,000 ppm and a Mg concentration of about 47,000 ppm, which resemble the Ca and Mg concentrations of the concentrated optimal fluid. However, the Na concentration in this highly evaporatively concentrated seawater would be about 5300, which is about a factor of seven lower than that of the concentrated optimal fluid. Thus, the optimal fluid composition found from this sensitivity analysis is unlike any modern or ancient evaporatively concentrated seawater. This suggests the Cl/Br ratio of the Ozark MVT ore fluids were modified by processes other than evaporative concentration, as the Cl/Br ratio of Middle Devonian to Cambrian seawater that has been evaporatively concentrated by a factor of about 90 averages

between 173 and 278 (table 3.1) whereas Cl/Br ratios of the Ozark MVT ore fluids are as low as 46 (table 3.1; Shelton et al., 2009).

3.6.2 Flow-through Model

Figure 3.7 A and B shows the change in fluid composition and abundance of minerals precipitated as a function of progress of reaction with granite for the flow-through model, using the same initial reactant fluid composition and mineral assemblage used in the base case titration model. Comparing these results to the results of the base case titration model shown in figure 3.3, it is clear that the patterns of mineral precipitation and changes in fluid composition are very similar to one another. The main difference in fluid composition is that in the flow-through model, the concentration of Mg declines more sharply between a ξ value of about 0.25 and 0.7 compared to the titration model, whereas the trajectories of the concentrations of Na, Ca and K in the two models are nearly identical. The main differences in the patterns of mineral precipitation are that in the flow-through model mineral precipitation is continuous whereas in the titration model Mg-saponite, Ca-saponite, and Mg-nontronite dissolve after earlier periods of precipitation. In addition, in the flow-through model Ca-nontronite is precipitated. The similarities between the titration and flow-through models demonstrate that fluid composition and mineral alteration patterns for the reaction of a sedimentary brine with a granite are relatively insensitive to whether or not the precipitated minerals remain in contact with the fluid. This implies that the fluid composition and mineral alteration patterns are also relatively insensitive to the velocity of the fluid, provided that the kinetics of reaction remain fast relative to the rate of flow.

3.6.3 Binary Fluid Mixing Models

As shown in Chapter 2, the sulfide ore mineral precipitation process in each Ozark MVT district most likely consisted principally of mixing between a Pb- and Zn-rich, sulfur-poor ore fluid that had a high Ca/Na and low Cl/Br ratio, and a fluid that had the converse properties. It is possible, however, that the ore fluid underwent one or more earlier stages of mixing prior to the mixing that ultimately led to ore precipitation. If the ore fluid originated some time between the Cambrian through Mississippian, tens to hundreds of millions of years would have been available for a proto-ore fluid to have mixed with other basinal fluids before precipitating MVT deposits in the Pennsylvanian-Permian. To test this scenario, simple binary fluid mixing models were conducted involving a hypothetical halite dissolution (HHD) brine and the Cambrian evaporatively concentrated model seawater utilized as the reactant fluid in the previous reaction path simulations to see if the average composition of the Ozark MVT ore fluids could be produced.

The results of the calculations show that this mixing scenario would work best for a HHD brine composition characterized by Na as the predominant cation, low concentrations of Mg, and an overall salinity similar to that of the Ozark MVT ore fluids (table 3.2). A mixture consisting of 80% of this HHD brine and 20% of the Cambrian evaporatively concentrated model seawater has Na and K concentrations close to the average Na and K concentrations of the Ozark MVT ore fluids (figure 3.8). However, the average concentration of Ca in the Ozark MVT ore fluids is reached for a mixture containing only about 60% HHD brine, and the average concentration of Mg is reached

for a mixture containing about 95% HHD brine. Thus, for this mixing process to produce a fluid with the overall average major element composition of Ozark MVT ore fluids, it must have been concomitant with another process that introduced Ca and removed Mg from solution, e.g. dolomitization of calcite. Reaction path calculations of a mixture consisting of 80% HHD brine and 20% of the Cambrian evaporatively concentrated model seawater reacting with calcite demonstrate that the Na and K concentration are insignificantly modified whereas the Ca and Mg concentrations are significantly modified by a 1:1 exchange of Mg for Ca in the fluid. Specifically, the reaction path calculations show that one kilogram of the fluid mixture reacting with 22 cm^3 of calcite will result in the exact average composition of the Ozark MVT ore fluid. This is shown graphically in figure 3.8 where the red and orange arrows point to the model fluid compositions resulting from reaction of the fluid mixture with calcite.

For a mixture consisting of 80% HHD brine and 20% Cambrian evaporatively concentrated model seawater, the resultant Cl/Br ratio of 314 is over a factor of six greater than the lowest Cl/Br ratios of Ozark MVT ore fluids, which as noted previously were obtained from in situ LA-ICP-MS analysis of fluid inclusions and thus are thought to be more accurate than the higher values obtained from bulk leachate analyses (Stoffell et al, 2008; table 3.1). One possible explanation may be that the HHD brine had an anomalously low Cl/Br ratio, perhaps caused by the recrystallization of halite. For example, Stoessell and Carpenter (1986) showed that the Br content of a halite-saturated fluid that is causing recrystallization of halite can increase by over 1,000 ppm. In addition, if the HHD brine acquired its salinity from the dissolution of Br-rich halite in

the first place, then the Cl/Br ratio of the HHD brine could have been lowered even further.

Halite precipitated from seawater typically has Br concentrations in the range of 50 to 270 ppm, though Br concentrations in halite as high as 3,000 ppm have been reported (Warren, 2006). The Cl/Br ratio of the initial HHD brine was modified using equation 1 and a distribution coefficient (D) of 0.34 (from Hermann, 1972).

$$D=\left(\frac{Br}{Cl}\right)_{mineral}\Big/\left(\frac{Br}{Cl}\right)_{solution} \quad (1)$$

Figure 3.8 shows the Cl/Br ratio as a function of mixing of the Cambrian evaporatively concentrated model seawater with HHD brine with initial Cl/Br ratios of seawater and Cl/Br ratios acquired from recrystallization of halite containing 200 and 500 ppm Br. For a mixture consisting of 80% HHD brine and 20% Cambrian evaporatively concentrated model seawater the Cl/Br ratios are 204 and 114 for a HHD brine that recrystallized halite with Br concentrations of 200 and 500 ppm, respectively. The results indicate that a low Cl/Br ratio resembling that of Ozark MVT ore fluids can be produced in a fluid mixture containing a high proportion of a fluid whose salinity was derived from halite dissolution, provided that the Br content of HHD brine was increased by recrystallization of Br-rich halite.

3.7 Discussion

The reaction path and binary mixing models each indicate that the high Na concentration and low Cl/Br ratio of the Ozark MVT ore fluid require a very specific

fluid evolution history. In the reaction path models, reaction of evaporatively concentrated seawater with granite does not predict the composition of Ozark MVT ore fluids. The inability to transform an evaporatively concentrated seawater into the Ozark MVT demonstrates no clear correlation exists between degree of evaporation and Cl/Br ratio for Ozark MVT ore fluids. In the binary mixing model, mixing between the Cambrian evaporatively concentrated seawater and the HHD brine will converge on the Ozark MVT ore fluid composition if the HHD brine was enriched in Br through recrystallization of Br-rich halite and reacted with calcite to modify the Ca and Mg concentrations of the mixture. The very specific scenario of this model implies that it is unlikely to have occurred naturally as the fluid composition ranges and Br enrichment scenarios are so narrow. Therefore, in both model types it appears that the Cl/Br ratio of the fluids could have been modified by some other process.

Investigations of the composition of Canadian Shield crustal brines have shown that fluid and rock reactions can indeed modify the Cl/Br ratio of saline fluids (Fritz and Frape, 1982; Frape and Fritz, 1987; Gascoyne et al. 1987). Experimental leachate studies have demonstrated that water reacting with granitic rocks has Cl/Br ratios from 56 to 266, with an average value of about 100 (Frape and Fritz, 1987; Seelig and Bucher, 2010). If the Ozark MVT ore fluids reacted with granitic basement rock, these studies suggest the Cl/Br ratio of the fluid could have been modified. If this is the mechanism by which the Ozark MVT ore fluids acquired their low Cl/Br ratios, then a highly evaporatively concentrated seawater is not a necessary component in the evolutionary history of MVT ore fluids. Instead, lower degrees of seawater evaporation and modification of the Cl/Br ratio, lowered through reaction with granite, could have produced a fluid similar in

composition to the Ozark MVT ore fluids. In addition, weakly evaporated seawater is much less reactive with granite, due to much lower Ca and Mg concentrations, and has an ionic strength comparable to the Ozark MVT ore fluids. Therefore, based on the high Ca concentrations of Paleozoic seawater and the ability of granites to modify the Cl/Br ratio of fluids, the Ozark MVT ore fluids could be the product of reaction between a weakly evaporatively concentrated ancient seawater and granite.

The reaction path models presented indicate that rock volumes of about 1,500 cm^3 are required to transform every kilogram of evaporatively concentrated seawater into Ozark MVT ore fluid compositions. For a model fluid density of 1.1 g/cm^3, this would equate to a water to rock volume ratio of about 0.73. The feasibility of this water to rock ratio can be examined by mass balance calculations of the volume of granite required for a fluid to attain the high Pb concentrations characteristic of Ozark MVT ore fluids. For example, one liter (L) of fluid extracting all of the Pb from 2,000 cm^3 of a low-Ca granite with a Pb concentration of 19 ppm (Faure, 1998) would result in an aqueous Pb concentration of 17 ppm. By extension, one L of fluid would have to extract all the Pb from 150,000 cm^3 to acquire a Pb concentration of about1,000 ppm, which is near the upper limit of measured values in Ozark MVT ore fluids. Assuming a density of 1.1 g/cm^3 for the fluid, the water to rock ratio would be 0.0073. This water to rock ratio is two orders of magnitude lower than predicted by the reaction path models and suggests the model fluid had interacted with a greater volume of rock than required to change its major cation concentrations to that of the Ozark MVT ore fluid. Thus, if the granitic basement were the Pb source rock and the ore fluid were an evaporatively concentrated seawater, reactions depleting the ore fluid of Ca, Mg and K must have been inhibited

kinetically or the granitic rocks were enriched in Pb by at factor of 50 to allow such small water to rock ratios determined from the reaction path models. The possibility of high Pb content in the Ozark Plateau basement is supported by the variably elevated U and Pb concentrations up to a factor of eight compared to typical granite compositions (Nabelek and Russ-Nabelek, 1990; Goldhaber et al., 1994; Faure, 1998).

Historically, investigations of Ozark Plateau MVT ore fluid compositions have considered Cl and Br to behave as conservative elements and thus to be good indicators of salinity origin. This assumption has led to a common interpretation that the low Cl/Br ratios in MVT ore fluids indicates that the fluids acquired their salinity through high degrees of evaporative concentration of seawater (Crocetti and Holland 1989; Viets, 1996, Kendrick et al., 2002). However, the major element concentrations and salinity of Ozark MVT ore fluids are much lower than suggested by the Cl/Br ratios and indicates that either the precursor evaporatively concentrated seawater fluid mixed with a more dilute fluid, such as a halite dissolution brine, or the Cl/Br ratios were modified by reaction with Br bearing minerals like biotite and muscovite in granite. The reaction path and mixing models presented in this study suggest that Cl/Br ratios cannot predict the origin of salinity for Ozark MVT ore fluids due to the complex evolutionary history they may have experienced. Instead, Cl/Br ratios of Ozark MVT ore fluids may be an indicator of interaction with the granitic basement and in effect an indicator of ore precipitating potential. Further experimental studies of Br and Cl distribution coefficients between silicate minerals and saline fluids will be necessary to understand the complex geochemical evolutionary history of the Ozark MVT ore fluids more fully.

3.8 Conclusions

The reaction path models presented in this study have revealed some important insights into the origins of Ozark Plateau MVT ore fluids.

1) Ancient evaporatively concentrated seawater with Cl/Br ratios similar to those of Ozark MVT ore fluids have major cation concentrations that differ by over one order of magnitude, indicating that if the Ozark MVT ore fluids originated as highly evaporatively concentrated seawater they subsequently must have been modified significantly.

2) Reaction path models of evaporatively concentrated seawater reacting with granite do not predict the cation concentrations of Ozark MVT ore fluids. An optimal fluid composition reacting with granite does predict the cation concentrations of Ozark MVT ore fluids, but this fluid is unlike any known natural evaporatively concentrated seawater.

3) A fluid mixture consisting of 20% evaporatively concentrated seawater and 80% HHD brine that reacted with calcite could have Na, Ca, Mg, and K concentrations that resemble the average concentrations of Ozark MVT fluids. For this fluid mixture also to have the Cl/Br ratio of Ozark MVT ore fluids, the HHD brine would had to have equilibrated with Br-rich halite prior to mixing or dissolved Br-rich halite.

4) Mass balance calculations indicate that one L of Ozark MVT ore fluid would need to have reacted with 15,000 cm^3 of granite to acquire its high Pb content. This volume of

granite is much greater than that required to modify highly evaporatively concentrated seawater to the composition of Ozark MVT ore fluids.

5) The reaction path and binary mixing models presented suggest that the Cl/Br ratios of Ozark MVT ore fluids are unlikely to have been derived solely from seawater evaporation. Instead, the Cl/Br ratios of Ozark MVT ore fluids may be the result of interaction with halogen bearing silicates in the Ozark Plateau's Precambrian granitic basement.

3.9 References

Aleinikoff, J. N., Walter, M., Kunk, M.J., and Hearn, P. P., J r., 1993, Do ages of authigenic K-feldspar date the formation of Mississippi Valley-type Pb-Zn deposits, central and southeastern United States?: Pb isotopic evidence: Geology, v. 21, p. 73-76.

Appold, M. S. and Garven, G., 1999, The hydrology of ore formation in the Southeast Missouri district: Numerical models of topography-driven fluid flow during the Ouachita orogeny: Economic Geology, v. 94, p. 913-936.

Appold, M. S., Numelin, T. J., Shepherd, T. J., and Chenery, S. R., 2004, Limits on the metal content of fluid inclusions in gangue minerals from the Viburnum Trend, southeast Missouri, determined by laser ablation ICPMS: Economic Geology, v. 99, p. 185-198.

Appold, M. S. and Nunn, J. A., 2005, Hydrology of the western Arkoma basin and Ozark platform during the Ouachita orogeny: implications for Mississippi Valley-type ore formation in the Tri-State Zn-Pb district: Geofluids, v. 5, p. 308-325.

Appold, M. S., and Wenz, Z. J., 2011, Composition of ore fluid inclusions from the Viburnum Trend, Southeast Missouri District, United States: Implications for transport and precipitation mechanisms: Economic Geology, v. 106, p. 55-78.

Bickford, M. E., Sides, J. R., and Cullers, R. L., 1981, Chemical evolution of magmas in the Proterozoic terrane of the St. Francois Mountains, southeastern Missouri; 1, Field, petrographic, and major element data: Journal of Geophysical Research, v. 86, p. 10365-10386.

Brockie, D. C., Hare, E. H., Jr, and Dingess, P. R., 1968, The geology and ore deposits of the Tri-State district of Missouri, Kansas and Oklahoma, *in* Ridge, J. D., editor, Ore deposits of the United States, 1933–1967: The Graton- Sales Volume: New York, American Institute of Mining, Metallurgical and Petroleum Engineers, p. 400-430.

Coveney, R. M., Jr., Ragan, V. M., Brannon, J. C., 2000, Temporal benchmarks for modeling Phanerozoic flow of basinal brines and hydrocarbons in the southern mid-continent based on radiometrically dated calcite: Geology, v. 28, p. 795-798.

Crocetti, C. A., Holland, H. D., and McKenna, L. W., 1988, Isotopic composition of lead in galenas from the Viburnum Trend, Missouri: Economic Geology, v. 83, p. 355-376.

Crocetti, C. A., and Holland, H. D., 1989, Sulfur-lead isotope systematics and the composition of fluid inclusions in galena from the Viburnum Trend, Missouri: Economic Geology, v. 84, p. 2196-2216.

Diehl, S. F., and Goldhaber, M. B., 1993, Feldspar diagenesis in Cambrian clastic rocks of the southern Ozarks and Reelfoot rift, southeastern Missouri and northeastern Arkansas—implication for Mississippi Valley-type ore genesis: U. S. Geological Survey Bulletin 1989-F, p. F1-F17.

Deloule, E., Allegre, C., and Doe, B., 1986, Lead and sulfur isotope microstratigraphy in galena crystals in Mississippi Valley-type deposits: Economic Geology, v. 81, p. 1307-1321.

Doe, B. R., and Delevaux, M. H., 1972, Source of lead in southeast Missouri galena ores: Economic Geology, v. 67, p. 409-425.

Faure, G., 1998, Principles and applications of geochemistry 2nd edition: New Jersey, Prentice Hall, 600 p.

Faure, G., and Mensing, T. M., 2005, Isotopes principles and applications 3rd edition: New Jersey, John Wiley and Sons Inc., 897 p.

Fontes, J. Ch., and Matray, J. M., 1993, Geochemistry and origin of formation brines from the Paris Basin, France: Chemical Geology, v. 109, p. 149-175.

Frape, S. K., and Fritz, P., 1987, Geochemical trends for groundwater from the Canadian Shield, *in* Fritz, P. and Frape, S. K., editors, Saline Water and Gases in Crystalline Rocks, Geological Association of Canada Special Paper 33, p. 19-38.

Fritz, P., and Frape, S. K., 1982, Saline groundwaters in the Canadian Shield—a first overview: Chemical Geology, v. 36, p. 179-190.

Garven, G., Ge, S., Person, M. A., Sverjensky, D. A., 1993, Genesis of stratabound ore deposits in the mid-continent basins of North America. I. The role of regional groundwater flow: American Journal of Science, v. 293, p. 497-568.

Gascoyne, M., Davison, C. C., Ross, J. D., and Pearson R., 1987, Saline groundwaters and brines in plutons in the Canadian Shield, *in* Fritz, P. and Frape, S. K., editors, Saline Water and Gases in Crystalline Rocks, Geological Association of Canada Special Paper 33, p. 53-68.

Goldhaber, M. B., Church, S. E., Doe, B. R., Aleinikoff, J. N., Brannon, J. C., Podosek, F. A., Mosier, E. L., Taylor, C. D., and Gent, C. A, 1994, Lead and sulfur isotope investigation of Paleozoic sedimentary rocks from the southern midcontinent of the United States: Implications for paleohydrology and ore genesis of the southeast Missouri lead belts: Economic Geology, v. 90, p. 1875-1910.

Gregg, J. M., 1985, Regional epigenetic dolomitization in the Bonneterre Dolomite (Cambrian), southeastern Missouri: Geology, v. 13, p. 503-506.

Gregg, J. M., and Shelton, K. L., 1989, Minor and trace element distributions in the Bonneterre Dolomite (Cambrian), southeast Missouri: Evidence for possible multiple basin fluid sources and pathways during lead-zinc mineralization: Geological Society of America Bulletin, v. 101, p. 221–230.

Hagni, R. D., 1983, Ore microscopy, paragenetic sequence, trace element content, and fluid inclusion studies of the coper-lead-zinc deposits of the southeast Missouri district, *in* Kisvarsanyi, G., Grant, S. K., Pratt, W. F., and Koenig, J. W., editors, International Conference on Mississippi Valley-type Lead-Zinc Deposits: Rolla, Missouri, University of Missouri-Rolla Press, Proceedings, p. 243-256.

Helgeson H. C., Kirkham,D. H., and Flowers, G. C., 1981, Theoretical prediction of the thermodynamic behavior of aqueous electrolytes at high pressures and temperatures. IV. Calculation of activity coefficients, and apparent molal and standard and relative partial molal properties to 600 °C and 5 kb: American Journal of Science, v. 281, p. 1249-1516.

Hermann, A. G., 1972, Bromine distribution coefficients for halite precipitated from modern seawater under natural conditions: Contributions to Mineralogy and Petrology, v. 37, p. 249-252.

Horita, J., Zimmermann, H., and Holland, H. D., 2002, Chemical evolution of seawater during the Phanerozoic: Implications from the record of marine evaporites: Geochimica et Cosmochimica Acta, v. 66, p. 3733-3756.

Imes, J. L., 1990, Major geohydrologic units and adjacent to the Ozark Plateaus province, Missouri, Arkansas, Kansas, and Oklahoma: U.S. Geological Survey Hydrologic Investigations Atlas HA-711-A, scale 1:750,000.

Imes, J. L., and Smith, B. J., 1990, Areal extent, stratigraphic relation, and geohydrologic properties of regional geohydrologic units in southern Missouri: U.S. Geological Survey Hydrologic Investigations Atlas HA-711-I.

Kendrick, M. A., Burgess, R., Leach, D., and Pattrick, R. A. D., 2002, Hydrothermal fluid origins in Mississippi Valley-type ore districts: Combined noble gas (He, Ar, Kr) and halogen (Cl, Br, I) analysis of fluid inclusions from the Illinois-Kentucky fluorspar district, Viburnum Trend, and Tri-State districts, mid-continent United States: Economic Geology, v. 97, p. 453-470.

Leach, D. L., 1973, Possible relationship of Pb-Zn mineralization in the Ozarks to Ouachita Orogeny: Geological Society of America Abstracts with Programs, v. 5, no. 3, p. 269.

Leach, D. L., 1979, Temperature and salinity of the fluids responsible for minor occurrences of sphalerite in the Ozark region of Missouri: Economic Geology, v. 74, p. 931-937.

Leach, D. L., 1994, Genesis of the Ozark Mississippi Valley-type metallogenic province, Missouri, Arkansas, Kansas and Oklahoma, USA, *in* Fontboté, L., and Boni, M., editors,Sediment-hosted Zn-Pb ores: Berlin, Springer-Verlag, p. 104-138.

Leach, D. L., Nelson, R. C., and Williams, D., 1975, Fluid inclusion studies in the northern Arkansas zinc district: Economic Geology, v. 70, p. 1084-1091.

Leach, D. L. and Rowan, E. L., 1986, Genetic link between Ouachita fold belt tectonism and the Mississippi Valley-type lead-zinc deposits of the Ozarks: Geology, v. 14, p. 931-935.

Long, K. R., Kelly, W. C., Ohle, E. L., and Lohmann K. C., 1986, Ground preparation and zinc mineralization in bedded and breccia ores of the Monte Cristo mine, northern Arkansas: Economic Geology, v. 81, p. 809-830.

Lowenstein, T. K., Timofeeff, M. N., Brennan, S.T., Hardie, L. A., and Demicco, R. V., 2001, Oscillations in Phanerozoic seawater chemistry: Evidence from fluid inclusions: Science, v. 294, p. 1086-1088.

Lowenstein, T. K., Hardie, L. A., Timofeeff, M. N., and Demicco, R.V., 2003, Secular variation in seawater chemistry and the origin of calcium chloride basinal brines: Geology, v. 31, p. 857-860.

McCaffrey M. A., Lazar B., and Holland H. D., 1987, The evaporation path of seawater and the coprecipitation of Br^- and K^+ with halite: Journal of Sedimentary Petrology, v. 57, p. 928-937.

McKnight, E. T., and Fischer, R. P., 1970, Geology and ore deposits of the Picher Field, Oklahoma and Kansas: U.S. Geological Survey Professional Paper 588, 165 p.

Nabelek, P. I., and Russ-Nabelek, C., 1990, The role of fluorine in the petrogenesis of magmatic segregations in the St. Francois volcano-plutonic terrane, southeastern Missouri, *in* Stein, H. J., and Hannah, J. L., editors, Ore bearing granite systems; Petrogenesis and mineralizing processes: Geological Society of America Special Paper 246, p. 71-87.

Newhouse, W. H., 1933, Temperature of formation of the Mississippi Valley lead-zinc deposits: Economic Geology, v. 28, p. 744-750.

Ragan, V. M., 1994, Mineralogy and fluid inclusion geochemistry of Tri-State–type mineralization in eastern Kansas: Economic Geology, v. 89, p. 1411-1418.

Ragan, V. M., Coveney, R. M., Jr., and Brannon, J. C., 1996, Migration paths for fluids and the northern limits of the Tri-State district from fluid inclusions and radiogenic isotopes, *in* Sangster, D.F., editor, Carbonate-hosted lead-zinc deposits: Society of Economic Geologists Special Publication 4, p. 419-431.

Roedder, E., 1963, Studies of fluid inclusions II: Freezing data and their interpretations: Economic Geology, v. 58, 167-211.

Roedder, E., 1967, Fluid inclusions as samples of ore fluids, *in* Barnes, H. L., editor, Geochemistry of Hydrothermal Ore Deposits: New York, Holt, Rinehart, and Winston, p. 515-574.

Roedder, E., 1977, Fluid inclusion studies of ore deposits in the Viburnum Trend, southeast Missouri: Economic Geology, v. 72, p. 474-479.

Rowan, E. L., and Leach, D. L., 1989, Constraints from fluid inclusions on sulfide precipitation mechanisms and ore fluid migration in the Viburnum Trend lead district, Missouri: Economic Geology, v. 84, p. 1948-1965.

Schmidt, R. A., 1962, Temperatures of mineral formation in the Miami-Picher district as indicated by liquid inclusions: Economic Geology, v. 57, p. 1-20.

Seelig, U., and Bucher, K., 2010, Halogens in water from the crystalline basement of the Gotthard rail base tunnel (central Alps): Geochimica et Cosmochimica Acta, v. 74, p. 2581-2595.

Shelton, K. L., Bauer, R. M., and Gregg, J. M., 1992, Fluid inclusion studies of regionally extensive epigenetic dolomites, Bonneterre Dolomite (Cambrian), southeast Missouri: Evidence of multiple fluids during dolomitization and lead-zinc mineralization: Geological Society of America Bulletin, v. 104, p. 675-683.

Shelton, K. L., Burstein, I. B., Hagni, R. D., Vierrether, C. B., Grant, S. K., Hennigh, Q. T., Bradley, M. F., and Brandom, R. T., 1995, Sulfur isotope evidence for penetration of MVT fluids into igneous basement rocks, southeast Missouri, U.S.A.: Mineralium Deposita, v. 30, p. 339-350.

Shelton, K. L., Gregg, J. M., and Johnson, A. W., 2009, Replacement dolomites and ore sulfides as recorders of multiple fluids and fluid sources in the Southeast Missouri Mississippi Valley-type District: Halogen-$^{87}Sr/^{86}Sr$-$\delta^{18}O$-$\delta^{34}S$ systematics in the Bonneterre Dolomite: Economic Geology, v. 104, pp. 733-748.

Siebenthal, C. E., 1916, Origin of the zinc and lead deposits of the Joplin region, Missouri, Kansas, Oklahoma: U.S. Geological Survey Bulletin 606, 283 p.

Stoffell, B., Appold, M. S., Wilkinson, J. J., McClean, N. A., and Jeffries, T. E., 2008, Geochemistry and evolution of Mississippi Valley-type mineralizing brines from the Tri- State and northern Arkansas districts determined by LA-ICP-MS microanalysis of fluid inclusions: Economic Geology, v. 103, p. 1411-1435.

Stoessell, R. K., and Carpenter, A. B., 1986, Stoichiometric saturation tests of $NaCl_{1-x}Br_x$ and $KCl_{1-x}Br_x$: Geochimica et Cosmochimica Acta, v. 50, p. 1465-1474.

Thacker, J. L., and Anderson, K. H., 1977, The geologic setting of the southeast Missouri lead district—regional geologic history, structure, and stratigraphy: Economic Geology, v. 72, p. 339-348.

Viets, J. G., Hostra, A. F., and Emsbo, P., 1996, Solute compositions of fluid inclusions in sphalerite from North American and European Mississippi Valley-type ore deposits: Ore fluids derived from evaporated seawater: Society of Economic Geologists Special Publication 4, p. 465-482.

Viets, J. G., and Leach, D. L., 1990, Genetic implications of regional and temporal trends in ore fluid geochemistry of Mississippi Valley-type deposits in the Ozark region: Economic Geology, v. 85, p. 842-861.

Warren, J. K., 2006, Evaporites: Sediments, resources and Hydrocarbons: Berlin, Springer-Verlag, 1035 p.

Wenz, Z. J., Appold, M. S., Shelton, K. L., and Tesfaye, S., under review, Geochemistry of Mississippi Valley-type Mineralizing Fluids of the Ozark Plateau: A Regional Synthesis

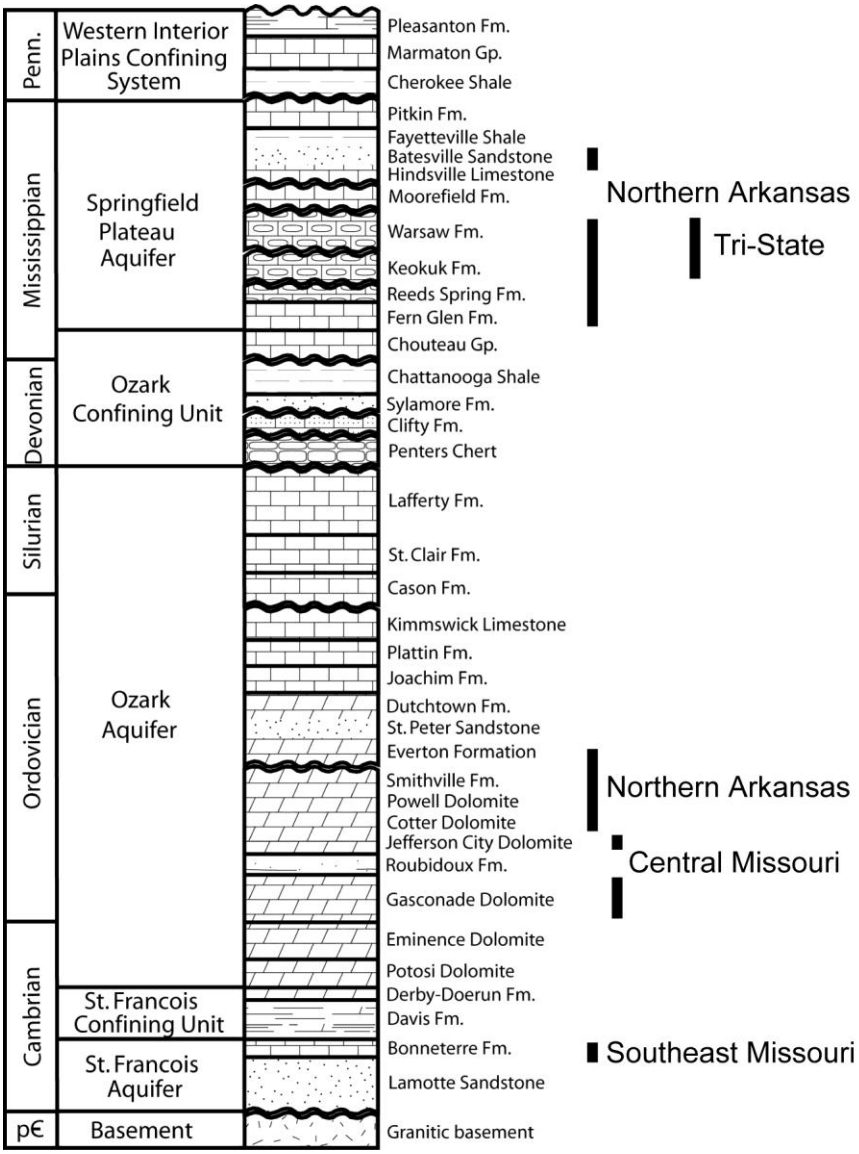

Fig. 3.1 Generalized stratigraphic section for the Ozark Plateau. Stratigraphic locations of the ore deposits are indicated by black bars (from Appold and Garven, 1999; data assembled from Brockie and others, 1968; Leach and others, 1975; Thacker and Anderson, 1977; Imes, 1990 and Imes and Smith, 1990).

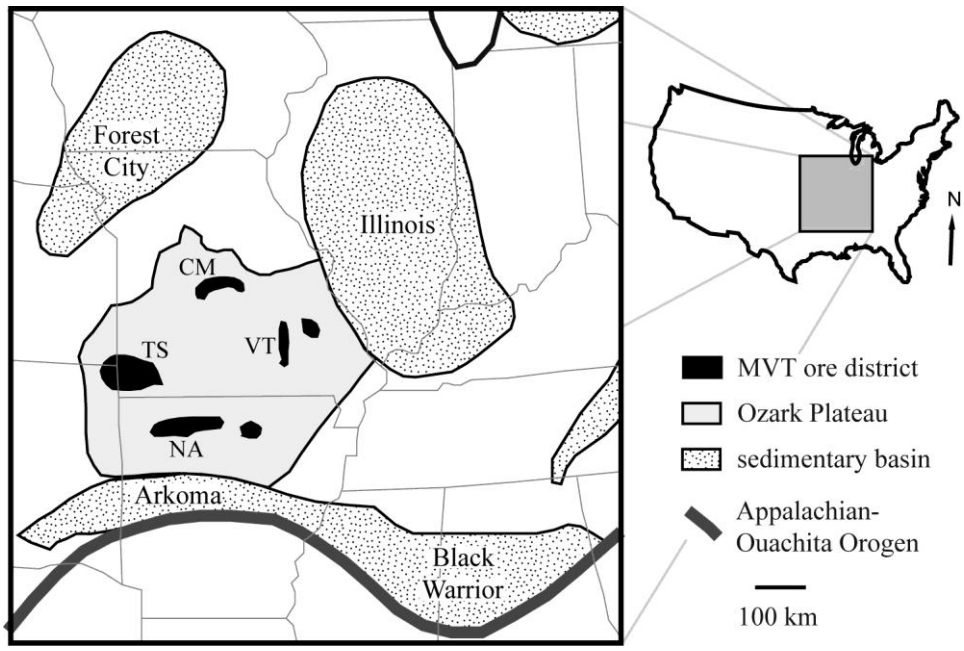

Fig. 3.2 Regional map of the Ozark Plateau and sedimentary basins showing the location of the Ozark MVT deposits (modified after Appold and Garven, 1999). Abbreviations: CM- Central Missouri district, NA- Northern Arkansas district, TS- Tri-State district, VT- Viburnum Trend.

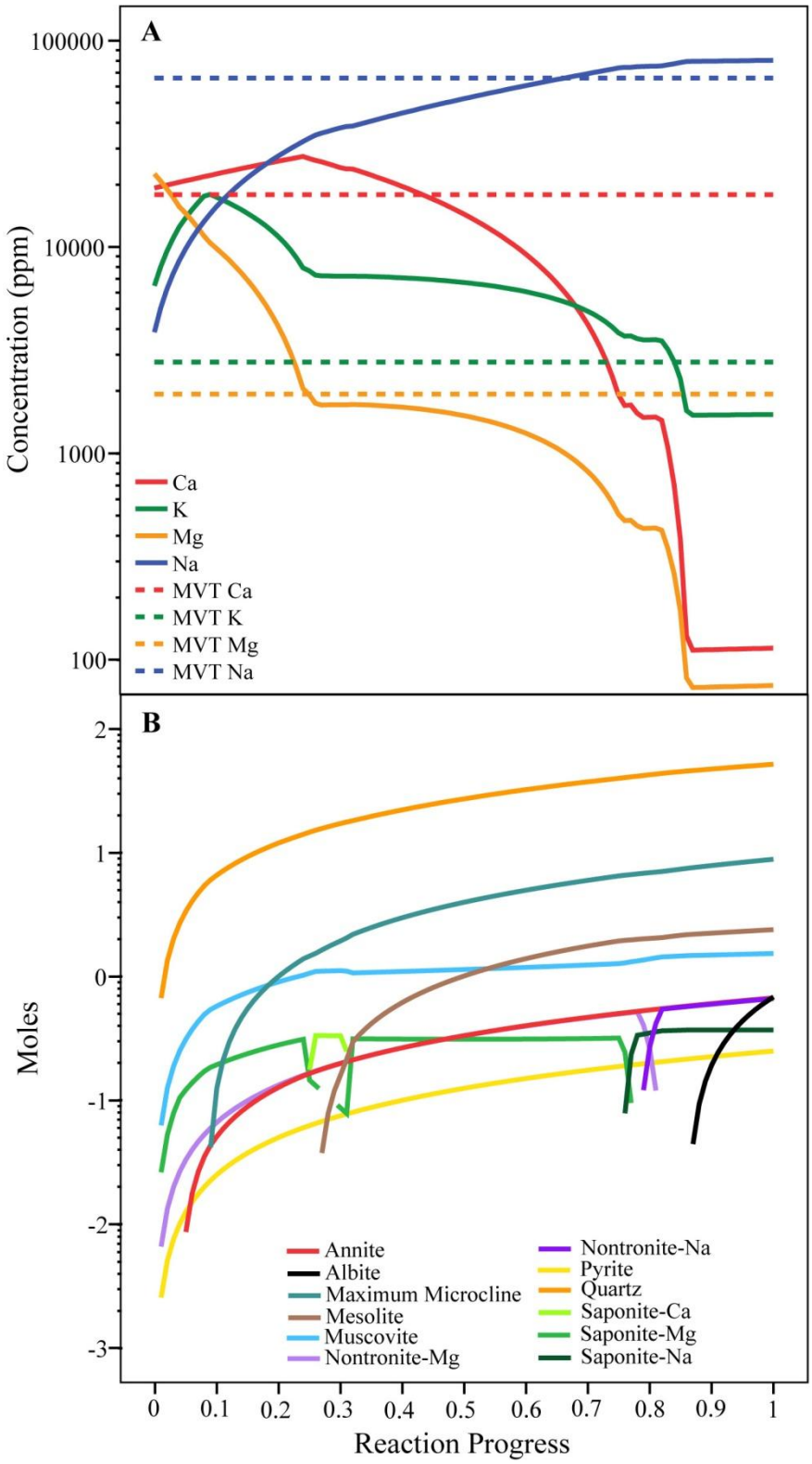

Fig. 3.3 Cambrian seawater titration model reaction path results for fluid composition and minerals present in the system. In A, the dashed lines represent the average composition of the Ozark MVT ore fluid.

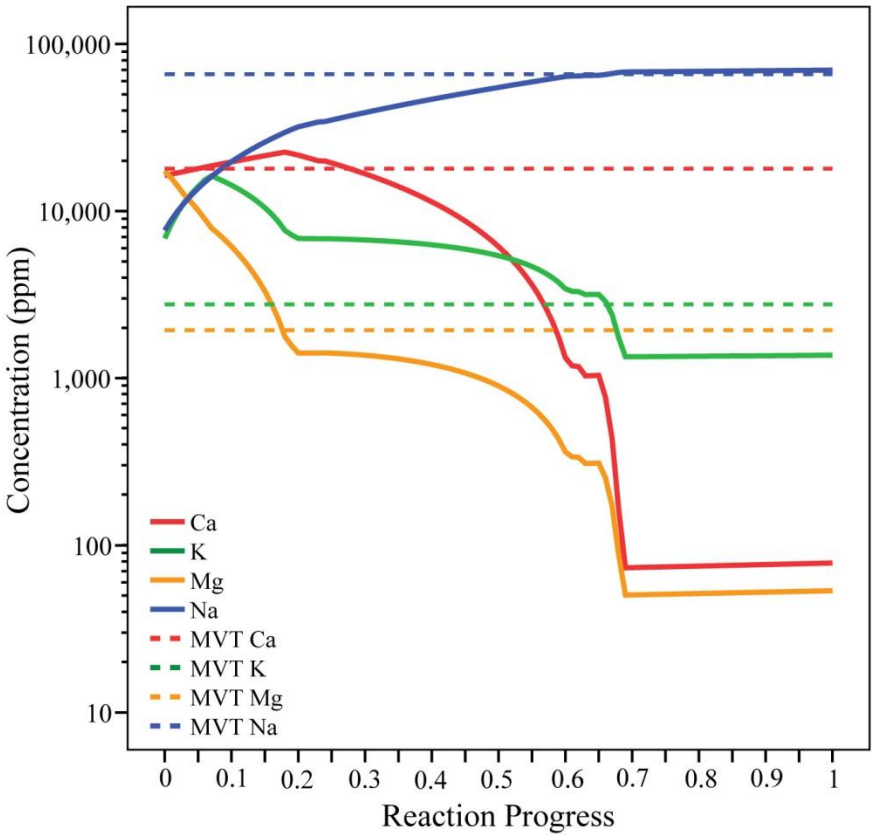

Figure 3.4 Late Silurian seawater titration model reaction path results for fluid composition. The dashed lines represent the average composition of the Ozark MVT ore fluid.

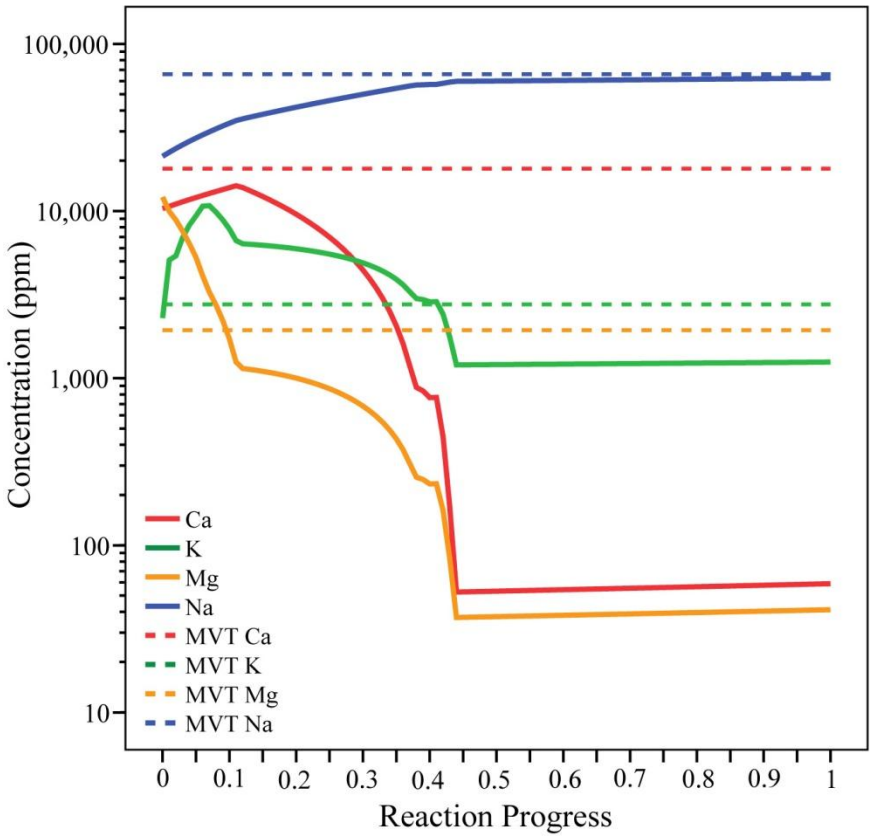

Figure 3.5 Middle Devonian seawater titration model reaction path results for fluid composition. The dashed lines represent the average composition of the Ozark MVT ore fluid.

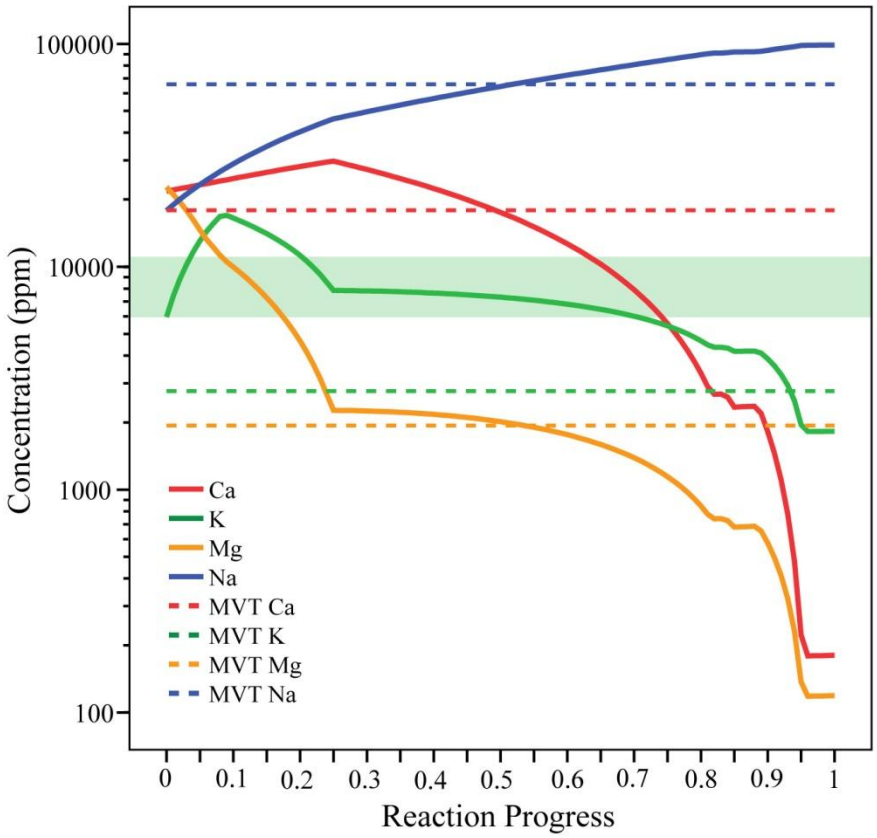

Fig. 3.6 Titration model reaction path results of the optimal fluid composition. The dashed lines represent the average composition of the Ozark MVT ore fluid. The light green shaded zone represents the range of K concentrations from the Viburnum Trend main stage Ag-rich sphalerite-hosted fluid inclusions.

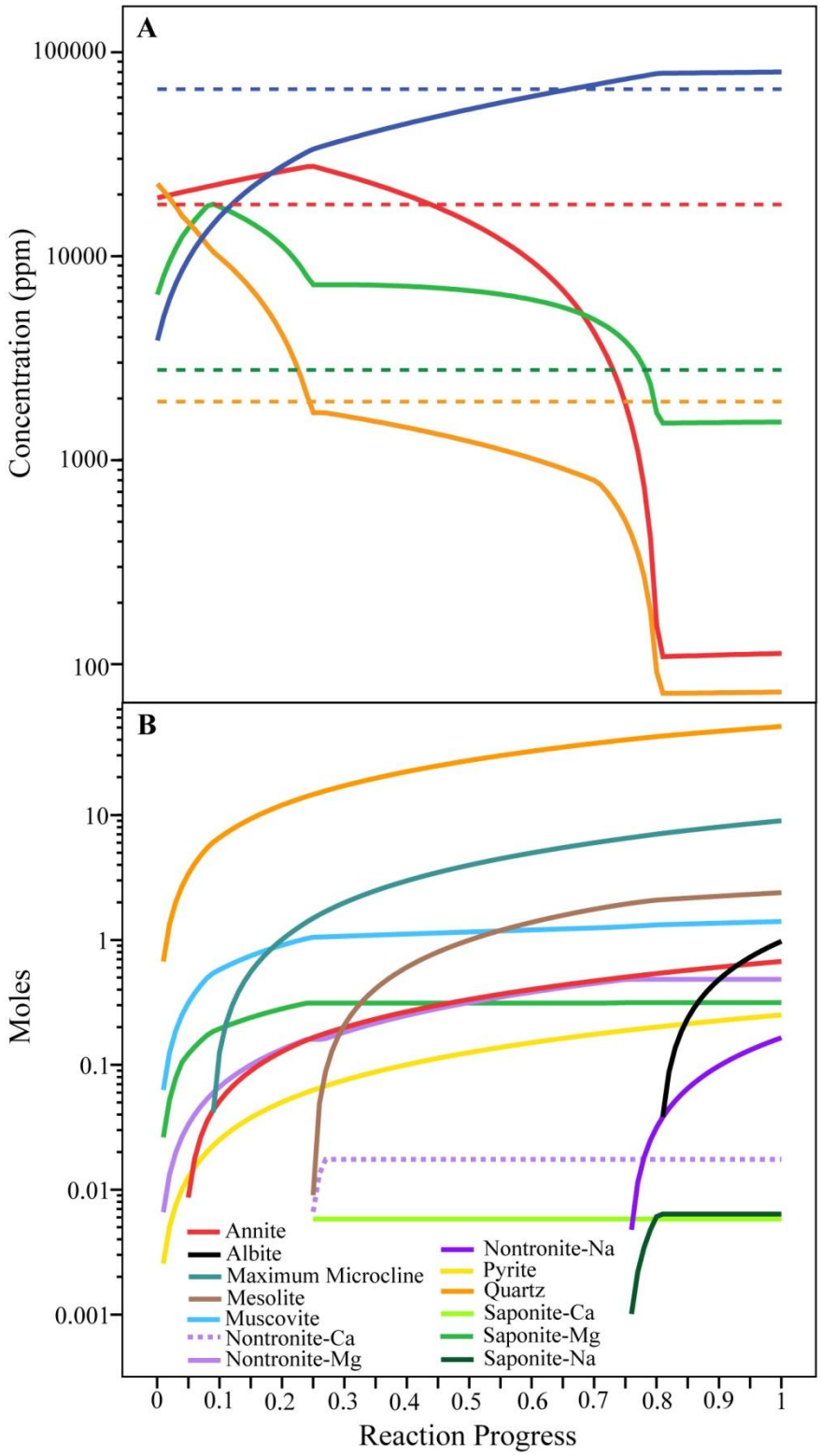

Fig. 3.7 Flow through model reaction path results for fluid composition and minerals present in the system. In the composition plot, dashed lines represent the average composition of the Ozark MVT ore fluid.

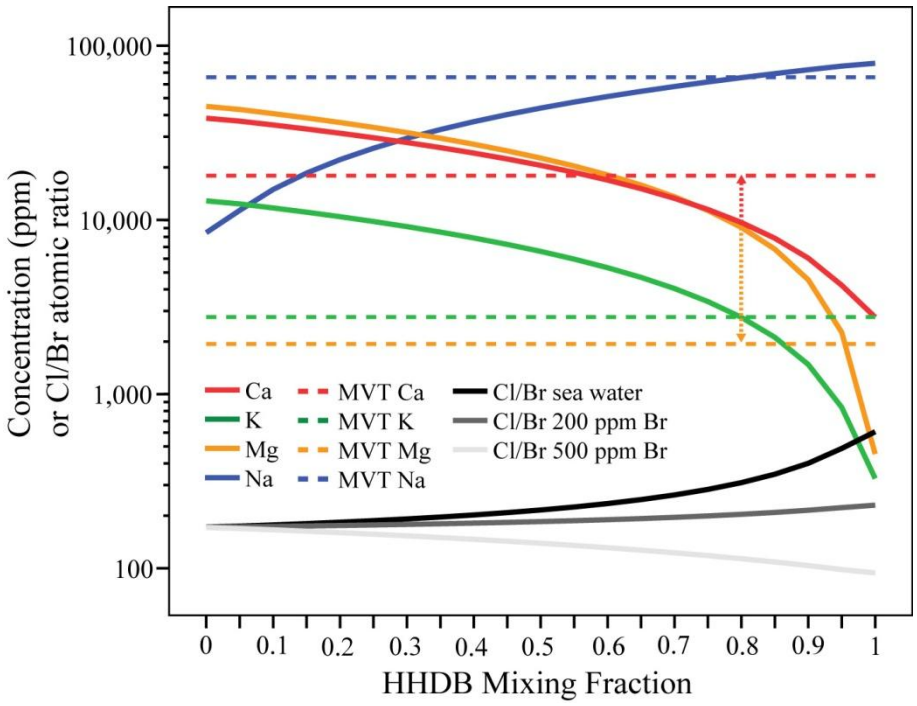

Fig. 3.8 Binary mixing model results. Dashed lines represent the average Ozark MVT ore fluid composition. Arrows on short dash lines point to the Ca and Mg concentrations for a 0.8 HHD brine mixture which reacted with calcite allowing a 1:1 molar exchange of Ca for Mg.

Table 3.1 Compositions of modern and ancient seawater and the Ozark MVT ore fluid.

Fluid Type	Na (ppm)	K (ppm)	Mg (ppm)	Ca (ppm)	Cl/Br atomic ratio
Ozark MVT ore fluid	65853	2769	1938	17929	90-100 (46-269*)
Cambrian ECSW	7731	12990	45290	38710	172
Late Silurian ECSW	15320	13720	34810	32590	173
Middle Devonian ECSW	42620	4584	24310	20730	278
modern ECSW	2889	3626	60513	0	77
Early Paleozoic 45x ECSW	31000	12000	29000	27000	157
Ideal ECSW	36000	12000	46000	44000	na
HHD brine	80000	200	0	2400	650, 232,93

ECSW= evaporatively concentrated seawater, * Cl/Br ratio of mainstage sulfides from the Viburnum Trend from Shelton et al. (2009). Modern seawater compositions are from McCaffery et al. (1987).

Table 3.2 Initial compositions of modeled fluids.

Variable	Cambrian ECSW	Late Silurian ECSW	Devonian ECSW	Optimal ECSW	HHD brine
Na (ppm)	3866	7660	21310	18000	80000
Mg (ppm)	22645	17405	12155	23000	0
K (ppm)	6495	6860	2292	6000	200
Ca (ppm)	19355	16295	10365	22000	2400
Cl (ppm)	110550	97600	86800	135000	84707
Br (ppm)	1448	1269	1269	1269	293
SiO_2(aq) (ppm)	1.0E-07	1.0E-07	1.0E-07	1.0E-07	-
Al (ppm)	0.002	0.002	0.002	0.002	-
Fe (ppm)	0.002	0.002	0.002	0.002	-
S (ppm)	9	9	9	9	-
pH	8	8	8	8	-
log fO_2	-53	-53	-53	-53	-

ECSW = evaporatively concentrated seawater

Table 3.3 Granite reactant mineral volume percent.

Mineral Reactant	Volume (cm^3)	Volume %
quartz	1020	34.00%
K-feldspar	1080	36.00%
albite	619.2	20.64%
anorthite	100.8	3.36%
annite	90	3.00%
pyrite	6	0.20%
muscovite	60	2.00%
magnetite	12	0.40%
hematite	12	0.40%

Table 3.4 Composition of reactant and reaction path precipitated minerals.

Mineral	Composition
Albite	$NaAlSi_3O_8$
Annite	$KFe_3AlSi_3O_{10}(OH)_2$
Anorthite	$CaAl_2Si_2O_5$
Hematite	Fe_2O_3
K-feldspar	$KAlSi_3O_8$
Magnetite	Fe_3O_4
Mesolite	$Na_{0.676}Ca_{0.657}Al_{1.99}Si_{3.01}O_{10} \cdot 2.647\ H_2O$
Muscovite	$KAl_3Si_3O_{10}(OH)_2$
Nontronite-Ca	$Ca_{0.165}Fe_2Al_{0.33}Si_{3.67} \cdot 12\ H_2O$
Nontronite-Mg	$Mg_{0.165}Fe_2Al_{0.33}Si_{3.67} \cdot 12\ H_2O$
Nontronite-Na	$Na_{0.33}Fe_2Al_{0.33}Si_{3.67} \cdot 12\ H_2O$
Pyrite	FeS_2
Quartz	SiO_2
Saponite-Ca	$Ca_{0.165}Mg_3Al_{0.33}Si_{3.67}O_{10}(OH)_2$
Saponite-K	$K_{0.33}Mg_3Al_{0.33}Si_{3.67}O_{10}(OH)_2$
Saponite-Mg	$Mg_{3.165}Al_{.33}Si_{3.67}O_{10}(OH)_2$
Saponite-Na	$Na_{0.33}Mg_3Al_{0.33}Si_{3.67}O_{10}(OH)_2$

APPENDIX 1

Sample	Th	Tm	area	Origin	NaCl eq wt%	Na	Mg	K	Ca	Cu	Sr	Ba	Pb
Viburnum Trend Sphalerite													
35_8V22_1_2_2_4	67	-2.5	35	s	4	1.4E+04	4.9E+02	1.0E+03	6.0E+02	-	1.4E+01	-	-
35_8V22_1_1_1_4	72	-2.5	72	s	4	1.2E+04	1.5E+03	7.5E+02	6.7E+02	-	4.7E+01	-	-
35_8V22_2_1_1_4	90	-23.1	32	p	24.4	7.4E+04	5.1E+03	7.1E+03	7.6E+03	-	2.3E+02	-	-
35_8V22_3_1_1_4	76	-20.8	70	p	22.8	7.5E+04	1.2E+03	1.5E+03	1.1E+04	-	2.7E+02	9.3E+00	-
35_8V22_4b_2_1_4	102	-22.8	35	p	24.2	7.3E+04	1.9E+03	4.5E+03	1.4E+04	-	5.4E+02	6.9E+00	-
35_8V22_4b_3_1_4	103	-22.8	40	p	24.2	7.1E+04	-	2.3E+03	1.8E+04	-	5.0E+02	1.7E+01	-
35_8V22_4b___4	nd	-22.8	171	p	24.2	7.1E+04	2.1E+03	2.1E+03	1.7E+04	-	4.9E+02	1.5E+01	-
81V22_1_2_1_5	93	-15.3	210	p	18.9	5.9E+04	1.3E+03	2.1E+03	1.0E+04	-	2.8E+02	1.1E+01	-
81V22_1_3_1_5	93	-15.2	162	p	18.8	5.8E+04	1.2E+03	2.1E+03	1.1E+04	-	3.5E+02	1.4E+01	-
81V22_2_3_1_5	114	-15.5	84	p	19	4.5E+04	4.3E+03	8.1E+03	1.5E+04	-	4.2E+02	1.6E+01	-
81V22_2_1_1_5	115	-15.5	63	p	19	5.5E+04	1.4E+03	3.8E+03	1.4E+04	-	4.4E+02	1.0E+01	-
81V22_2_2_1_5	114	-15.5	64	p	19	5.5E+04	1.7E+03	3.6E+03	1.3E+04	-	4.5E+02	1.6E+01	-
81V22_3_2_1_5	89	-22.1	18	p	23.8	5.8E+04	5.3E+03	1.1E+04	1.7E+04	-	4.3E+02	-	-
81V22_3_3_1_5	87	-22.1	63	p	23.8	6.1E+04	5.3E+03	9.1E+03	1.6E+04	-	5.0E+02	5.7E+00	-
81V22_3_1_1_5	89	-22.2	42	p	23.8	5.9E+04	4.9E+03	9.6E+03	1.8E+04	-	5.2E+02	6.1E+00	-
81V22_3_4_1_5	87	-22.1	20	p	23.8	6.2E+04	5.1E+03	7.3E+03	1.6E+04	-	5.5E+02	-	-
MAG13_1_2_1_5	102	-22.4	90	p	23.9	7.0E+04	-	4.2E+03	1.8E+04	-	7.3E+02	3.0E+01	-
MAG13_1_5_1_5	111	-22.4	180	p	23.9	6.4E+04	1.9E+03	2.6E+03	2.2E+04	-	9.4E+02	4.0E+01	-
MAG13_2_2_1_5	132	-23.1	308	p	24.4	6.9E+04	1.7E+03	3.3E+03	2.0E+04	-	7.4E+02	3.9E+01	5.1E+01
MAG13_2_1_1_5	130	-23.1	345	p	24.4	7.1E+04	1.6E+03	2.8E+03	1.8E+04	-	6.8E+02	3.3E+01	7.4E+01
MAG13_2_3_1_5	116	-23.1	290	p	24.4	6.7E+04	1.8E+03	2.6E+03	2.2E+04	-	8.6E+02	4.2E+01	-
MAG13_2_4_1_5	125	-23.1	100	p	24.4	6.7E+04	1.7E+03	2.3E+03	2.2E+04	-	8.4E+02	3.2E+01	-
MAG13_2_5_1_5	134	-23.1	92	p	24.4	6.9E+04	1.4E+03	-	2.2E+04	-	8.4E+02	4.2E+01	-
MAG13_3_1_1_4	116	-21.7	49	p	23.5	6.9E+04	1.5E+03	2.4E+03	1.7E+04	-	8.4E+02	2.9E+01	-
MAG13_3_5_1_6	114	-15.3	280	s	18.9	5.4E+04	1.5E+03	2.0E+03	1.4E+04	-	8.4E+02	1.2E+01	-
MAG13_3_1_1_6	117	-15.3	216	s	18.9	5.3E+04	1.5E+03	2.1E+03	1.6E+04	-	9.0E+02	1.5E+01	5.0E+02
MAG13_3_2_1_6	114	-15.3	95	s	18.9	4.8E+04	2.3E+03	2.2E+03	1.8E+04	-	1.1E+03	1.6E+01	1.1E+03
MAG13_4_1_1_4	106	-15.5	168	p	19	5.9E+04	1.0E+03	2.0E+03	1.1E+04	-	5.7E+02	1.2E+01	-
MAG13_4_3_1_4	110	-15.5	80	p	19	5.4E+04	1.8E+03	2.3E+03	1.4E+04	-	8.3E+02	2.1E+01	-
MAG13_4_2_1_4	110	-15.5	28	p	19	5.4E+04	-	-	1.5E+04	-	9.1E+02	-	-
MAG13_6_1_1_4	118	-23.1	63	p	24.4	7.5E+04	7.8E+02	3.6E+03	1.5E+04	-	5.9E+02	2.0E+01	-
MAG13_1a_1_1_6	135	-22.6	988	p	24.1	6.1E+04	1.8E+03	3.3E+03	2.5E+04	-	9.9E+02	4.6E+01	1.4E+02

MAG13_1b_1_1_6	133	-22.6	168	p	24.1	6.2E+04	2.2E+03	3.1E+03	2.4E+04	-	9.6E+02	3.8E+01	1.5E+03
MAG13_1c_3_2_4	119	-22.7	68	p	24.5	7.7E+04	-	3.9E+03	1.3E+04	-	6.2E+02	2.9E+01	-
MAG13_1c_1_1_6	115	-22.6	140	s	24.1	6.6E+04	1.5E+03	3.4E+03	2.1E+04	-	8.3E+02	3.5E+01	-
MAG13_1c_2_1_6	115	-22.6	48	s	24.1	5.2E+04	3.4E+03	4.1E+03	3.0E+04	-	1.3E+03	5.6E+01	-
MAG13_2a_1_1_6	115	-15.4	153	s	19	5.5E+04	1.4E+03	2.9E+03	1.4E+04	-	8.7E+02	1.8E+01	-
MAG13_2a_5_1_6	115	-15.4	160	s	19	5.4E+04	1.4E+03	2.6E+03	1.4E+04	-	7.0E+02	1.6E+01	-
MAG13_2a_4_1_6	115	-15.4	198	s	19	5.5E+04	1.7E+03	2.3E+03	1.4E+04	-	8.4E+02	1.1E+01	-
MAG13_2a_2_1_6	116	-15.4	396	s	19	5.2E+04	1.5E+03	2.5E+03	1.6E+04	-	9.5E+02	2.1E+01	-
MAG13_2a_3_1_6	115	-15.5	126	s	19	5.1E+04	1.6E+03	2.3E+03	1.7E+04	-	1.1E+03	2.1E+01	-
MAG13_2b_3_2_4	110	-15.5	80	p	19	5.4E+04	1.5E+03	2.0E+03	1.5E+04	-	8.1E+02	1.4E+01	-
MAG13A_1_1_1_3	116	-15.8	270	p	19.3	6.0E+04	1.1E+03	2.3E+03	1.1E+04	-	7.2E+02	1.9E+01	1.7E+02
MAG13A_1_3_1_3	113	-15.3	112	p	18.9	5.4E+04	1.4E+03	2.6E+03	1.4E+04	-	9.3E+02	1.6E+01	5.2E+01
MAG13A_1_2_1_3	108	-15.6	56	p	19.1	5.3E+04	1.6E+03	2.7E+03	1.6E+04	-	9.8E+02	1.8E+01	2.6E+02
MAG13A_1_5_1_3	116	-15.3	960	p	18.9	5.2E+04	1.5E+03	2.7E+03	1.6E+04	-	9.2E+02	1.5E+01	5.2E+01
MAG13A_1_4_1_3	105	-15.3	32	p	18.9	5.3E+04	1.6E+03	2.0E+03	1.6E+04	-	8.3E+02	1.2E+01	1.3E+02
MAG13A_2_1_1_3	111	-15.3	126	p	18.9	5.5E+04	1.0E+03	2.6E+03	1.4E+04	-	8.4E+02	1.3E+01	5.6E+01
MAG13A_2_4_1_3	114	-15.3	20	p	18.9	5.6E+04	8.4E+02	1.4E+03	1.4E+04	-	8.2E+02	2.7E+01	-
MAG13B_2_2_1_3	118	-22.6	24	p	24.1	6.6E+04	1.5E+03	3.4E+03	2.1E+04	-	8.4E+02	3.0E+01	2.7E+02
MAG13B_2_1_1_3	118	-22.6	18	p	24.1	6.6E+04	1.9E+03	2.4E+03	2.1E+04	-	8.5E+02	1.9E+01	-
VTSW2E_1_1_1_3	101	-20.8	24	p	22.9	7.0E+04	1.9E+03	8.6E+03	9.3E+03	-	2.5E+02	1.1E+01	-
VTSW2E_1_4_1_3	100	-20.8	35	p	22.9	6.3E+04	2.2E+03	6.1E+03	1.7E+04	-	1.1E+03	5.6E+01	-
VTSW2E_2_1_1_3	100	-20.8	30	p	22.9	6.0E+04	4.6E+03	1.0E+04	1.4E+04	-	3.4E+02	6.3E+00	-
WF2_1_1_1_5	102	-23.3	128	p	24.5	7.1E+04	2.2E+03	2.4E+03	1.8E+04	-	6.1E+02	2.0E+01	-
WF2_1_2_1_5	105	-23.3	64	p	24.5	7.3E+04	1.9E+03	2.0E+03	1.7E+04	-	6.1E+02	7.2E+01	-
WF2_2_1_1_4	112	-20.5	143	p	22.7	7.5E+04	1.2E+03	2.1E+03	9.8E+03	-	3.5E+02	9.7E+00	-
WF2_2_3_1_5	112	-23.3	63	p	24.5	6.6E+04	2.7E+03	4.2E+03	2.0E+04	-	6.2E+02	2.8E+01	-
WF2_2_1_1_5	124	-23.2	364	p	24.5	7.0E+04	1.9E+03	3.8E+03	1.8E+04	-	6.5E+02	2.5E+01	-
WF2_2_2_1_5	115	-22.9	108	p	24.3	6.8E+04	2.2E+03	2.5E+03	2.0E+04	-	6.9E+02	5.4E+01	-
WF2_3_2_1_5	115	-23.2	36	p	24.5	7.3E+04	-	3.8E+03	1.8E+04	-	6.5E+02	-	-
WF2_3_1_1_5	114	-23.2	322	p	24.5	7.3E+04	1.6E+03	3.1E+03	1.7E+04	-	6.0E+02	2.4E+01	-
WF2_3_1_1_4	108	-20.4	72	p	22.6	6.9E+04	1.5E+03	2.4E+03	1.4E+04	-	4.4E+02	1.5E+01	-
WF2_3_4_1_6	112	-22.9	221	s	24.3	6.9E+04	1.9E+03	3.0E+03	1.9E+04	-	7.0E+02	2.0E+01	-
WF2_3_2_1_6	112	-22.9	182	s	24.3	6.9E+04	1.7E+03	2.9E+03	2.0E+04	-	7.2E+02	2.4E+01	-
WF2_3_1_1_6	112	-22.9	221	s	24.3	6.9E+04	1.9E+03	2.7E+03	1.9E+04	-	7.0E+02	2.4E+01	-
WF2_3_3_1_6	113	-22.9	247	s	24.3	6.9E+04	2.0E+03	2.7E+03	1.9E+04	-	7.1E+02	2.1E+01	-
WF2_4_2_1_6	110	-22.8	198	p	24.2	7.2E+04	1.8E+03	2.8E+03	1.6E+04	-	5.0E+02	1.4E+01	-

WF2_4_1_1_6	110	-22.8	110	p	24.2	6.9E+04	2.1E+03	2.7E+03	1.9E+04	-	6.0E+02	1.4E+01	-
WF2_1a_1_1_6	131	-22.8	80	s	24.2	7.3E+04	1.2E+03	3.2E+03	1.6E+04	-	8.0E+02	3.0E+01	-
WF2_1a_2_1_6	131	-22.8	80	s	24.2	7.3E+04	1.1E+03	3.2E+03	1.7E+04	-	6.4E+02	1.2E+01	-
WF2_1z_2_1_4	96	-21.0	24	s	23	7.6E+04	4.2E+03	3.5E+03	4.6E+03	-	1.3E+02	-	-
WF2_1z_1_1_4	100	-21.0	84	s	23	6.1E+04	6.5E+03	7.8E+03	1.2E+04	-	4.2E+02	5.8E+00	-
WF2B_2_2_1_3	107	-22.5	45	p	24	6.8E+04	2.0E+03	2.3E+03	1.9E+04	-	7.8E+02	1.8E+01	-
WF2B_2_1_1_3	106	-22.5	255	p	24	6.9E+04	2.0E+03	2.1E+03	1.8E+04	-	5.6E+02	1.5E+01	-
Tri-State Sphalerite													
TSBS3-2_3_1_1_1	106	-20.9	325	p	23	7.3E+04	1.0E+03	1.5E+03	1.3E+04	-	8.8E+02	2.3E+01	-
TSBS3-2_3_2_1_1	101	-21.1	120	p	23.1	6.1E+04	1.7E+03	-	2.3E+04	-	8.8E+02	1.6E+01	-
TSBS3-2_4_1_1_1	nd	-21.0	78	p	23	5.7E+04	2.0E+03	6.5E+03	2.2E+04	-	1.1E+03	2.2E+01	1.5E+03
TSBS3-2_4_2_1_1	nd	-21.0	80	p	23	4.4E+04	1.7E+03	6.8E+03	3.5E+04	-	9.7E+02	-	6.7E+02
TSBS3-2_4_3_1_1	nd	-21.0	144	p	23	6.4E+04	1.8E+03	1.7E+03	1.9E+04	-	1.2E+03	2.5E+01	1.2E+03
TSBS3-2_7_3_1_1	109	-15.8	310	s	19.3	5.1E+04	1.8E+03	2.9E+03	1.8E+04	-	8.8E+02	1.2E+01	-
TSBS3-2_7_2_1_1	99	-15.8	1080	s	19.3	5.3E+04	1.8E+03	2.3E+03	1.7E+04	-	9.2E+02	1.8E+01	-
TSBS3-2_7_5_1_1	114	-15.8	338	s	19.3	5.4E+04	1.3E+03	1.8E+03	1.7E+04	-	8.3E+02	1.5E+01	-
TSBS3-2_13_6_1_1	102	-15.8	132	s	19.3	5.0E+04	1.8E+03	3.5E+03	1.9E+04	-	8.1E+02	1.0E+01	-
TSBS3-2_13_10_1_1	98	-15.8	154	s	19.4	5.1E+04	1.8E+03	2.3E+03	1.9E+04	-	9.2E+02	2.2E+01	-
TSBS3-2_13_7_1_1	95	-15.9	126	s	19.4	5.9E+04	1.5E+03	-	1.2E+04	-	1.0E+03	1.1E+01	-
TSBS3-2_13_8_1_1	100	-15.9	140	s	19.4	5.1E+04	1.7E+03	-	1.8E+04	-	1.1E+03	1.4E+01	-
TSBS5-2_1_1_1_3	110	-22.5	136	p	24	7.2E+04	1.7E+03	2.5E+03	1.6E+04	-	5.8E+02	1.6E+01	1.2E+02
TSBS5-2_2_3_1_3	120	-12.4	300	s	16.3	4.8E+04	1.0E+03	1.7E+03	1.2E+04	-	6.3E+02	1.4E+01	-
TSBS5-2_2_1_1_3	121	-12.4	270	s	16.3	4.4E+04	1.6E+03	1.8E+03	1.4E+04	-	7.2E+02	1.3E+01	-
TSBS5-2_2_2_1_3	120	-12.4	90	s	16.3	4.5E+04	-	-	1.4E+04	-	5.7E+02	1.8E+01	-
TSBS5-2_3_2_2_2	117	-22.2	336	p	23.8	6.7E+04	1.7E+03	3.6E+03	1.9E+04	-	7.6E+02	4.1E+01	-
TSBS5-2_3_1_1_2	119	-22.2	270	p	23.8	6.6E+04	1.6E+03	3.2E+03	2.0E+04	-	7.7E+02	3.9E+01	8.7E+02
TSBS5-2_3_3_2_2	117	-22.2	96	p	23.8	6.7E+04	1.6E+03	2.8E+03	1.9E+04	-	7.7E+02	2.9E+01	4.8E+02
TSBS5-2_3_4_1_2	119	-22.2	30	p	23.8	7.0E+04	-	-	1.9E+04	-	8.1E+02	4.7E+01	-
TSBS5-2_4_2_1_3	109	-22.5	120	p	24	7.1E+04	1.8E+03	2.6E+03	1.7E+04	-	6.0E+02	1.7E+01	4.2E+01
TSBS5-2_4_1_1_3	111	-22.5	154	p	24	6.8E+04	1.9E+03	2.7E+03	1.9E+04	-	6.9E+02	1.6E+01	1.7E+02
TSBS5-2_4_4_1_3	112	-22.5	126	p	24	6.6E+04	2.2E+03	2.7E+03	2.1E+04	-	7.9E+02	1.8E+01	-
TSBS5-2_4_6_1_3	111	-22.5	77	p	24	6.9E+04	1.8E+03	2.4E+03	1.9E+04	-	7.0E+02	2.2E+01	-
TSBS5-2_4_3_1_3	108	-22.5	84	p	24	7.0E+04	1.8E+03	2.2E+03	1.8E+04	-	6.6E+02	1.9E+01	2.0E+02
TSBS5-2_4_5_1_3	109	-22.5	120	p	24	6.8E+04	2.0E+03	2.3E+03	1.9E+04	-	6.8E+02	1.8E+01	-
TSBS5-2_3d_2_1_3	131	-22.9	72	p	24.3	6.6E+04	2.1E+03	3.8E+03	2.1E+04	-	7.6E+02	2.8E+01	-
TSBS5-2_3d_1_1_3	131	-22.9	364	p	24.3	6.9E+04	1.7E+03	3.0E+03	1.9E+04	-	7.0E+02	4.0E+01	-

TSBS5-2_3d_3_1_3	131	-22.9	364	p	24.3	6.8E+04	1.5E+03	3.1E+03	2.1E+04	-	7.7E+02	3.6E+01	-
TSBS5-2_3d_4_1_3	131	-22.9	50	p	24.3	6.6E+04	1.8E+03	3.2E+03	2.2E+04	-	9.2E+02	5.0E+01	-
TSBS5-2_3d_5_1_3	131	-22.9	115	p	24.3	6.7E+04	1.5E+03	2.9E+03	2.1E+04	-	8.0E+02	4.1E+01	-
TSCM2-1_2_3_1_2	113	-17.2	56	p	20.4	6.0E+04	1.6E+03	2.6E+03	1.4E+04	-	8.2E+02	1.1E+01	-
TSCM2-1_2_2_1_2	113	-16.9	90	p	20.1	5.8E+04	2.1E+03	2.1E+03	1.5E+04	-	1.0E+03	1.5E+01	-
TSCM2-1_2_4_1_2	113	-16.9	63	p	20.1	5.7E+04	1.6E+03	1.9E+03	1.7E+04	-	8.6E+02	1.7E+01	-
TSCM2-1_3_5_1_3	110	-18.0	368	p	21	6.1E+04	1.7E+03	2.4E+03	1.5E+04	-	8.5E+02	1.7E+01	-
TSCM2-1_3_3_1_3	104	-18.0	210	p	21	5.9E+04	1.9E+03	2.7E+03	1.7E+04	-	9.5E+02	1.2E+01	5.3E+01
TSCM2-1_3_2_1_3	110	-18.0	1120	p	21	6.0E+04	1.8E+03	2.4E+03	1.6E+04	-	9.2E+02	1.8E+01	-
TSCM2-1_3_1_1_3	106	-18.0	560	p	21	6.6E+04	1.5E+03	1.6E+03	1.1E+04	-	5.5E+02	1.0E+01	6.6E+01
TSCM2-1_3_4_1_2	91	-16.8	198	s	20.1	5.7E+04	-	-	1.8E+04	-	1.1E+03	1.1E+01	-
TSCM2-1_4_3_1_2	115	-18.2	63	p	21.1	6.2E+04	1.5E+03	2.1E+03	1.5E+04	-	8.8E+02	1.2E+01	-
TSCM2-1_4_1_1_2	115	-18.2	90	p	21.1	6.0E+04	1.6E+03	2.2E+03	1.7E+04	-	8.7E+02	1.0E+01	-
TSCM2-1_4_2_1_2	116	-18.4	42	p	21.1	6.0E+04	1.9E+03	-	1.6E+04	-	9.2E+02	2.2E+01	-
TSCM2-1_1a_4_1_3	107	-18.3	84	p	21.2	5.9E+04	1.3E+03	2.9E+03	1.8E+04	-	9.3E+02	1.8E+01	-
TSCM2-1_1a_1_1_3	106	-18.3	84	p	21.2	5.9E+04	2.2E+03	2.7E+03	1.7E+04	-	9.8E+02	1.7E+01	-
TSCM2-1_1a_3_1_3	106	-18.1	300	p	21	5.8E+04	1.8E+03	2.5E+03	1.8E+04	8.1E+02	9.7E+02	1.7E+01	7.8E+01
TSCM2-1_1a_2_1_3	106	-18.3	200	p	21.2	6.0E+04	2.1E+03	2.3E+03	1.6E+04	-	1.2E+03	1.5E+01	1.4E+02
TSCM2-1_1b_7_1_3	110	-18.1	35	p	21	5.7E+04	2.4E+03	2.8E+03	1.8E+04	-	1.0E+03	1.6E+01	-
TSCM2-1_1b_5_1_3	108	-18.3	161	p	21.2	5.8E+04	1.9E+03	2.3E+03	1.8E+04	-	9.9E+02	1.8E+01	1.2E+02
TSCM2-1_1b_6_1_3	108	-18.1	30	p	21	6.2E+04	2.1E+03	-	1.5E+04	-	8.7E+02	8.6E+00	-
TSCM2-1_2a_2_1_3	104	-18.1	160	p	21	5.9E+04	1.8E+03	2.3E+03	1.7E+04	-	9.3E+02	1.6E+01	1.5E+01
TSCM2-1_2a_4_2_3	104	-18.1	210	p	21	5.9E+04	1.9E+03	2.3E+03	1.7E+04	-	9.9E+02	1.4E+01	-
TSCM2-1_2a_3_1_3	104	-18.1	108	p	21	5.2E+04	2.9E+03	2.4E+03	2.2E+04	1.2E+03	1.2E+03	2.5E+01	3.0E+02
TSDW2-8_1_2_1_2	106	-23.4	136	p	24.6	7.5E+04	1.8E+03	2.3E+03	1.5E+04	-	4.8E+02	1.8E+01	2.1E+01
TSDW2-8_1_1_1_2	107	-23.4	260	p	24.6	7.6E+04	1.9E+03	2.1E+03	1.5E+04	-	4.9E+02	1.5E+01	7.7E+01
TSDW2-8_1_3_1_2	106	-23.4	176	p	24.6	7.3E+04	2.0E+03	2.2E+03	1.7E+04	-	5.9E+02	1.9E+01	5.0E+01
TSDW2-8_1_2_1_1	102	-22.7	60	p	24.1	6.6E+04	1.9E+03	2.1E+03	2.2E+04	-	4.8E+02	9.8E+00	5.0E+01
TSDW2-8_1_1_1_1	102	-22.7	180	p	24.1	6.6E+04	3.0E+03	-	2.1E+04	-	7.2E+02	1.5E+01	3.4E+01
TSDW2-8_2_2_1_1	100	-23.1	220	p	24.4	7.1E+04	2.3E+03	2.7E+03	1.8E+04	-	5.7E+02	2.0E+01	1.9E+01
TSDW2-8_2_1_1_1	100	-23.0	345	p	24.3	7.1E+04	2.3E+03	2.6E+03	1.8E+04	-	5.7E+02	2.0E+01	2.2E+01
TSDW2-8_3_1_1_1	94	-23.0	187	p	24.3	6.6E+04	2.9E+03	2.7E+03	2.1E+04	-	7.9E+02	8.5E+00	1.8E+01
TSDW2-8_4_1_1_1	92	-22.7	336	p	24.1	6.7E+04	2.2E+03	3.0E+03	2.0E+04	-	5.4E+02	1.6E+01	-
TSDW2-8_5_1_1_1	98	-22.7	468	p	24.1	7.2E+04	2.0E+03	2.3E+03	1.6E+04	-	5.0E+02	1.6E+01	1.3E+01
TSDW2-9_2_3_1_2	104	-23.2	88	p	24.5	7.2E+04	2.0E+03	2.1E+03	1.6E+04	1.5E+03	6.0E+02	1.6E+01	1.7E+02
TSDW2-9_2_5_1_2	104	-23.2	165	p	24.5	6.8E+04	2.1E+03	2.7E+03	2.1E+04	1.2E+03	5.8E+02	1.5E+01	9.6E+02

TSDW2-9_2_1_1_2	108	-23.2	90	p	24.5	6.8E+04	1.5E+03	2.5E+03	2.0E+04	1.6E+03	6.7E+02	1.9E+01	1.0E+02
TSDW2-9_2_4_1_2	104	-23.2	130	p	24.5	6.9E+04	2.2E+03	2.3E+03	1.9E+04	1.4E+03	5.9E+02	1.8E+01	1.3E+02
TSDW2-9_2_2_1_2	109	-23.2	77	p	24.5	7.2E+04	1.8E+03	1.7E+03	1.7E+04	1.7E+03	7.1E+02	1.9E+01	1.1E+02
TSGY2-3_3_3_1_2	108	-23.2	104	p	24.5	6.7E+04	1.4E+03	3.1E+03	2.2E+04	-	9.5E+02	3.2E+01	-
TSGY2-3_3_1_1_2	109	-23.0	150	p	24.3	6.5E+04	1.9E+03	2.9E+03	2.3E+04	-	9.8E+02	2.8E+01	-
TSGY2-3_3_2_1_2	109	-23.1	90	p	24.4	6.9E+04	1.7E+03	2.2E+03	2.0E+04	-	8.0E+02	2.7E+01	-
TSNC1-1_2_5_2_1	111	-22.7	105	p	24.1	6.7E+04	1.8E+03	4.5E+03	1.9E+04	-	8.4E+02	2.7E+01	6.7E+02
TSNC1-1_2_6_2_1	95	-22.7	60	p	24.1	6.3E+04	5.5E+03	-	1.9E+04	-	4.5E+02	2.6E+01	1.5E+02
TSNC1-1_2_4_2_1	100	-22.7	60	p	24.1	8.1E+04	3.9E+03	-	-	-	6.3E+02	-	7.8E+02
TSNC1-2_2_1_1_3	95	-22.5	352	p	24	7.1E+04	1.6E+03	2.3E+03	1.8E+04	-	6.6E+02	1.4E+01	-
TSNC1-2_1a_5_1_3	98	-23.1	120	p	24.4	6.9E+04	1.9E+03	2.9E+03	2.0E+04	-	7.4E+02	2.0E+01	-
TSNC1-2_1a_4_1_3	102	-23.1	135	p	24.4	6.9E+04	1.9E+03	2.5E+03	2.0E+04	-	6.7E+02	1.9E+01	-
TSNC1-2_1a_3_1_3	99	-23.1	72	p	24.4	7.2E+04	1.4E+03	2.3E+03	1.8E+04	-	6.2E+02	2.0E+01	-
TSNC1-2_1a_1_1_3	97	-23.1	48	p	24.4	7.0E+04	2.0E+03	2.5E+03	1.9E+04	-	6.4E+02	1.8E+01	-
TSNC1-2_1a_2_1_3	99	-23.1	72	p	24.4	6.7E+04	2.0E+03	2.5E+03	2.2E+04	-	7.0E+02	1.9E+01	-
TSNC1-2_1b_6_1?_3	97	-23.1	210	p	24.4	7.1E+04	1.7E+03	2.9E+03	1.8E+04	-	6.8E+02	2.0E+01	-
TSNC1-2_1b_8_1?_3	102	-23.1	102	p	24.4	6.9E+04	1.8E+03	2.6E+03	2.0E+04	-	6.6E+02	1.7E+01	-
TSOR2-3_1_1_1_5	113	-23.3	156	p	24.5	7.2E+04	2.1E+03	3.2E+03	1.7E+04	-	6.9E+02	2.7E+01	-
TSOR2-3_1_4_1_5	115	-23.2	45	p	24.5	6.7E+04	2.8E+03	3.6E+03	2.0E+04	-	7.7E+02	3.8E+01	-
TSOR2-3_1_5_1_5	115	-23.2	36	p	24.5	6.5E+04	3.8E+03	3.3E+03	2.0E+04	-	6.7E+02	2.0E+01	-
TSOR2-3_1_6_1_5	116	-23.2	42	p	24.5	6.2E+04	2.2E+03	3.7E+03	2.5E+04	-	6.8E+02	3.5E+01	-
TSOR2-3_1_3_1_5	113	-23.2	64	p	24.5	7.0E+04	2.2E+03	2.6E+03	1.8E+04	-	7.2E+02	4.5E+01	-
TSOR2-3_1_1_1_2	110	-23.2	176	p	24.5	7.2E+04	2.2E+03	2.1E+03	1.7E+04	-	6.2E+02	2.3E+01	-
TSOR2-3_1_2_1_5	115	-23.2	140	p	24.5	7.0E+04	1.7E+03	2.3E+03	1.9E+04	-	5.7E+02	1.9E+01	-
TSOR2-3_1_2_1_2	111	-23.2	40	p	24.5	7.3E+04	1.6E+03	-	1.7E+04	-	5.7E+02	2.2E+01	-
TSPC2-1_1_3_1_2	109	-22.8	120	s	24.2	6.8E+04	1.3E+03	3.9E+03	2.0E+04	-	8.4E+02	4.3E+01	4.2E+02
TSPC2-1_1_2_1_2	109	-22.8	95	s	24.2	6.9E+04	1.6E+03	2.5E+03	2.0E+04	-	8.1E+02	4.1E+01	-
TSPC2-1_1_1_1_2	109	-22.8	45	s	24.2	7.0E+04	-	-	2.1E+04	-	7.9E+02	1.9E+01	-
TSPC2-1_2_1_1_2	123	-22.7	3128	s	24.1	7.2E+04	1.3E+03	3.6E+03	1.6E+04	-	6.9E+02	3.3E+01	-
TSPC2-1_2_2_1_3	113	-22.7	936	s	24.1	6.5E+04	1.6E+03	3.0E+03	2.3E+04	-	9.7E+02	4.1E+01	6.9E+01
TSPC2-1_3_6_1_2	121	-23.1	33	p	24.4	6.6E+04	2.1E+03	4.8E+03	2.0E+04	-	6.4E+02	1.6E+01	6.4E+02
TSPC2-1_3_1_1_2	119	-23.1	96	p	24.4	7.2E+04	2.0E+03	1.9E+03	1.8E+04	-	6.2E+02	1.4E+01	2.6E+02
TSPC2-1_3_4_1_2	123	-23.1	135	p	24.4	7.0E+04	2.0E+03	2.0E+03	1.9E+04	-	6.2E+02	2.3E+01	2.3E+02
TSPC2-1_3_5_1_2	122	-23.2	42	p	24.5	7.0E+04	2.5E+03	-	1.9E+04	-	7.2E+02	1.9E+01	-
TSPC2-1_3_2_1_2	119	-23.2	84	p	24.5	6.9E+04	1.9E+03	-	2.1E+04	-	6.3E+02	1.7E+01	2.8E+02
TSPC2-1_4_6_1_2	106	-22.8	120	p	24.2	7.2E+04	1.7E+03	2.6E+03	1.7E+04	-	6.3E+02	1.4E+01	-

TSPC2-1_4_1_1_2	107	-22.8	162	p	24.2	7.3E+04	2.6E+03	-	1.5E+04	-	6.1E+02	8.9E+00	-
TSPC2-1_5_1_1_2	113	-22.9	434	p	24.3	7.2E+04	1.6E+03	2.3E+03	1.7E+04	-	6.0E+02	1.5E+01	-
TSPC2-1_5_2_1_2	112	-22.9	176	p	24.3	7.1E+04	1.8E+03	2.3E+03	1.8E+04	-	6.5E+02	1.6E+01	-
TSPC2-1_5_3_1_2	112	-22.9	105	p	24.3	6.4E+04	2.3E+03	2.6E+03	2.3E+04	-	7.7E+02	1.7E+01	-
TSPC2-1_1a_2_1_6	119	-22.7	192	s	24.1	6.9E+04	1.9E+03	2.5E+03	1.9E+04	-	7.5E+02	1.8E+01	6.3E+01
TSPC2-1_1a_1_1_6	119	-22.7	180	s	24.1	7.1E+04	1.8E+03	2.1E+03	1.7E+04	-	5.8E+02	1.8E+01	6.2E+01
TSPC2-1_1a_3_1_6	119	-22.7	160	s	24.1	6.8E+04	2.2E+03	2.4E+03	2.0E+04	-	6.8E+02	1.9E+01	1.3E+02
TSPC2-1_1b_1_1_6	122	-22.5	294	s	24	7.1E+04	1.8E+03	2.4E+03	1.7E+04	-	6.1E+02	1.7E+01	1.8E+01
TSPC2-1_1b_2_1_6	119	-22.5	200	s	24	7.1E+04	1.7E+03	2.3E+03	1.7E+04	-	6.0E+02	1.8E+01	2.7E+01
TSPC2-1_1b_4_1_6	121	-22.5	280	s	24	6.9E+04	1.8E+03	2.3E+03	1.9E+04	-	6.5E+02	1.8E+01	5.3E+01
TSPC2-1_1b_3_1_6	121	-22.5	294	s	24	7.0E+04	1.7E+03	2.1E+03	1.8E+04	-	5.9E+02	1.5E+01	2.3E+01
TSPC2-1_1c_1_1_6	116	-22.9	416	p	24.3	6.8E+04	2.2E+03	2.3E+03	2.0E+04	-	7.0E+02	1.6E+01	-
TSPC2-1_1c_2_1_6	111	-22.9	75	p	24.3	6.6E+04	3.0E+03	2.1E+03	2.1E+04	-	7.9E+02	2.6E+01	-
TSTR1-2_1a_1_1_6	112	-18.4	220	p	21.3	6.7E+04	1.0E+03	2.8E+03	1.1E+04	-	6.8E+02	1.3E+01	4.9E+00
TSTR1-7_1_1_1_3	nd	-21.5	950	p	23.4	5.6E+04	2.7E+03	3.1E+03	2.6E+04	-	1.1E+03	2.3E+01	5.4E+01
TSTR1-7_2_3_2_3	110	-21.3	144	p	23.2	6.6E+04	1.8E+03	2.5E+03	1.8E+04	-	8.1E+02	2.5E+01	1.8E+02
TSTR1-7_2_2_2_3	108	-21.5	490	p	23.4	6.6E+04	1.9E+03	2.4E+03	1.9E+04	-	8.6E+02	2.1E+01	-
TSTR1-7_3_5_3_3	111	-21.3	84	p	23.2	6.5E+04	1.9E+03	2.6E+03	1.9E+04	-	8.7E+02	2.4E+01	-
TSTR1-7_3_7_3_3	111	-20.8	108	p	22.9	6.3E+04	1.9E+03	2.6E+03	2.0E+04	-	9.3E+02	2.1E+01	-
TSTR1-7_3_8_3_3	108	-20.8	170	p	22.9	6.1E+04	1.8E+03	2.7E+03	2.1E+04	-	1.0E+03	1.8E+01	-
TSTR1-7_3_6_3_3	112	-20.8	240	p	22.9	6.0E+04	1.9E+03	2.8E+03	2.2E+04	-	9.5E+02	2.0E+01	2.1E+01
TSTR1-7_4_9_4_3	111	-20.8	144	p	22.9	6.6E+04	2.0E+03	2.4E+03	1.8E+04	-	8.1E+02	2.0E+01	2.8E+02
TSTR1-7_4_10_4_3	111	-20.8	204	p	22.9	6.2E+04	2.0E+03	2.4E+03	2.0E+04	-	9.0E+02	2.7E+01	1.1E+02
TSTR1-7_5_11_1_3	108	-21.3	168	p	23.2	6.4E+04	2.5E+03	3.0E+03	1.9E+04	-	9.6E+02	1.6E+01	-
TSTR1-7_5_10_1_3	112	-20.7	140	p	22.8	6.5E+04	1.8E+03	2.6E+03	1.8E+04	-	9.0E+02	1.9E+01	-
TSTR1-7_5_12_6_3	111	-22.5	182	p	24	6.6E+04	2.7E+03	2.8E+03	1.9E+04	-	9.9E+02	3.2E+01	6.2E+01
TSTR1-7_5_9_1_3	111	-21.3	234	p	23.2	6.4E+04	2.9E+03	2.5E+03	1.9E+04	-	8.0E+02	2.0E+01	1.1E+02
TSTR1-7_5_14_6_3	112	-21.9	207	p	23.6	6.6E+04	1.8E+03	2.5E+03	2.0E+04	-	7.1E+02	2.7E+01	6.3E+01
TSTR1-7_5_13_6_3	112	-22.5	209	p	24	6.7E+04	2.4E+03	2.5E+03	2.0E+04	-	9.9E+02	2.1E+01	1.7E+02
TSTR1-7_5_12_1_3	108	-20.7	286	p	22.8	6.1E+04	2.3E+03	2.2E+03	2.1E+04	-	1.1E+03	3.2E+01	9.0E+01
TSTR1-7_5_11_5_3	112	-22.5	968	p	24	5.9E+04	2.6E+03	2.8E+03	2.6E+04	-	1.1E+03	3.5E+01	1.0E+01
TSTR1-7_6_2_1_2	112	-21.3	720	p	23.2	6.5E+04	2.1E+03	2.9E+03	1.9E+04	-	1.0E+03	2.0E+01	6.6E+00
TSTR1-7_6_1_1_2	108	-21.3	660	p	23.2	7.0E+04	1.5E+03	2.4E+03	1.5E+04	-	7.2E+02	2.1E+01	4.1E+00
TSTR1-7_6_17_8_3	113	-22.9	136	p	24.3	6.9E+04	1.6E+03	2.7E+03	2.0E+04	-	7.6E+02	2.8E+01	8.7E+01
TSTR1-7_6_15_7_3	109	-22.9	570	p	24.3	6.0E+04	2.2E+03	2.5E+03	2.7E+04	-	1.1E+03	2.7E+01	1.5E+01
TSTR1-7_6_3_1_2	108	-21.3	42	p	23.2	7.2E+04	1.8E+03	-	1.2E+04	-	6.7E+02	1.3E+01	6.9E+01

TSTR1-7_7_8_1_2	110	-21.3	133	p	23.2	6.6E+04	2.0E+03	2.9E+03	1.8E+04	-	8.5E+02	3.0E+01	4.8E+02
TSTR1-7_7_7_1_2	110	-21.3	930	p	23.2	6.8E+04	1.8E+03	2.5E+03	1.7E+04	-	7.1E+02	1.8E+01	1.2E+01
TSTR1-7_7_19_9_3	108	-20.5	1088	p	22.7	6.7E+04	1.7E+03	2.1E+03	1.6E+04	-	7.3E+02	1.5E+01	6.2E+00
TSTR1-7_8_6_1_2	108	-21.3	238	p	23.2	7.0E+04	1.5E+03	2.6E+03	1.5E+04	-	6.8E+02	2.1E+01	3.2E+01
TSTR1-7_8_5_1_2	113	-21.3	190	p	23.2	6.9E+04	1.9E+03	2.7E+03	1.6E+04	-	7.5E+02	2.4E+01	1.1E+02
TSTR1-7_8_4_1_2	110	-21.3	143	p	23.2	7.1E+04	1.3E+03	2.2E+03	1.5E+04	-	6.7E+02	1.8E+01	7.3E+01
TSTR1-7_1a_1_1_6	113	-23.1	220	p	24.4	7.1E+04	1.7E+03	2.6E+03	1.8E+04	-	8.3E+02	2.3E+01	-
TSTR1-7_1b_1_1_6	112	-22.4	414	p	23.9	6.4E+04	2.1E+03	3.3E+03	2.2E+04	-	9.3E+02	2.5E+01	-
TSTR1-7_1c_1_1_6	112	-22.4	238	p	23.9	7.5E+04	1.6E+03	2.2E+03	1.4E+04	-	5.8E+02	1.9E+01	-
TSTR1-7_1c_2_1_6	113	-22.4	160	p	23.9	6.7E+04	1.9E+03	2.5E+03	2.0E+04	-	8.8E+02	2.4E+01	-
TSWB3-9_1_9_1_2	124	-23.2	88	p	24.5	7.3E+04	1.6E+03	2.9E+03	1.7E+04	-	6.6E+02	1.2E+01	-
TSWB3-9_1_12_1_2	120	-23.2	54	p	24.5	7.4E+04	1.4E+03	2.7E+03	1.6E+04	-	6.4E+02	2.1E+01	2.5E+02
TSWB3-9_1_1_1_2	116	-23.2	1083	p	24.5	7.4E+04	1.6E+03	2.4E+03	1.6E+04	-	5.5E+02	1.6E+01	-
TSWB3-9_1_8_1_2	119	-23.2	104	p	24.5	7.3E+04	1.5E+03	2.3E+03	1.7E+04	-	5.8E+02	2.2E+01	-
TSWB3-9_1_2_1_2	118	-23.2	312	p	24.5	7.1E+04	1.7E+03	1.9E+03	1.9E+04	-	6.5E+02	1.5E+01	1.7E+02
TSWB3-9_1_6_1_2	120	-23.2	104	p	24.5	7.4E+04	1.4E+03	1.7E+03	1.7E+04	-	7.1E+02	1.5E+01	-
TSWB3-9_2_1_1_3	121	-22.9	104	s	24.3	6.9E+04	2.4E+03	2.4E+03	1.9E+04	-	7.9E+02	1.5E+01	-
TSWB3-9_2_7_1_3	121	-22.9	54	s	24.3	7.0E+04	2.0E+03	2.4E+03	1.9E+04	-	6.4E+02	1.6E+01	-
TSWB3-9_2_6_1_3	122	-22.9	90	s	24.3	6.8E+04	2.4E+03	2.5E+03	2.0E+04	-	7.0E+02	1.9E+01	-
TSWB3-9_2_4_1_3	122	-22.9	50	s	24.3	6.9E+04	2.1E+03	2.2E+03	1.9E+04	-	7.2E+02	1.7E+01	-
TSWB3-9_2_5_1_3	120	-22.9	70	s	24.3	6.7E+04	2.4E+03	2.2E+03	2.1E+04	-	7.0E+02	2.1E+01	-
TSWB3-9_2_2_1_3	121	-22.9	132	s	24.3	6.8E+04	2.2E+03	2.1E+03	2.0E+04	-	7.4E+02	1.9E+01	-
TSWC1-3_3_5_1_3	102	-16.5	96	p	19.8	5.8E+04	1.8E+03	2.0E+03	1.4E+04	3.7E+02	1.1E+03	1.0E+01	1.3E+02
TSWC1-3_3_1_1_3	102	-16.5	130	p	19.8	5.5E+04	2.0E+03	1.8E+03	1.7E+04	-	1.1E+03	8.8E+00	-
TSWC1-3_3_3_1_3	119	-16.5	456	p	19.8	5.0E+04	2.4E+03	2.1E+03	2.0E+04	-	1.2E+03	1.5E+01	-
TSWC1-3_3_4_1_3	102	-16.5	70	p	19.8	5.4E+04	1.8E+03	-	1.8E+04	-	1.1E+03	1.5E+01	1.4E+02
TSWC1-3_3_2_1_3	100	-16.5	40	p	19.8	5.4E+04	2.1E+03	-	1.8E+04	-	1.0E+03	7.5E+00	-
TSWC1-3_4_7_1_3	102	-16.5	66	p	19.8	5.3E+04	2.0E+03	3.1E+03	1.7E+04	7.6E+02	9.6E+02	1.7E+01	3.0E+02
TSWC1-3_4_6_1_3	102	-16.5	98	p	19.8	5.4E+04	2.1E+03	2.6E+03	1.6E+04	3.9E+02	1.1E+03	1.4E+01	2.2E+02
TSWC1-3_4_8_1_3	102	-16.5	77	p	19.8	5.4E+04	1.6E+03	1.7E+03	1.8E+04	5.8E+02	8.7E+02	9.8E+00	2.1E+02
Tri-State Quartz													
TSDW2-2_1_1_1_1	106	-21.9	198	p	23.6	7.8E+04	9.7E+02	-	1.1E+04	-	5.2E+02	1.5E+01	-
TSDW2-2_1_3_1_1	107	-22.1	64	p	23.8	7.2E+04	1.7E+03	1.5E+03	1.6E+04	-	5.3E+02	2.3E+01	-
TSDW2-2_2_1_1_1	63	-21.5	323	s	23.4	7.6E+04	1.0E+03	1.7E+03	1.1E+04	-	3.8E+02	1.5E+01	-
TSDW2-2_2_4_1_2	68	-21.8	70	s	23.6	6.7E+04	1.0E+03	-	2.0E+04	-	6.3E+02	1.8E+01	-
TSDW2-2_4_1_1_2	101	-22.1	70	s	23.8	8.0E+04	5.5E+02	1.3E+03	9.8E+03	-	3.4E+02	7.6E+00	-

TSDW2-2_5_1_1_2	101	-22.3	396	s	23.9	7.4E+04	1.4E+02	2.4E+03	1.6E+04	-	5.2E+02	1.6E+01	-
TSDW2-2_5_2_1_2	92	-22.2	286	s	23.8	8.1E+04	-	2.2E+03	9.0E+03	-	2.9E+02	7.4E+00	-
TSWC1-2_1c_5_1_2	115	-22.7	352	s	24.1	7.2E+04	1.8E+03	2.2E+03	1.6E+04	-	5.1E+02	1.6E+01	-
TSWC1-2_6a_1_1_2	134	-22.6	465	s	24.1	7.4E+04	4.4E+02	2.1E+03	1.7E+04	-	4.7E+02	1.3E+01	1.2E+00
TSWC1-2_6b_2_1_2	110	-22.7	399	s	24.1	8.0E+04	9.6E+02	2.5E+03	1.0E+04	-	3.4E+02	1.3E+01	1.6E+00
TSWC1-2_6b_5_1_2	113	-22.7	132	s	24.1	8.0E+04	7.1E+02	1.8E+03	1.1E+04	-	3.7E+02	1.4E+01	-
TSWC1-2_5_1_1_3	nd	-22.1	161	s	23.8	7.9E+04	7.1E+02	2.5E+03	1.1E+04	-	3.2E+02	1.5E+01	2.9E+00
TSWC1-2_5_2_1_3	87	-22.1	468	s	23.8	7.7E+04	5.1E+01	1.8E+03	1.4E+04	-	4.4E+02	1.7E+01	2.1E+00
TSWC1-2_5_3_1_3	123	-22.5	110	s	24	7.6E+04	3.0E+02	2.4E+03	1.5E+04	-	4.3E+02	1.7E+01	-
TSWC1-2_5_4_1_3	140	-22.5	80	s	24	7.7E+04	2.6E+02	2.3E+03	1.4E+04	-	4.2E+02	1.7E+01	-
TSWC1-2_5_7_1_3	128	-22.5	96	s	24	7.7E+04	-	1.8E+03	1.4E+04	-	3.9E+02	1.4E+01	-
TSWC1-2_1_6_1_1	113	-22.5	176	p	24	8.8E+04	1.4E+03	-	-	-	5.9E+02	1.9E+01	-
TSWC1-2_1c_6_1_2	78	-22.7	425	s	24.1	7.1E+04	1.7E+03	2.5E+03	1.7E+04	-	5.9E+02	1.6E+01	6.1E-01
Northern Arkansas Sphalerite													
NACP1-8_1_1_1_1	110	-20.4	297	p	22.6	6.6E+04	1.6E+03	2.2E+03	1.7E+04	-	5.8E+02	1.7E+01	-
NACP1-8_1_2_1_1	nd	-20.4	108	p	22.6	6.4E+04	1.9E+03	2.2E+03	1.8E+04	-	6.6E+02	1.9E+01	-
NACP1-8_2_1_1_2	100	-22.2	48	p	23.8	6.4E+04	2.0E+03	7.5E+03	1.9E+04	-	5.3E+02	4.3E+01	-
NACP1-8_2_2_1_1	99	-22.7	475	p	24.1	7.2E+04	1.7E+03	2.0E+03	1.7E+04	-	5.3E+02	1.6E+01	-
NACP1-8_2_2_1_2	97	-22.2	70	p	23.8	6.8E+04	2.1E+03	2.2E+03	1.9E+04	-	6.5E+02	1.9E+01	-
NACP1-8_2_3__1	nd	-22.7	170	p	24.1	6.7E+04	2.7E+03	2.2E+03	2.0E+04	-	6.6E+02	1.5E+01	-
NACP1-8_2_1_1_1	103	-22.5	372	p	24	6.2E+04	1.9E+03	1.9E+03	2.5E+04	-	5.5E+02	1.7E+01	-
NACP1-8_3_1_1_3	112	-22.5	126	p	24	7.0E+04	1.8E+03	2.2E+03	1.7E+04	5.9E+02	6.1E+02	1.6E+01	1.3E+02
NACP1-8_3_2_1_3	112	-22.5	88	p	24	6.9E+04	1.8E+03	2.2E+03	1.8E+04	7.2E+02	6.4E+02	1.8E+01	5.9E+01
NACP1-8_3_3_1_3	112	-22.5	104	p	24	6.6E+04	2.0E+03	2.4E+03	2.0E+04	1.3E+03	8.0E+02	1.9E+01	1.2E+02
NACP1-8_3_4_1_3	107	-22.5	42	p	24	6.8E+04	1.5E+03	2.3E+03	2.0E+04	-	7.9E+02	1.6E+01	-
NACP1-8_3_4__1	nd	-22.1	60	p	23.8	6.5E+04	2.9E+03	-	2.0E+04	-	7.1E+02	1.6E+01	-
NACP1-8_3_1_1_1	116	-22.1	98	p	23.8	5.9E+04	2.2E+03	-	2.7E+04	-	1.1E+03	1.4E+01	-
NACP1-8_4_4__2	nd	-21.6	0	p	23.4	6.8E+04	2.0E+03	2.5E+03	1.7E+04	-	7.2E+02	1.6E+01	-
NACP1-8_4_2_1_2	87	-21.6	133	p	23.4	6.6E+04	1.5E+03	2.4E+03	2.0E+04	-	6.4E+02	1.7E+01	-
NACP1-8_5_3_1_1	nd	-23.4	532	p	24.6	7.2E+04	1.6E+03	3.0E+03	1.8E+04	-	6.1E+02	1.7E+01	-
NACP1-8_5_2_1_1	101	-23.4	220	p	24.6	6.7E+04	2.4E+03	3.3E+03	2.1E+04	-	7.2E+02	2.6E+01	-
NACP1-8_5_1_1_1	109	-23.2	486	p	24.5	6.9E+04	1.8E+03	2.7E+03	2.0E+04	-	6.5E+02	1.7E+01	-
NACP1-8_5_3_1_3	103	-22.6	93	p	24.1	7.4E+04	2.1E+03	2.2E+03	1.4E+04	-	5.3E+02	1.7E+01	-
NACP1-8_5_2_1_3	103	-22.6	320	p	24.1	7.1E+04	1.7E+03	2.3E+03	1.7E+04	-	5.8E+02	1.5E+01	-
NACP1-8_5_4_1_3	103	-22.6	112	p	24.1	6.9E+04	1.7E+03	2.5E+03	1.9E+04	-	6.6E+02	1.5E+01	-
NACP1-8_5_1_1_3	109	-22.6	385	p	24.1	6.9E+04	2.0E+03	2.4E+03	1.9E+04	-	6.5E+02	1.5E+01	-

NAEX1-14_1_1_1_2	110	-22.0	222	p	23.7	6.7E+04	2.4E+03	4.6E+03	1.7E+04	-	5.2E+02	1.6E+01	-
NAEX1-14_1_2_1_2	111	-22.2	30	p	23.8	7.2E+04	1.6E+03	2.2E+03	1.6E+04	-	5.0E+02	1.5E+01	-
NAEX1-2_1_1_1_2	102	-22.9	0	p	24.3	7.1E+04	1.8E+03	2.4E+03	1.8E+04	-	5.6E+02	1.8E+01	-
NAEX1-2_1_2_1_2	101	-22.9	0	p	24.3	7.2E+04	1.6E+03	1.9E+03	1.7E+04	-	6.1E+02	2.2E+01	-
NAEX1-2_1_3_1_2	101	-22.9	0	p	24.3	7.2E+04	-	-	1.8E+04	-	6.1E+02	2.1E+01	-
NAEX1-2_1_2_1_3	95	-22.5	30	s	24	6.7E+04	2.1E+03	2.4E+03	2.1E+04	-	6.5E+02	1.8E+01	-
NAEX1-2_1_1_1_3	95	-22.5	130	s	24	6.5E+04	2.4E+03	2.5E+03	2.2E+04	-	8.0E+02	2.0E+01	-
NAEX1-2_1_3_1_3	95	-22.5	20	s	24	7.0E+04	1.8E+03	1.9E+03	1.8E+04	-	5.8E+02	2.8E+01	-
NAEX1-2_2A_1_1_3	108	-22.6	168	s	24.1	7.2E+04	1.8E+03	2.3E+03	1.6E+04	-	4.8E+02	1.5E+01	-
NAEX1-2_2B_2_1_3	101	-22.6	72	s	24.1	7.0E+04	2.2E+03	2.5E+03	1.7E+04	-	4.9E+02	1.6E+01	3.1E+02
NAEX1-2_2B_3_1_3	113	-22.6	18	s	24.1	6.9E+04	2.3E+03	2.0E+03	1.9E+04	-	6.0E+02	4.5E+00	2.6E+02
NAEX1-2_3A_1_1_3	105	-21.8	189	s	23.6	6.9E+04	1.8E+03	2.6E+03	1.7E+04	-	4.8E+02	1.7E+01	8.5E+02
NAEX1-2_3B_3_1_3	106	-22.0	45	s	23.7	6.4E+04	2.2E+03	2.7E+03	2.1E+04	-	6.9E+02	1.6E+01	-
NAEX1-2_3B_2_1_3	105	-22.0	153	s	23.7	7.1E+04	2.1E+03	1.9E+03	1.5E+04	-	4.9E+02	1.2E+01	-
NAEX1-2_3C_5_1_3	104	-21.8	108	s	23.5	6.9E+04	1.5E+03	2.6E+03	1.7E+04	-	5.6E+02	1.4E+01	-
NAEX1-2_3C_4_1_3	104	-22.0	35	s	23.7	7.5E+04	9.4E+02	1.9E+03	1.4E+04	-	4.7E+02	1.2E+01	-
NAEX1-7_1_1_1_3	114	-21.8	360	p	23.6	6.7E+04	1.9E+03	2.2E+03	1.9E+04	-	6.0E+02	1.7E+01	4.5E+01
NAEX1-7_1_2_1_3	108	-21.8	70	p	23.6	6.2E+04	2.2E+03	2.4E+03	2.3E+04	-	7.0E+02	1.7E+01	2.1E+03
NAEX1-7_2_3_1_2	114	-16.1	80	p	19.5	5.4E+04	1.2E+03	3.6E+03	1.6E+04	-	9.6E+02	2.4E+01	1.9E+03
NAEX1-7_2_1_1_2	116	-16.1	748	p	19.5	5.2E+04	1.4E+03	2.6E+03	1.4E+04	-	8.5E+02	1.1E+01	1.0E+02
NAEX1-7_2_2_1_2	114	-16.1	247	p	19.5	5.3E+04	1.7E+03	2.2E+03	1.7E+04	-	1.1E+03	8.8E+00	-
NAEX1-7_2_4_1_2	114	-16.1	88	p	19.5	5.3E+04	2.1E+03	2.0E+03	1.7E+04	-	8.2E+02	1.1E+01	8.5E+02
NAEX1-7_4_1_1_2	114	-20.4	220	s	22.6	6.7E+04	1.6E+03	2.1E+03	1.6E+04	-	5.3E+02	1.5E+01	8.3E+01
NAEX1-7_4_2_1_2	114	-20.6	80	s	22.8	6.6E+04	1.7E+03	1.5E+03	1.8E+04	-	4.3E+02	9.8E+00	-
NAEX1-7_1a_2_1_2	130	-21.1	91	p	23.1	5.3E+04	1.5E+03	3.7E+03	2.2E+04	-	8.8E+02	5.5E+01	-
NAEX1-8_8_2_1_1	276	-20.0	392	p	22.4	6.2E+04	1.6E+03	2.9E+03	1.9E+04	-	7.6E+02	2.0E+01	-
NAEX1-8_8_1_1_1	329	-20.0	702	p	22.4	5.7E+04	1.9E+03	2.8E+03	2.4E+04	-	9.5E+02	2.4E+01	-
NAJP1-10_2_2_1_2	102	-22.7	64	p	24.1	6.8E+04	2.6E+03	2.3E+03	1.9E+04	1.9E+03	6.2E+02	2.0E+01	2.8E+02
NAJP1-10_2_3_1_2	103	-22.7	70	p	24.1	6.6E+04	2.1E+03	2.1E+03	1.8E+04	2.8E+03	7.0E+02	2.0E+01	-
NAJP1-10_2_1_1_2	104	-22.8	480	p	24.2	6.9E+04	2.1E+03	2.0E+03	1.8E+04	7.0E+02	5.6E+02	1.9E+01	4.7E+01
NAJP1-10_2_4_1_2	103	-22.8	156	p	24.2	6.9E+04	2.0E+03	2.0E+03	1.9E+04	4.4E+02	4.8E+02	1.4E+01	9.5E+01
NAJP1-10_4_1_1_2	111	-22.8	180	p	24.3	7.8E+04	1.3E+03	2.1E+03	1.2E+04	-	4.9E+02	1.5E+01	-
NAJP1-10_4_2_1_2	111	-22.8	70	p	24.2	6.7E+04	2.2E+03	2.0E+03	1.8E+04	3.3E+03	5.6E+02	1.5E+01	-
NAJP1-10_4_3_1_2	105	-22.9	50	p	24.2	7.2E+04	2.8E+03	-	1.5E+04	-	6.1E+02	2.4E+01	-
NAJP1-3_1_2_1_3	100	-21.5	117	p	23.4	7.1E+04	1.5E+03	2.1E+03	1.5E+04	-	4.9E+02	1.5E+01	4.9E+01
NAJP1-3_1_1_1_3	100	-21.5	180	p	23.4	6.8E+04	1.9E+03	2.3E+03	1.7E+04	-	5.3E+02	2.0E+01	7.9E+01

NAJP1-3_4_2_1_1	101	-22.5	315	p	24	7.1E+04	1.9E+03	2.5E+03	1.7E+04	7.5E+01	5.4E+02	1.5E+01	1.7E+01
NAJP1-3_4_1_1_1	100	-22.5	476	p	24	6.8E+04	2.6E+03	2.4E+03	1.8E+04	2.3E+02	5.2E+02	1.9E+01	6.4E+02
NAJP1-3_4_4_1_1	nd	-22.5	294	p	24	6.8E+04	2.2E+03	2.3E+03	1.9E+04	4.3E+02	5.3E+02	1.6E+01	6.0E+01
NAJP1-3_4_5_1_1	nd	-22.5	399	p	24	6.6E+04	2.1E+03	2.4E+03	2.1E+04	1.4E+02	5.9E+02	1.2E+01	3.0E+01
NAJP1-3o_1_1_1_1	101	-23.0	372	p	24.3	6.6E+04	2.5E+03	4.2E+03	2.0E+04	-	6.1E+02	1.3E+01	-
NALB1-1_1_1_1_6	134	-22.0	120	p	23.7	7.1E+04	1.6E+03	2.9E+03	1.5E+04	-	4.2E+02	1.9E+01	2.3E+02
NALB1-1_1_3_1_6	nd	-22.1	36	p	23.8	6.8E+04	2.0E+03	2.0E+03	1.9E+04	-	4.5E+02	-	3.4E+02
NALB1-1_1_2_1_6	134	-22.0	36	p	23.7	6.7E+04	1.9E+03	-	2.0E+04	-	5.1E+02	1.5E+01	2.9E+02
NALB1-1_2_2_1_6	91	-22.2	92	s	23.8	7.3E+04	1.2E+03	2.1E+03	1.6E+04	-	5.2E+02	1.8E+01	-
NALB1-1_2_1_1_6	136	-23.2	154	s	24.5	6.7E+04	2.4E+03	2.4E+03	2.1E+04	-	6.1E+02	1.9E+01	-
NALB1-1_3_1_1_2	89	-22.9	210	p	24.3	6.9E+04	2.2E+03	2.2E+03	2.0E+04	-	6.5E+02	1.6E+01	2.9E+01
NALB1-1_3_2_1_2	89	-22.9	80	p	24.3	6.8E+04	2.5E+03	-	1.7E+04	1.7E+03	5.1E+02	1.2E+01	3.2E+03
NALB1-1_1b_2_1_2	108	-22.1	35	p	23.8	6.9E+04	2.3E+03	2.2E+03	1.7E+04	-	5.7E+02	2.1E+01	-
NALB1-1_1b_1_1_2	107	-22.0	300	p	23.7	7.0E+04	1.9E+03	2.0E+03	1.7E+04	-	5.5E+02	1.7E+01	-
NALB1-1_1b_1_2_6	94	-21.3	77	s	23.2	6.6E+04	1.9E+03	3.3E+03	1.8E+04	-	4.4E+02	1.4E+01	-
NALB1-1_1b_2_2_6	94	-21.3	60	s	23.2	6.2E+04	2.6E+03	2.5E+03	2.1E+04	-	5.1E+02	1.7E+01	-
NALD1-2_1_1_1_4	125	-21.0	54	s	23	7.1E+04	1.7E+03	3.3E+03	1.3E+04	-	3.2E+02	1.3E+01	-
NALD1-2_1_2_1_4	117	-21.0	32	s	23	6.7E+04	1.9E+03	3.3E+03	1.6E+04	-	3.3E+02	1.2E+01	-
NALD1-2_1_1_1_1	114	-20.1	345	s	22.4	6.7E+04	1.7E+03	5.4E+03	1.3E+04	-	2.7E+02	8.0E+00	-
NALD1-2_2_1_1_1	106	-19.5	2580	p	22	6.5E+04	1.8E+03	2.9E+03	1.6E+04	-	3.3E+02	1.2E+01	3.4E+01
NALD1-2_2_2_1_4	102	-21.5	35	s	23.4	7.5E+04	1.6E+03	2.8E+03	1.1E+04	-	3.7E+02	2.1E+01	-
NALD1-2_2_1_1_4	102	-21.5	80	s	23.4	7.4E+04	1.3E+03	2.7E+03	1.2E+04	-	3.7E+02	1.2E+01	-
NALD1-4_1_2_1_4	60	-22.4	60	p	23.9	7.4E+04	1.4E+03	2.5E+03	1.5E+04	-	5.0E+02	1.2E+01	-
NALD1-4_1_4_1_2	116	-22.8	50	p	24.2	6.8E+04	1.5E+03	3.0E+03	2.1E+04	-	7.7E+02	5.3E+01	-
NALD1-4_1_1_1_4	106	-19.9	247	p	22.3	6.2E+04	2.2E+03	2.5E+03	1.9E+04	-	7.3E+02	1.2E+01	-
NALD1-4_2_6__	nd	-21.7	0	p	23.5	6.9E+04	1.7E+03	2.6E+03	1.7E+04	-	1.0E+03	1.3E+01	-
NALD1-4_2_2_1_6	115	-18.4	1122	p	21.3	5.8E+04	1.8E+03	2.8E+03	1.8E+04	-	9.7E+02	1.7E+01	5.6E+00
NALD1-4_2_3_1_6	118	-18.4	768	p	21.3	5.9E+04	1.9E+03	2.6E+03	1.8E+04	-	9.8E+02	1.5E+01	2.7E+01
NALD1-4_2_5_1_6	130	-21.7	220	p	23.5	6.5E+04	1.5E+03	2.8E+03	2.0E+04	-	8.3E+02	3.3E+01	8.7E+01
NALD1-4_2_1_1_6	115	-18.4	400	p	21.3	6.6E+04	1.2E+03	1.6E+03	1.3E+04	-	6.2E+02	9.4E+00	1.5E+00
NALD1-4_2_4_1_6	116	-18.4	1575	p	21.3	4.3E+04	2.3E+03	3.6E+03	3.0E+04	-	9.7E+02	4.4E+01	2.7E+01
NALD1-4_1a_1_1_3	110	-22.2	204	p	23.8	6.9E+04	2.0E+03	2.1E+03	1.8E+04	-	5.3E+02	1.7E+01	4.5E+01
NALD1-4_1c_10_3_3	113	-21.5	36	p	23.4	6.4E+04	2.3E+03	2.8E+03	2.0E+04	-	1.0E+03	1.6E+01	1.5E+02
NALD1-4_1c_9_3_3	113	-21.5	80	p	23.4	6.7E+04	2.0E+03	2.5E+03	1.7E+04	-	9.0E+02	1.4E+01	-
NALD1-4_1c_8_3_3	111	-21.5	126	p	23.4	6.7E+04	1.8E+03	2.2E+03	1.8E+04	-	9.0E+02	1.4E+01	5.0E+01
NALD1-4_1c_7_3_3	117	-21.8	91	p	23.6	6.9E+04	1.8E+03	2.0E+03	1.7E+04	-	5.3E+02	1.6E+01	6.0E+01

NALD1-4_2a_1_1_4	122	-20.4	252	p	22.6	6.3E+04	2.0E+03	2.6E+03	1.9E+04	-	1.0E+03	2.1E+01	6.0E+01
NALD1-4_2a_2_1_4	145	-22.4	180	p	23.9	6.1E+04	1.4E+03	3.2E+03	2.5E+04	-	8.2E+02	3.3E+01	5.6E+01
NALD1-4_2a_3_1_4	145	-22.4	54	p	23.9	5.4E+04	1.2E+03	2.2E+03	3.3E+04	-	6.9E+02	4.3E+01	8.9E+01
NALD1-4_2b_4_1_4	145	-22.4	170	p	23.9	6.9E+04	1.2E+03	3.0E+03	1.9E+04	-	7.7E+02	3.5E+01	7.3E+01
NALD1-4_2b_6_1_4	145	-22.4	132	p	23.9	6.8E+04	1.5E+03	3.0E+03	2.0E+04	-	8.0E+02	5.0E+01	4.5E+01
NALD1-4_2b_5_1_4	145	-22.4	216	p	23.9	5.8E+04	1.8E+03	2.8E+03	2.9E+04	-	8.0E+02	3.2E+01	9.0E+01
NAMC1-1_2_1_1_1	137	-23.0	80	p	24.3	6.9E+04	1.8E+03	-	2.0E+04	-	5.7E+02	2.4E+01	-
NAMC1-1_4_2_1_1	111	-23.2	80	p	24.5	7.4E+04	5.8E+02	3.3E+03	1.7E+04	-	3.9E+02	1.8E+01	-
NAMC1-1_4_1_1_1	111	-23.2	459	p	24.5	7.1E+04	1.9E+03	2.4E+03	1.9E+04	-	5.6E+02	1.7E+01	-
NAMC1-1_5_5_2_1	nd	-23.0	72	p	24.3	7.1E+04	1.6E+03	1.3E+03	1.9E+04	4.4E+02	5.6E+02	2.9E+01	3.9E+02
NAMC1-1_5_4_1_1	nd	-23.0	480	p	24.3	7.3E+04	2.4E+03	1.5E+03	1.6E+04	-	5.3E+02	2.7E+01	-
NAMC1-1_5_2_1_1	139	-23.0	371	p	24.3	7.0E+04	1.8E+03	1.5E+03	1.9E+04	-	5.5E+02	2.7E+01	-
NAMC1-1_5_3_1_1	134	-23.0	255	p	24.3	6.9E+04	2.4E+03	1.4E+03	2.0E+04	-	6.7E+02	3.1E+01	-
NAMC1-1_12_5_1_2	104	-22.3	136	s	23.9	7.0E+04	1.4E+03	2.7E+03	1.8E+04	-	5.4E+02	1.6E+01	-
NAMC1-1_12_2_1_2	103	-22.3	56	s	23.9	7.1E+04	1.5E+03	2.5E+03	1.7E+04	-	6.2E+02	1.8E+01	-
NAMC1-1_12_4_1_2	103	-22.3	66	s	23.9	7.0E+04	2.0E+03	2.5E+03	1.7E+04	-	5.8E+02	1.9E+01	-
NAMC1-1_12_1_1_2	100	-22.3	120	s	23.9	7.0E+04	1.9E+03	2.5E+03	1.7E+04	-	5.6E+02	1.8E+01	-
NAMC1-1_12_3_1_2	103	-22.3	64	s	23.9	6.8E+04	2.0E+03	1.9E+03	1.9E+04	-	5.1E+02	2.3E+01	-
NAMC1-1_12_6_1_2	104	-22.3	90	s	23.9	7.1E+04	1.8E+03	1.7E+03	1.7E+04	-	5.3E+02	2.0E+01	-
NAMC1-1_13_2_1_2	100	-22.2	190	s	23.8	7.1E+04	1.8E+03	2.2E+03	1.6E+04	-	5.5E+02	1.4E+01	-
NAMC1-1_13_1_1_2	107	-22.2	400	s	23.8	7.1E+04	1.7E+03	2.2E+03	1.7E+04	-	5.1E+02	1.6E+01	-
NAMC1-1_14_1_1_2	130	-22.3	192	p	23.9	7.1E+04	1.7E+03	2.7E+03	1.5E+04	1.1E+03	4.7E+02	1.6E+01	1.6E+02
NAMC1-1_14_4_2_2	130	-22.3	70	p	23.9	7.1E+04	1.5E+03	2.5E+03	1.7E+04	-	5.1E+02	1.7E+01	-
NAMC1-1_14_2_2_2	134	-22.3	60	p	23.9	7.5E+04	1.7E+03	-	1.5E+04	-	5.0E+02	1.8E+01	-
NAMC1-1_14_3_2_2	132	-22.3	30	p	23.9	7.0E+04	-	-	1.7E+04	-	5.8E+02	1.0E+01	-
NAMC1-1_15_1_1_2	104	-22.4	105	p	23.9	7.3E+04	1.7E+03	2.4E+03	1.5E+04	-	4.6E+02	1.9E+01	-
NAMC1-1_15_4_1_2	104	-22.4	84	p	23.9	7.1E+04	2.0E+03	2.4E+03	1.7E+04	-	5.0E+02	1.7E+01	-
NAMC1-1_15_3_1_2	104	-22.4	72	p	23.9	7.5E+04	1.3E+03	1.4E+03	1.5E+04	-	4.5E+02	1.9E+01	-
NAMC1-1_17_3_2_2	129	-22.3	56	p	23.9	7.1E+04	1.3E+03	3.3E+03	1.7E+04	-	5.2E+02	1.5E+01	-
NAMC1-1_17_2_1_2	125	-22.3	78	p	23.9	7.3E+04	1.7E+03	1.7E+03	1.6E+04	-	4.9E+02	1.7E+01	-
NAMC1-1_17_4_2_2	129	-22.3	66	p	23.9	7.2E+04	2.0E+03	-	1.6E+04	-	5.0E+02	9.9E+00	-
NAMC1-1_15b_7_1_2	109	-22.4	120	p	23.9	7.2E+04	1.7E+03	2.4E+03	1.6E+04	-	5.0E+02	1.4E+01	-
NAMC1-1_15b_8_1_2	108	-22.4	72	p	23.9	7.3E+04	1.7E+03	2.0E+03	1.5E+04	-	5.3E+02	2.4E+01	-
NAMC1-1_15b_6_1_2	108	-22.4	96	p	23.9	7.1E+04	1.5E+03	1.7E+03	1.7E+04	-	5.4E+02	1.4E+01	-
NAMC1-1_7a_3_1_2	106	-22.4	88	p	23.9	7.3E+04	1.2E+03	2.4E+03	1.6E+04	3.2E+03	4.7E+02	1.8E+01	2.4E+02
NAMC1-1_7a_6_1_2	106	-22.4	99	p	23.9	7.0E+04	2.1E+03	2.3E+03	1.7E+04	-	5.4E+02	1.6E+01	-

NAMC1-1_7a_8_1_2	106	-22.4	91	p	23.9	7.0E+04	2.1E+03	2.3E+03	1.7E+04	-	5.4E+02	1.6E+01	-
NAMC1-1_7a_4_1_2	106	-22.4	168	p	23.9	7.2E+04	1.7E+03	2.1E+03	1.6E+04	6.8E+02	5.3E+02	1.5E+01	8.2E+01
NAMC1-1_7a_5_1_2	106	-22.4	110	p	23.9	7.2E+04	1.7E+03	1.4E+03	1.7E+04	-	4.9E+02	1.5E+01	-
NAMC1-1_7a_7_1_2	106	-22.4	81	p	23.9	6.8E+04	2.5E+03	-	1.9E+04	-	6.4E+02	1.8E+01	-
NAMC1-1_7b_2_1_2	106	-22.4	81	p	23.9	6.9E+04	2.1E+03	2.2E+03	1.8E+04	-	5.2E+02	1.2E+01	-
NAPA1-1_1_4_1_4	106	-20.9	120	p	23	6.8E+04	1.8E+03	2.8E+03	1.5E+04	-	4.4E+02	1.5E+01	-
NAPA1-1_1_1_1_4	106	-20.9	384	p	23	6.8E+04	1.8E+03	2.7E+03	1.6E+04	-	4.4E+02	1.3E+01	-
NAPA1-1_1_2_1_4	106	-20.9	84	p	23	6.2E+04	1.9E+03	3.5E+03	2.0E+04	-	6.8E+02	1.4E+01	-
NAPA1-1_1_3_1_4	106	-20.9	180	p	23	6.8E+04	1.6E+03	2.7E+03	1.6E+04	-	4.1E+02	1.4E+01	-
NAPA1-13_1_3_1_4	101	-21.4	66	s	23.3	7.1E+04	1.5E+03	2.8E+03	1.4E+04	-	4.1E+02	9.9E+00	1.8E+02
NAPA1-13_1_1_1_4	101	-21.3	224	s	23.2	6.9E+04	1.7E+03	2.8E+03	1.6E+04	6.9E+01	5.0E+02	1.0E+01	2.7E+02
NAPA1-13_1_2_1_4	101	-21.4	77	s	23.3	6.9E+04	1.7E+03	2.7E+03	1.6E+04	-	4.0E+02	1.6E+01	1.0E+02
NAPA1-13_2_2_1_2	102	-21.2	63	p	23.2	6.2E+04	2.5E+03	3.5E+03	2.0E+04	-	6.5E+02	2.6E+01	-
NAPA1-13_2_1_1_2	102	-21.2	40	p	23.2	6.9E+04	1.6E+03	2.7E+03	1.6E+04	-	3.6E+02	1.4E+01	-
NAPA1-13_2_1_1_1	nd	-21.1	96	p	23.1	6.4E+04	2.2E+03	2.7E+03	1.9E+04	-	5.5E+02	1.3E+01	-
NAPA1-13_2_3_1_2	102	-21.2	56	p	23.2	5.2E+04	1.8E+03	3.3E+03	3.1E+04	-	7.5E+02	2.2E+01	-
NAPA1-13_2_1_1_4	95	-21.0	432	s	23	7.0E+04	1.5E+03	2.6E+03	1.4E+04	3.3E+02	3.8E+02	1.3E+01	5.2E+01
NAPA1-13_3_1_1_1	102	-21.1	341	s	23.1	6.6E+04	2.1E+03	2.7E+03	1.7E+04	-	3.8E+02	1.9E+01	-
NAPA1-13_3_4_1_1	nd	-21.0	220	s	23	6.4E+04	1.8E+03	2.8E+03	2.0E+04	-	4.0E+02	1.2E+01	-
NAPA1-13_4_1_1_4	105	-21.5	494	p	23.4	5.5E+04	2.7E+03	3.5E+03	2.7E+04	-	6.6E+02	1.7E+01	-
NAPA1-13_6_2_1_1	101	-21.5	918	s	23.4	6.7E+04	1.9E+03	2.7E+03	1.8E+04	-	4.0E+02	1.3E+01	-
NAPA1-13_6_3_1_1	140	-21.0	319	s	23	6.0E+04	2.6E+03	1.9E+03	2.3E+04	-	5.5E+02	1.7E+01	-
NAPA1-13_1a_4_1_6	108	-20.9	132	p	23	7.3E+04	8.4E+02	3.3E+03	1.2E+04	-	3.6E+02	6.7E+00	-
NAPA1-13_1a_3_1_6	107	-20.9	196	p	23	6.6E+04	1.7E+03	3.8E+03	1.7E+04	-	4.7E+02	1.4E+01	-
NAPA1-13_1a_2_1_6	107	-20.9	140	p	23	7.0E+04	1.4E+03	3.0E+03	1.4E+04	-	3.9E+02	1.0E+01	-
NAPA1-13_1a_5_1_6	107	-20.9	130	p	23	6.9E+04	1.7E+03	3.0E+03	1.5E+04	-	3.8E+02	9.5E+00	-
NAPA1-13_1a_1_1_6	106	-20.9	480	p	23	6.9E+04	1.7E+03	2.9E+03	1.5E+04	-	4.0E+02	1.1E+01	3.3E+02
NAPA1-13_1b_1_1_6	103	-20.9	322	p	23	6.7E+04	1.8E+03	2.8E+03	1.6E+04	-	4.2E+02	1.4E+01	-
NAPA1-13_1b_5_1_6	106	-20.9	96	s	23	6.7E+04	1.9E+03	2.8E+03	1.6E+04	-	4.2E+02	1.6E+01	-
NAPA1-13_1b_4_1_6	105	-20.9	63	s	23	6.5E+04	1.8E+03	3.0E+03	1.8E+04	-	4.7E+02	1.9E+01	-
NAPA1-13_2b_7_1_2	103	-21.2	135	p	23.2	7.0E+04	1.6E+03	2.9E+03	1.5E+04	-	3.7E+02	1.4E+01	-
NAPA1-13_2b_8_1_2	102	-21.2	104	p	23.2	6.8E+04	1.8E+03	2.9E+03	1.6E+04	-	4.0E+02	1.3E+01	-
NAPA1-13_2b_5_1_2	102	-21.2	56	p	23.2	7.0E+04	1.5E+03	2.6E+03	1.5E+04	-	3.6E+02	1.1E+01	-
NAPA1-13_2b_6_1_2	102	-21.2	130	p	23.2	6.8E+04	1.8E+03	2.4E+03	1.7E+04	-	4.2E+02	1.3E+01	-
NAPA1-13_2b_2_1_4	101	-21.1	88	s	23.1	6.9E+04	2.0E+03	2.9E+03	1.4E+04	7.4E+02	4.1E+02	1.7E+01	7.5E+01
NAPA1-13_2p_1_2_2	nd	-21.2	0	p	23.2	7.2E+04	1.5E+03	3.7E+03	1.3E+04	-	6.3E+02	1.3E+01	-

NAPA1-13_2p_2_2_2	nd	-21.2	0	p	23.2	7.4E+04	1.3E+03	2.1E+03	1.3E+04	-	3.1E+02	9.2E+00	-
NAPA1-13_3a_3_1_4	103	-21.4	45	s	23.3	7.7E+04	1.7E+03	3.0E+03	8.7E+03	-	2.7E+02	9.6E+00	-
NAPA1-13_3a_1_1_4	98	-21.4	168	s	23.3	7.1E+04	1.7E+03	2.8E+03	1.5E+04	-	3.6E+02	1.4E+01	-
NAPA1-13_3b_2_1_4	102	-21.4	154	s	23.3	7.0E+04	1.7E+03	2.7E+03	1.5E+04	1.6E+02	3.3E+02	1.4E+01	1.4E+02
NAPA1-13_4b_4_1_4	104	-21.6	90	p	23.4	7.0E+04	1.2E+03	3.2E+03	1.6E+04	-	4.4E+02	6.4E+00	-
NAPA1-13_4b_3_1_4	104	-21.6	196	p	23.4	7.1E+04	1.7E+03	2.8E+03	1.5E+04	-	3.8E+02	1.3E+01	-
NAPA1-13_6a_1_1_4	99	-21.5	152	s	23.4	7.0E+04	1.8E+03	2.7E+03	1.5E+04	-	3.9E+02	1.2E+01	2.4E+02
NAPA1-13_6b_2_1_4	99	-21.6	48	s	23.4	7.0E+04	2.3E+03	3.1E+03	1.5E+04	-	4.4E+02	-	-
NAPA1-13_6b_3_1_4	99	-21.5	77	s	23.4	7.0E+04	1.6E+03	2.9E+03	1.6E+04	-	3.8E+02	1.4E+01	-
NAPA1-13_6b_4_1_4	99	-21.5	50	s	23.4	6.8E+04	1.8E+03	2.5E+03	1.7E+04	-	3.8E+02	1.6E+01	-
NAPA1-13B_1_2_1_1	91	-21.6	242	p	23.4	6.6E+04	1.7E+03	3.7E+03	1.9E+04	-	4.0E+02	1.0E+01	-
NAPA1-13B_1_1_1_1	99	-21.8	160	p	23.6	4.1E+04	2.6E+03	6.7E+03	3.9E+04	-	5.9E+02	1.2E+01	-
NAPA1-13B_1_3_1_1	81	-21.9	210	p	23.6	7.1E+04	1.5E+03	2.6E+03	1.6E+04	-	4.8E+02	1.0E+01	-
NAPA1-13B_1_4_2_1	74	-21.3	410	s	23.2	6.0E+04	1.2E+03	4.4E+03	2.3E+04	-	4.9E+02	2.0E+01	-
Northern Arkansas Quartz													
NAPA1-13_1_1_1_1	113	-22.0	1071	s	23.7	5.1E+04	4.2E+03	3.5E+03	2.8E+04	-	1.7E+03	2.0E+01	-
NAPA1-13_1_3_1_1	97	-22.0	170	s	23.7	7.4E+04	1.5E+03	2.5E+03	1.3E+04	-	5.2E+02	1.7E+01	-
NAPA1-13_1_4_1_1	91	-22.0	546	s	23.7	6.7E+04	1.8E+03	-	1.9E+04	-	7.6E+02	2.9E+01	-
NAPA1-13_1_5_1_1	87	-22.1	225	s	23.8	8.2E+04	1.0E+03	1.6E+03	7.4E+03	-	3.0E+02	6.6E+00	-
NAPA1-13_1_6_1_1	99	-22.1	285	s	23.8	7.6E+04	7.2E+02	1.2E+03	1.4E+04	-	3.6E+02	1.4E+01	-
NAPA1-13_1a_3_1_2	106	-22.0	92	s	23.7	7.4E+04	5.5E+02	2.4E+03	1.5E+04	-	4.6E+02	1.2E+01	-
NAPA1-13_1b_5_1_2	110	-22.0	192	s	23.7	7.2E+04	9.6E+02	1.5E+03	1.6E+04	-	4.9E+02	1.0E+01	-
NAPA1-13_1b_7_1_2	106	-22.0	168	s	23.7	7.0E+04	9.6E+02	2.9E+03	1.7E+04	-	6.0E+02	2.9E+01	-
NAPA1-13_2a_1_1_6	120	-22.0	300	s	23.7	7.2E+04	2.1E+03	2.1E+03	1.4E+04	-	4.9E+02	1.6E+01	-
NAPA1-13_2a_2_1_6	106	-21.9	91	s	23.6	7.0E+04	2.5E+03	2.3E+03	1.5E+04	-	5.0E+02	1.5E+01	-
NAPA1-13_2a_3_1_6	111	-21.9	176	s	23.6	7.0E+04	2.0E+03	2.3E+03	1.6E+04	-	5.3E+02	1.8E+01	-
NAPA1-13_2c_1_1_6	125	-22.0	108	s	23.7	7.5E+04	3.0E+03	2.0E+03	1.0E+04	-	4.1E+02	1.2E+01	-
Central Missouri Sphalerite													
CMBN_1_1_1_6	110	-22.4	232	s	23.9	6.7E+04	2.0E+03	2.9E+03	1.9E+04	-	7.7E+02	2.3E+01	-
CMBN_2_1_1_5	104	-22.7	140	p	24.1	6.9E+04	2.1E+03	2.6E+03	1.8E+04	-	6.5E+02	2.1E+01	-
CMBN_2_2_1_5	103	-22.7	60	p	24.1	6.8E+04	1.8E+03	2.7E+03	1.9E+04	-	7.4E+02	1.9E+01	-
CMBN_2_5_1_5	107	-22.5	56	p	24	6.4E+04	1.9E+03	3.2E+03	2.2E+04	-	8.4E+02	1.3E+01	-
CMBN_2_1_1_6	108	-22.4	160	p	23.9	6.8E+04	1.9E+03	2.6E+03	1.9E+04	-	7.0E+02	1.6E+01	-
CMBN_2_3_1_6	106	-22.4	50	p	23.9	6.5E+04	1.8E+03	2.6E+03	2.1E+04	-	7.6E+02	1.8E+01	-
CMBN_2_2_1_6	107	-22.4	126	p	23.9	6.5E+04	2.7E+03	2.4E+03	2.0E+04	-	7.4E+02	2.1E+01	-
CMBN_2_4_1_5	103	-22.7	36	p	24.1	6.8E+04	2.0E+03	2.0E+03	1.9E+04	-	7.6E+02	1.8E+01	-

CMBN_3_3_1_5	103	-22.4	200	s	23.9	7.0E+04	1.7E+03	2.7E+03	1.7E+04	-	6.2E+02	1.7E+01	-
CMBN_3_1_1_5	102	-22.4	697	s	23.9	6.9E+04	1.9E+03	2.8E+03	1.8E+04	-	7.2E+02	3.4E+01	-
CMBN_3_2_1_5	103	-22.4	136	s	23.9	6.4E+04	2.3E+03	2.9E+03	2.1E+04	-	7.5E+02	2.1E+01	-
CMBN_4_2_1_5	102	-22.3	192	p	23.9	6.6E+04	1.9E+03	2.7E+03	2.1E+04	-	7.6E+02	2.1E+01	-
CMBN_4_1_1_5	102	-22.3	180	p	23.9	6.6E+04	2.1E+03	2.4E+03	2.0E+04	-	7.2E+02	1.5E+01	-
CMBN_5_3_2_5	102	-22.2	20	p	23.8	6.0E+04	5.5E+03	6.9E+03	1.8E+04	-	6.4E+02	9.1E+01	-
CMBN_5_1_1_5	106	-22.2	80	p	23.8	6.6E+04	1.8E+03	3.4E+03	2.0E+04	-	7.4E+02	-	-
CMBN_5_2_2_5	104	-22.2	84	p	23.8	6.2E+04	3.2E+03	2.1E+03	2.2E+04	-	7.7E+02	2.6E+01	-
CMBN_5_4_2_5	106	-22.1	175	s	23.8	6.6E+04	2.1E+03	2.7E+03	2.0E+04	-	7.1E+02	2.1E+01	-
CMBN_6_2_1_5	106	-22.4	63	p	23.9	6.7E+04	2.2E+03	3.1E+03	1.9E+04	-	7.3E+02	1.4E+01	-
CMBN_6_1_1_5	103	-22.4	396	p	23.9	6.7E+04	2.4E+03	2.6E+03	1.9E+04	-	6.6E+02	2.2E+01	-
CMBN_7_2_1_5	93	-22.3	77	s	23.9	7.2E+04	8.4E+02	3.2E+03	1.6E+04	-	6.5E+02	2.2E+01	-
CMBN_7_4_1_5	95	-22.1	78	s	23.8	6.6E+04	1.7E+03	2.8E+03	2.0E+04	-	7.2E+02	2.6E+01	-
CMBN_7_3_1_5	96	-22.1	160	s	23.8	6.9E+04	1.6E+03	2.4E+03	1.8E+04	-	6.4E+02	2.0E+01	-
CMBN_7_1_1_5	94	-22.3	54	s	23.9	6.8E+04	-	-	2.1E+04	-	6.8E+02	-	-
CMBN_8_4_2_5	94	-22.0	48	p	23.7	6.8E+04	1.2E+03	2.6E+03	1.9E+04	-	7.0E+02	1.4E+01	-
CMBN_8_3_2_5	94	-22.0	245	p	23.7	6.6E+04	1.9E+03	2.5E+03	2.0E+04	-	7.2E+02	1.1E+01	-
CMBN_8_1_1_5	97	-22.2	85	p	23.8	5.8E+04	3.0E+03	1.8E+03	2.7E+04	-	8.2E+02	1.6E+01	-
CMBN_9_2_1_5	95	-21.9	36	p	23.6	6.8E+04	1.7E+03	2.9E+03	1.8E+04	-	7.1E+02	1.9E+01	-
CMBN_9_3_1_5	95	-22.1	28	p	23.8	7.0E+04	1.6E+03	2.5E+03	1.7E+04	-	5.8E+02	2.3E+01	-
CMBN_9_1_1_5	95	-22.0	119	p	23.7	6.8E+04	1.8E+03	2.1E+03	1.8E+04	-	7.0E+02	2.0E+01	-
CMBN_10_6_1_5	103	-22.1	56	s	23.8	6.7E+04	2.6E+03	3.1E+03	1.8E+04	-	8.5E+02	2.2E+01	-
CMBN_10_3_1_5	101	-22.1	98	s	23.8	6.8E+04	1.6E+03	3.1E+03	1.8E+04	-	8.2E+02	1.6E+01	-
CMBN_10_4_1_5	101	-22.1	44	s	23.8	6.2E+04	2.1E+03	3.5E+03	2.3E+04	-	8.1E+02	2.6E+01	-
CMBN_10_1_1_5	100	-22.1	28	s	23.8	6.3E+04	2.9E+03	3.0E+03	2.1E+04	-	7.8E+02	3.5E+01	-
CMBN_10_2_1_5	104	-22.1	112	s	23.8	5.8E+04	3.2E+03	3.2E+03	2.5E+04	-	7.4E+02	6.3E+01	-
CMBN_10_5_1_5	101	-22.1	50	s	23.8	6.5E+04	2.8E+03	2.3E+03	2.0E+04	-	8.4E+02	2.7E+01	-
CMBN_11_2_1_5	92	-22.0	91	p	23.7	5.9E+04	2.3E+03	3.4E+03	2.5E+04	-	9.3E+02	3.3E+01	-
CMBN_11_3_2_5	102	-22.0	208	p	23.7	6.6E+04	2.1E+03	2.7E+03	2.0E+04	-	6.9E+02	2.0E+01	9.6E+01
CMBN_11_4_2_5	99	-22.0	63	p	23.7	6.6E+04	1.6E+03	2.1E+03	2.1E+04	-	6.6E+02	4.3E+01	6.6E+01
CMBN_12_1_1_5	105	-22.3	102	p	23.9	6.6E+04	2.1E+03	2.9E+03	2.1E+04	-	7.2E+02	2.2E+01	-
CMBN_12_2_1_5	102	-22.2	36	p	23.8	6.8E+04	1.8E+03	-	1.9E+04	-	7.5E+02	2.4E+01	-
CMBN_17_2_1_5	80	-22.4	72	?	23.9	6.5E+04	2.5E+03	3.5E+03	2.0E+04	-	7.4E+02	2.8E+01	-
CMBN_17_1_1_5	82	-22.4	119	?	23.9	7.0E+04	1.2E+03	1.9E+03	1.9E+04	-	7.1E+02	4.9E+01	-
CMBN_18_1_1_5	106	-22.2	144	p	23.9	6.4E+04	1.6E+03	3.6E+03	2.2E+04	-	7.6E+02	2.7E+01	-
CMBN_18_5_2_5	108	-22.3	224	p	23.9	6.7E+04	1.8E+03	2.8E+03	1.9E+04	-	7.0E+02	1.9E+01	-

CMBN_18_2_1_5	104	-22.3	144	p	23.9	6.7E+04	1.6E+03	2.8E+03	2.0E+04	-	7.2E+02	2.2E+01	-
CMBN_18_4_2_5	108	-22.3	336	p	23.9	6.7E+04	1.9E+03	2.6E+03	2.0E+04	-	7.2E+02	2.3E+01	-
CMBN_21_1_1_5	107	-22.5	590	p	24	6.7E+04	1.9E+03	3.0E+03	2.0E+04	-	7.1E+02	2.3E+01	-
CMBN_18b_1_1_5	107	-22.3	276	p	23.9	6.7E+04	2.5E+03	2.6E+03	1.9E+04	-	7.1E+02	1.8E+01	-
CMBN_18b_2_1_5	106	-22.3	216	p	23.9	6.7E+04	1.8E+03	2.7E+03	2.0E+04	-	6.9E+02	2.2E+01	-
CMBN_18b_3_1_5	106	-22.4	306	p	23.9	7.0E+04	1.7E+03	2.3E+03	1.8E+04	-	6.7E+02	1.8E+01	-
CMFD_1_1_1_5	72	-20.1	66	p	22.4	6.5E+04	2.1E+03	1.7E+03	1.7E+04	-	3.3E+02	1.7E+01	-
CMFD_1_1_1_6	87	-23.0	176	s	24.3	7.3E+04	1.5E+03	2.4E+03	1.7E+04	-	5.9E+02	1.6E+01	-
CMFD_1_3_1_6	87	-23.0	6	s	24.3	7.2E+04	-	-	1.9E+04	-	6.2E+02	-	-
CMFD_2_3_1_5	87	-20.9	42	p	23	6.8E+04	-	-	1.6E+04	-	6.4E+02	2.7E+01	-
CMFD_2_1_1_5	93	-20.9	135	s	23	6.7E+04	2.2E+03	2.2E+03	1.7E+04	-	5.5E+02	1.9E+01	-
CMFD_2_2_1_5	94	-21.7	160	s	23.5	6.8E+04	2.2E+03	2.0E+03	1.8E+04	-	5.2E+02	1.2E+01	-
CMFD_3_2_1_5	94	-14.5	80	s	18.2	5.2E+04	1.8E+03	2.6E+03	1.4E+04	-	8.8E+02	1.1E+01	-
CMFD_3_1_1_5	95	-14.5	84	s	18.2	5.1E+04	1.8E+03	2.7E+03	1.4E+04	-	9.5E+02	2.5E+01	-
CMFD_4_3_1_5	105	-23.4	120	p	24.6	8.3E+04	9.3E+02	3.6E+03	8.9E+03	-	3.3E+02	1.1E+01	-
CMFD_4_7_1_5	107	-23.1	602	p	24.4	7.7E+04	1.4E+03	2.3E+03	1.4E+04	-	5.0E+02	1.8E+01	-
CMFD_2b_2_1_6	nd	-23.0	18	s	24.3	6.8E+04	-	-	2.0E+04	-	9.2E+02	-	-
CMFD_2b_3_1_6	nd	-23.0	56	-	24.3	7.6E+04	2.8E+03	-	1.3E+04	-	3.4E+02	1.8E+01	-
CMFT_2_3_1_6	113	-22.2	153	p	23.8	7.1E+04	1.2E+03	2.7E+03	1.7E+04	-	6.3E+02	2.6E+01	-
CMFT_2_1_1_6	111	-22.1	644	p	23.8	6.8E+04	1.8E+03	2.9E+03	1.9E+04	-	6.9E+02	1.7E+01	-
CMFT_2_4_1_6	115	-22.1	319	p	23.8	6.8E+04	1.7E+03	2.8E+03	1.9E+04	-	7.5E+02	2.0E+01	-
CMFT_2_2_1_6	113	-22.2	224	p	23.8	6.6E+04	2.0E+03	2.5E+03	2.0E+04	-	7.3E+02	2.1E+01	2.3E+02
CMFT_4_2_1_6	109	-22.3	697	p	23.9	6.7E+04	1.8E+03	3.0E+03	2.0E+04	-	7.5E+02	2.1E+01	-
CMHL_3_1_1_6	82	-17.1	182	p	20.3	5.7E+04	1.6E+03	2.1E+03	1.7E+04	-	1.0E+03	1.2E+01	-
CMHL_3_3_1_6	77	-17.0	40	p	20.2	5.6E+04	2.1E+03	1.3E+03	1.7E+04	-	1.1E+03	1.5E+01	-
CMHL_3_2_1_6	83	-17.1	48	p	20.3	5.6E+04	1.7E+03	-	1.8E+04	-	1.1E+03	-	-
CMHL_1a_2_1_6	94	-17.3	84	p	20.4	5.5E+04	1.7E+03	3.0E+03	1.8E+04	-	1.1E+03	1.8E+01	-
CMHL_1a_5_1_6	81	-17.7	84	p	20.7	5.3E+04	2.9E+03	2.8E+03	1.9E+04	-	1.3E+03	2.5E+01	-
CMHL_1a_3_1_6	54	-17.5	98	p	20.6	5.5E+04	2.2E+03	2.5E+03	1.8E+04	-	1.2E+03	1.8E+01	-
CMTF_1_1_1_5	77	-21.7	50	p	23.5	6.6E+04	1.9E+03	3.7E+03	1.8E+04	-	6.3E+02	-	-
CMTF_1_2_1_6	111	-22.3	390	p	23.9	7.2E+04	1.5E+03	2.7E+03	1.6E+04	-	6.1E+02	1.9E+01	-
CMTF_1_1_1_6	114	-22.4	418	p	23.9	6.8E+04	1.8E+03	3.0E+03	1.9E+04	-	6.8E+02	2.6E+01	-
CMTF_1_5_1_6	111	-22.4	48	p	23.9	6.9E+04	2.1E+03	2.7E+03	1.8E+04	-	6.6E+02	1.5E+01	-
CMTF_1_4_1_6	111	-22.4	105	p	23.9	7.0E+04	1.4E+03	2.5E+03	1.8E+04	-	7.3E+02	2.6E+01	-
CMTF_1_3_1_6	111	-22.4	252	p	23.9	6.9E+04	1.7E+03	2.5E+03	1.8E+04	-	6.4E+02	2.1E+01	1.7E+02
CMTF_1_2_1_5	79	-21.7	15	p	23.5	6.2E+04	-	-	2.6E+04	-	7.9E+02	-	-

CMTF_1_3_2_5	100	-22.3	24	p	23.9	6.8E+04	-	-	2.3E+04	-	1.1E+03	6.4E+01	-
CMTF_1_4_2_5	100	-22.3	40	p	23.9	6.7E+04	-	-	1.2E+04	-	3.8E+02	-	-
CMTF_2_2_1_5	102	-22.1	70	p	23.8	6.9E+04	1.6E+03	3.5E+03	1.7E+04	-	6.2E+02	1.9E+01	-
CMTF_2_1_1_5	102	-22.1	35	p	23.8	6.6E+04	2.9E+03	3.3E+03	1.8E+04	-	8.7E+02	2.5E+01	-
CMTF_2_4_1_5	102	-22.1	48	p	23.8	6.8E+04	2.6E+03	3.0E+03	1.7E+04	-	5.9E+02	-	-
CMTF_2_5_1_5	102	-22.1	45	p	23.8	6.7E+04	2.1E+03	2.5E+03	1.9E+04	-	6.6E+02	-	-
CMTF_2_3_1_5	102	-22.1	66	p	23.8	6.5E+04	1.6E+03	2.3E+03	2.2E+04	-	6.5E+02	1.5E+01	-
CMTF_3_2_1_5	97	-22.9	55	p	24.1	7.0E+04	1.9E+03	2.9E+03	1.8E+04	-	6.7E+02	5.1E+01	-
CMTF_3_1_1_5	98	-22.9	105	p	24.1	6.7E+04	2.0E+03	2.4E+03	2.1E+04	-	6.6E+02	3.1E+01	-
CMTF_4_1_1_5	109	-22.5	161	p	24	6.6E+04	1.8E+03	3.2E+03	2.0E+04	-	8.3E+02	-	-
CMTF_4_2_1_5	109	-22.5	126	p	24	6.8E+04	1.8E+03	2.8E+03	1.9E+04	-	6.7E+02	-	-
CMTF_4_5_1_5	110	-22.5	80	p	24	7.0E+04	1.4E+03	2.5E+03	1.8E+04	-	6.5E+02	2.1E+01	-
CMTF_4_4_1_5	110	-22.5	42	p	24	6.9E+04	1.5E+03	2.5E+03	1.9E+04	-	6.9E+02	4.3E+01	-
CMTF_4_3_1_5	106	-22.6	32	p	24.1	6.7E+04	-	-	1.9E+04	-	7.5E+02	-	-
CMTF_5_5_1_5	85	-22.9	80	p	24.3	6.9E+04	1.8E+03	3.1E+03	1.9E+04	-	6.9E+02	2.2E+01	-
CMTF_5_1_1_5	85	-22.9	150	p	24.3	6.6E+04	2.2E+03	3.4E+03	2.1E+04	-	8.0E+02	-	-
CMTF_5_4_1_5	91	-22.7	55	p	24.1	6.9E+04	2.0E+03	2.8E+03	1.9E+04	-	7.0E+02	-	-
CMTF_5_3_1_5	92	-22.9	126	p	24.3	7.4E+04	1.6E+03	2.2E+03	1.6E+04	-	5.3E+02	-	-
CMTF_5_2_1_5	85	-22.9	60	p	24.3	7.0E+04	2.1E+03	2.1E+03	1.8E+04	-	7.2E+02	-	-
CMTF_6_2_1_5	90	-22.7	117	p	24.1	7.0E+04	1.5E+03	3.0E+03	1.8E+04	-	6.8E+02	1.8E+01	-
CMTF_6_1_1_5	90	-22.7	154	p	24.1	6.9E+04	1.5E+03	2.9E+03	1.9E+04	-	7.1E+02	1.7E+01	-
CMTF_6_3_2_5	89	-22.4	840	p	23.9	6.5E+04	2.0E+03	3.1E+03	2.1E+04	-	7.2E+02	1.8E+01	-
CMTF_7_3_1_5	106	-23.1	216	p	24.4	7.3E+04	1.5E+03	3.5E+03	1.6E+04	-	5.9E+02	1.2E+01	-
CMTF_7_2_1_5	100	-23.1	416	p	24.4	6.9E+04	1.9E+03	3.3E+03	1.9E+04	-	7.1E+02	1.6E+01	-
CMTF_7_1_1_5	99	-23.1	322	p	24.4	6.8E+04	1.9E+03	3.0E+03	2.0E+04	-	7.2E+02	1.5E+01	-
CMTF_8_1_1_5	72	-22.2	187	s	23.8	6.4E+04	2.3E+03	9.8E+02	2.8E+01	-	-	-	-
CMTF_8_2_1_5	93	-22.2	72	s	23.8	5.7E+04	5.8E+03	1.0E+03	8.3E+01	-	-	-	-

Abbreviations as follows: s = secondary; p = primary; - = below detection limit; nd = not determined. Detection limit for each analysis varied based on fluid inclusion depth, volume, and salinity. Detection limit values had the following approximate ranges (ppm): Na, Mg, K, Ca = 10's to 1,000's; Cu, Sr, Pb = 10's to 100's, and Ba = 1's to 10's.

APPENDIX 2

Sample	Th	Tm	area	Origin	NaCl eq. wt%	K/Na	Ca/Na	Ba/Na
Viburnum Trend Dolomite								
MAG13A_D1_1__3	158	-22.6	144	p	24.1	2.3E-02	nd	6.2E-05
MAG13A_D2_1__3	155	-22.6	68	p	24.1	2.2E-02	nd	7.0E-05
MAG13A_D3_1__3	120	-22.5	152	p	24	2.5E-02	nd	8.3E-05
VTSW2E_D2_1__3	105	-21.2	70	p	23.2	2.4E-02	nd	6.5E-05
VTSW2F_D1_1__3	107	-17.6	120	p	20.7	2.0E-02	nd	1.9E-05
VTSW2F_D2_1__3	129	-22.1	500	p	23.8	2.7E-02	nd	4.8E-05
VTSW2F_D4_1__3	131	-6.7	154	p	10.1	2.9E-02	nd	2.8E-05
VTSW2F_D4_2__3	125	-22.4	44	p	23.9	2.0E-02	nd	8.0E-05
VTSW2F_D5_1__3	106	-19.9	60	p	22.3	2.1E-02	nd	4.2E-05
WF2B_D1_1__3	137	-22.6	66	p	24.1	2.8E-02	nd	1.0E-04
81V22_D1_1__4	135	-22.5	72	p	24	2.0E-02	nd	9.6E-06
81V22_D1_4__4	127	-21.7	40	p	23.5	1.9E-02	nd	2.4E-05
VTSW2_D1_1_1_4	126	-5.5	60	p	8.5	3.7E-02	nd	3.7E-05
VTSW2_D1_3_2_4	111	-22.5	50	p	24	1.6E-02	nd	5.4E-05
VTSW2_D1_4_3_4	126	-22.5	80	p	24	2.6E-02	nd	9.9E-05
VTSW2_D1_6_4_4	119	-22.5	45	p	24	2.1E-02	nd	4.2E-05
VTSW2_D1_7_4_4	122	-22.5	120	p	24	1.9E-02	nd	5.5E-05
VTSW2_D1_9_5_4	122	-22.5	54	p	24	1.7E-02	nd	4.6E-05
VTSW2_D2_1__4	117	-22.8	234	p	24.2	1.8E-02	nd	5.3E-05
VTSW2_D2_2__4	117	-22.8	70	p	24.2	2.6E-02	nd	7.6E-05
VTSW2_D2_3__4	120	-22.8	110	p	24.2	2.2E-02	nd	3.8E-05
VTSW2_D2_6__4	124	-22.3	32	p	23.9	1.3E-02	nd	4.4E-05
WF2_D2a_1_1_6	193	-22.7	48	p	24.1	2.9E-02	nd	1.3E-04
Viburnum Trend Replacement Dolomite								
#7_1_1_1_6	117	-20.2	45	p	22.5	5.9E-02	nd	7.0E-05
#7_1b_2_1_6	118	-20.2	39	p	22.5	1.3E-01	nd	1.4E-04
#7_1b_3_1_6	111	-20.2	18	p	22.5	1.3E-01	nd	9.3E-05
#7_2_1_1_6	142	-12.3	28	p	16.2	1.4E-01	nd	2.8E-04
#7_4_1_1_5	77	-18.7	40	p	21.5	1.1E-01	nd	1.4E-04
#7_4_2_1_5	100	-18.7	36	p	21.5	6.7E-02	nd	9.4E-05
#7_4_3_1_5	133	-18.7	84	p	21.5	1.1E-01	nd	7.0E-05
#7_4_4_1_5	131	-18.7	9	p	21.5	1.5E-01	nd	4.6E-05
#7_4_1_1_6	126	-19.5	30	p	22.4	1.2E-01	nd	3.3E-04
Tri-State Calcite								
TSGY2-1__2_1_2	68	-4.2	144	p	6.7	-	nd	8.6E-05
TSGY2-1__3_1_2	67	-4.2	252	p	6.7	2.3E-02	nd	5.8E-05
TSGY2-1__2_1_2	78	-4.2	104	p	6.7	1.6E-02	nd	2.1E-04
Tri-State Dolomite								
TSNC1-2_D2b_1__3	109	-18.6	154	p	21.4	2.8E-02	nd	4.4E-05
TSNC1-2_D2b_2__3	129	-18.6	374	p	21.4	1.6E-02	nd	1.6E-05
TSNC1-2_D2b_3__3	129	-18.6	50	p	21.4	2.3E-02	nd	3.5E-05
TSNC1-2_D2b_4__3	109	-18.6	120	p	21.4	2.3E-02	nd	3.1E-05
TSNC1-2_D3_1__3	120	-22.1	36	p	23.8	3.5E-02	nd	6.5E-05
TSNC1-2_D3_2__3	121	-22.1	56	p	23.8	1.9E-02	nd	9.1E-05
TSNC1-2_D3_3__3	124	-22.1	16	p	23.8	-	nd	2.1E-04
TSNC1-2_D3_4__3	122	-22.1	180	p	23.8	2.4E-02	nd	6.8E-05
TSPC7-1_D1_1__3	132	-22.9	140	p	24.3	2.5E-02	nd	1.2E-04
TSPC7-1_D2_1__3	130	-22.9	160	p	24.3	3.8E-02	nd	4.1E-05
TSPC7-1_D4_1__3	123	-22.9	70	p	24.3	2.7E-02	nd	1.1E-04
TSTR1-3__D1_1_6	133	-22.8	48		24.2	3.0E-02	nd	9.7E-05
TSTR1-3__D2_2_6	133	-22.8	30	p	24.2	4.4E-02	nd	-

TSTR1-3__D3_3_6	131	-22.8	84	p	24.2	2.9E-02	nd	-
TSTR1-3__D4_4_6	133	-22.8	48	p	24.2	3.0E-02	nd	-
TSTR1-3__D5_5_6	109	-13.3	110	p	17.2	3.0E-02	nd	6.5E-05
TSTR1-3__D6_6_6	134	-22.8	288	p	24.2	3.0E-02	nd	9.6E-05
Northern Arkansas Dolomite								
NAMC1-4_1_1_1_2	142	-22.8	243	p	24	2.2E-02	nd	3.1E-05
NAMC1-4_2a_1_1_2	138	-22.4	126	p	23.9	2.8E-02	nd	4.1E-05
NAMC1-4_2b_3_3_2	137	-22.4	168	p	23.9	1.7E-02	nd	2.6E-05
NAEX1-7_D2_2__3	127	-21.1	56	p	23.1	2.4E-02	nd	2.6E-05
NAEX1-7_D3_3__3	128	-19.8	70	p	22.2	4.5E-02	nd	5.2E-05
NAEX1-7_D2_6__3	127	-21.1	60	p	23.1	-	nd	2.6E-05
NAJP1-1_D4_1__3	133	-21.4	360	p	23.3	2.4E-02	nd	6.8E-05
NAJP1-1_D5_1__3	117	-20.8	64	p	22.9	2.7E-02	nd	4.3E-05
NALD1-1_D1_1__3	133	-11.9	480	p	15.8	2.0E-02	nd	1.7E-05
NALD1-1_D2_1__3	119	-11.8	49	p	15.8	3.1E-02	nd	4.6E-05
NALD1-1_D4_1__3	137	-18.6	160	p	21.4	2.8E-02	nd	1.9E-05
NAPA1-1_D1_1__3	152	-22.9	28	p	24.3	2.5E-02	nd	1.1E-04
NAPA1-1_D3_1__3	148	-22.9	50	p	24.3	2.3E-02	nd	8.5E-05
NAPA1-1_D1_1__4	119	-18.7	32	p	21.5	2.7E-02	nd	2.6E-05
NAPA1-1_D1_2__4	137	-23.2	24	p	24.5	2.7E-02	nd	9.7E-05
NAPA1-1_D1_4__4	136	-23.4	20	p	24.6	-	nd	-
NAPA1-1_D1_6__4	116	-22.8	25	p	24.2	1.7E-02	nd	2.0E-05
NAPA1-1_D1_7__4	143	-23.1	50	p	24.4	2.0E-02	nd	3.4E-05
NAPA1-1_D1_8__4	147	-23.1	32	p	24.4	2.3E-02	nd	2.6E-05
NAPA1-1_D1_9__4	138	-22.8	50	p	24.2	-	nd	4.4E-05
NAPA1-1_D1_10__4	134	-22.8	42	p	24.2	-	nd	6.9E-05
NAPA1-1_D1_11__4	123	-17.7	54	p	20.7	2.7E-02	nd	-
Central Missouri Barite								
CMBN_B1_1__6	nd	-1.9	80	p	3.2	2.7E-01	1.1E-01	nd
CMBN_B2_1__6	nd	-1.9	32	p	3.2	2.2E-01	8.4E-02	nd
CMBN_B3_1__6	nd	-1.9	273	p	3.2	2.0E-01	1.4E-01	nd
CMTF_B1_1__6	nd	-8.1	91	p	11.8	5.1E-02	2.1E-02	nd
CMTF_B3_1__6	nd	-1.2	63	p	2.1	2.1E-01	8.5E-02	nd
CMTF_B3b_1__6	nd	-2.0	45	p	3.4	1.9E-01	1.8E-01	nd
CMTF_B4_1__6	133	-0.9	80	p	1.6	4.0E-02	3.6E-02	nd
CMTF_B5_1__6	nd	-4.4	192	p	7	7.1E-02	7.8E-02	nd
CMGO_B1_1__6	nd	-2.0	nd	p	3.4	1.4E-01	9.8E-02	nd
CMGO_B2_2__6	nd	-2.0	nd	p	3.4	1.5E-01	2.2E-02	nd
CMGO_B3_3__6	nd	-2.0	nd	p	3.4	5.5E-02	7.2E-02	nd
CMGO_B4_4__6	nd	-2.0	nd	p	3.4	9.0E-02	2.2E-02	nd

Abbreviations as follows: s = secondary; p = primary; - = below detection limit; nd = not determined.

VITA

Ph. D in geology, 2011, University of Missouri

Advisor: Dr. Martin Appold

Title: Geochemistry and Origins of Mississippi Valley Type Mineralizing Fluids of the Ozark Plateau

M. S. in geology, 2004, University of Alaska-Fairbanks

Advisor: Dr. Rainer Newberry

Title: Geology and Gold Mineralization of the Nyac District, SW Alaska

B. S. in geology, 2002, University of Minnesota-Duluth

Advisor: Dr. Richard Ojakangas

Senior Thesis: Geochemical and Mineralogical Correlation of Archean Pillow Basalt Flows in the Upper Ely Greenstone